From the
Walter-Brendel-Zentrum für Experimentelle Medizin
of the Ludwig-Maximilians-Universität München
Director: Prof. Dr. med. Ulrich Pohl

Sympathetic innervation of arteries drives rhythmic leukocyte adhesion to arteries and veins

Dissertation
zum Erwerb des Doctor of Philosophy (PhD)
an der Medizinischen Fakultät der
Ludwig-Maximilians-Universität

submitted by

Alba de Juan

from
Madrid, Spain

On
04/05/2018

Supervisor: Prof. Dr. Christoph Scheiermann

Second evaluator. Prof. Dr. Oliver Söhnlein

Dean: Prof. Dr. Reinhard Hickel

Date of oral defense: 20/07/2018

Acknowledgements

First of all, I would like to thank my supervisor Christoph Scheiermann for giving me this opportunity and his tremendous guidance over the past few years. His wise advice has been really important not only in my scientific career but in my private life as well.

I have to add that it would not have been the same without such excellent lab members: Louise, Chien Sin, Kerstin, Jasmin, Sophia, Robert, Stephan and Wenyan. They are not only awesome colleagues, they are friends, family and their support has been crucial, especially in the last stage of this PhD (sorry if I have been too grumpy sometimes!). I should not forget about Amelia and Eike, even though they were from another group, their help and friendship has been quite instrumental to get me to this point too.

My colleagues and I had the privilege of being part of the IRTG914, where we have benefited from plenty of courses, seminars, retreats and great opportunities for becoming better scientists. I am really grateful in particular, to Verena, our guardian angel who takes care of all the students of this Graduate program. I would like to mention as well my TAC members Oliver Söhnlein and Barbara Walzog for their helpful feedback in our annual meetings.

The first lab is like the first love: you never forget it. So I have to allude to my former supervisor, Óscar M. Pello who has been an essential person over the last years and he still is. I would like to acknowledge the rest of my colleagues at the CNIC, too, since I have learnt a lot from them. And, in particular, I would like to highlight Vicente Andrés and Andrés Hidalgo and their support, even nowadays.

Life outside of the lab is really important for me. That is why I am so thankful to all my “Munich family”, the fantastic people whom I have met here during these years and have made it easier being away from home. I could cite names forever but I would like to especially thank my “Munich parents” Rubén and Teresa, the other two thirds of the trident Sara and María and my wonderful flatmates and neighbors: Martin, Esther, Felix, Stefan, Thies, Chris and Almir.

Obviously, I cannot forget where I come from and how important it has been to receive the support from my friends and family at home. Even if they are not really familiar with what I am actually doing, their encouragement has been amazing. I would like to mention all my good friends but, in particular, my best friend Bárbara and her mother Montse. And of course, I cannot leave out my uncle Julián (mi Calvi), my aunt Maria Ángeles and my cousins Sergio, Raquel and Noelia that are like the older brother and sisters that I never had. Unfortunately, my grandfather Julián is not here anymore but I am pretty sure he would be quite proud of me and that makes me tremendously happy.

Finally, I have to thank my closest family, my parents Santos and Cecilia and the person I love the most in this life, my sister Tamara. “Jefe”, I would not be who I have become and I have would not achieved all these things without you. “Enana, mi sol y mis estrellas”, you are the person who knows me better than anybody else. Your unconditional faith in me and the way you see me as your role model makes me try to improve myself every single day. The passion I have for what I do it is the only reason that makes it bearable to be far from you. I love you!

Abstract

Leukocyte recruitment exhibits circadian, ~24h oscillations, which is dependent on local input by the sympathetic nervous system (SNS). Sympathetic nerves reach tissues alongside arterioles. Since smaller veins are devoid of sympathetic innervation but are the main site of leukocyte recruitment, it is unclear how these adrenergic stimuli reach veins to regulate leukocyte infiltration to tissues. Here, we demonstrate rhythmic differences in the ability of leukocytes to adhere to arteries and veins in an acute inflammatory scenario. Using *in vivo* quantitative imaging after TNF-α stimulation, we could observe higher leukocyte recruitment in the carotid artery in the morning and lower at night. It was the opposite situation in the case of the jugular vein; lower in the early morning and higher at night. We could confirm the same results in the microvasculature of the cremaster muscle, suggesting an intrinsic mechanism independent on the vessel location. Among different oscillatory cell adhesion molecules, intercellular adhesion molecule 1 (ICAM-1) fitted most closely with the recruitment data. Using genetically modified mice and blocking antibodies, we could confirm the functional importance of ICAM-1 in these oscillations in both vessels. As the SNS has in important role in rhythmic leukocyte recruitment, we next used pharmacological and surgical procedures for inducing denervation in our mice. We found ablated oscillations in leukocyte recruitment, as well as in *Icam1* gene expression. Similar results were obtained when we focused on the β2 adrenergic receptors, via β2-antagonists and *Adrb2*$^{-/-}$ mice. Surprisingly, when using *Ng2Cre x Bmal1*$^{flox/flox}$ mice, where mice lacked a molecular clock specifically in arteriolar pericytes, we could no longer see oscillations in both vessels, even though the genetic manipulation targeted the artery. This suggested that there was an effect from the artery that could have affected the vein. In terms of clinical relevance, acute cardiovascular complications occur predominantly at the onset of the behavioral activity phase and are the major cause of death in humans. Recent evidence points to a critical role for rhythmic leukocyte recruitment in the onset of vascular diseases. We could see that altered rhythmicity resulted in a heightened susceptibility to vaso-occlusion at different

times. Together, these data point to an important role of arteries in regulating rhythmic leukocyte recruitment to veins, which could have potential implications in driving time-of-day-dependent cardiovascular complications.

Table of contents

Acknowledgements 4
Abstract 6
Abbreviations 14
1 Introduction 18
1.1 Cardiovascular system 18
1.1.1 General overview 18
1.1.2 Vessels: differences between arteries and veins (structure and function) 20
1.1.3 The leukocyte adhesion cascade 24
1.2. Circadian rhythms 28
1.2.1 General overview 28
1.2.2 Entrainment and synchronization of the clock 29
1.2.3 The molecular clock 31
1.2.4 Clock genes links to immunology 32
1.2.5 Circadian rhythms and the immune system 34
1.2.6 Diseases associated with circadian rhythms 39
1.2.7 Shift workers and health complications 40
1.3 Sympathetic Nervous System 41
1.3.1 General overview 41
1.3.2 Role of the SNS in the vasculature 42
1.3.3 Adrenergic receptors 44
1.3.4 Adrenergic control of the immune system 45
2 Materials and Methods 48
2.1 Animals 48
2.1.1 Mouse strains 48
2.1.2 Genotyping 48
2.1.3 Tamoxifen preparation and treatment 51
2.2 Multichannel fluorescence intravital microscopy (MFIM) 51
2.2.1 Carotid artery and jugular vein imaging 51

2.2.2 Cremaster muscle imaging 55
2.3 Immunofluorescence on frozen sections 57
2.4 Adoptive transfer and flow cytometry experiments 60
2.5 Functional blocking of adhesion molecules and chemokine receptors 61
2.6 Denervation techniques 61
2.6.1 Chemical sympathetic denervation (6-OHDA) 61
2.6.2 Surgical sympathetic denervation (SCGx) 62
2.7 β_2 adrenergic receptor antagonist treatment 62
2.8 Thrombosis assay 63
2.9 RNA isolation 64
2.10 Reverse transcription 64
2.11 Quantitative real-time PCR 65
2.12 Statistical analyses 67
2.13 Antibody list 68
2.14 Reagents 69
3 Results 71
3.1. Differences in leukocyte adhesion between arteries and veins 71
3.2 Involvement of cell adhesion molecules and chemokines in diurnal leukocyte recruitment 76
3.3 Similar circadian oscillations in arteries and veins 82
3.4 Sympathetic control of circadian leukocyte recruitment in arteries and veins 86
3.5 Differences in adrenergic input between arteries and veins 94
3.6 Clinical relevance: circadian thrombosis 99
4 Discussion 104
4.1. Circadian differences in leukocyte recruitment between arteries and veins 105
4.2. Cell adhesion molecules and chemokines are involved in circadian recruitment 106
4.3. Differences in recruitment are independent of circadian clock gene expression 107
4.4 SNS controls rhythmic leukocyte recruitment in arteries and veins 109

4.5 Arteries drive rhythmic recruitment in arteries and veins 110
4.6 Different susceptibility in circadian thrombosis between arteries and veins111
5 References 114
6 Appendix 128
6. 1 Curriculum Vitae 128
6.2 Affidavit 131

List of figures

Figure 1.1 Cardiovascular System 19
Figure 1.2 Artery-vein network.. 20
Figure 1.3 Structural features of the vasculature. 22
Figure 1.4 General scheme of the leukocyte adhesion cascade. 26
Figure 1.5 Entrainment and synchronization of the clock. 30
Figure 1.6 The molecular clock. 32
Figure 1.7 Rhythms in immune cells parameters. 38
Figure 1.8 Innervation status of the vasculature by SNS 43

Figure 2. 1 PCR genotyping gels 50
Figure 2. 2 Carotid artery/jugular vein in vivo imaging 52
Figure 2. 3 Epifluorescence microscope set-up 53
Figure 2. 4 Representative example of mean fluorescence intensity measurement in adherent cells 54
Figure 2. 5 Cremaster muscle preparation 55
Figure 2. 6 MFIM of the cremasteric microcirculation 56
Figure 2. 7 Cremaster muscle MFIM 57
Figure 2. 8 Representative fluorescence imaging picture 58
Figure 2. 9 Representative example of quantitative expression analyses 59
Figure 2. 10 6-OHDA treatment scheme 62
Figure 2. 11 Set-up of phototoxicity-induced thrombus formation 63

Figure 3.1 Diurnal oscillations in leukocyte adhesion in large vessels 72
Figure 3.2 Differences in leukocyte recruitment in LyEGFP mice between morning and night 73
Figure 3.3 Differences in leukocyte adhesion in microvasculature 74
Figure 3.4 Differences in β2-integrins expression on adherent leukocytes 75
Figure 3.5 Relevance of the microenvironment in CFSE+ cells homing 76
Figure 3.6 Cell adhesion molecule oscillations after inflammation 77

Figure 3.7 Chemokine oscillations over 24h in an inflammatory scenario 78
Figure 3.8 ICAM-1 and VCAM-1 protein oscillations over 24h during inflammation 79
Figure 3.9 Leukocyte recruitment to large vessels in *Icam1*$^{-/-}$ mice 80
Figure 3.10 Importance of ICAM-1 and VCAM-1 in oscillatory recruitment in large vessels 81
Figure 3.11 Functional role of chemokines in oscillatory leukocyte recruitment in large vessels 82
Figure 3.12 PER2 daily oscillations in arteries and veins 83
Figure 3.13 Circadian clock genes oscillations in arteries and veins in steady state conditions 84
Figure 3.14 Circadian clock gene oscillations in arteries and veins in inflammatory conditions 85
Figure 3.15 *Tnfr1* and *Tnfr2* oscillations in large vessels 86
Figure 3.16 Leukocyte recruitment in animals with no sympathetic input 87
Figure 3.17 Leukocyte recruitment in animals after surgical denervation 88
Figure 3.18 Cell adhesion molecule expression after surgical denervation 89
Figure 3.19 Leukocyte recruitment in animals after acute β2 adrenergic receptor blockade 90
Figure 3.20 *Icam1* expression after acute β2 adrenergic receptor blockade 91
Figure 3.21 Leukocyte recruitment in mice after chronic β2 adrenergic receptor blockade 92
Figure 3.22 *Icam1* expression after chronic β2 adrenergic receptor blockade 92
Figure 3.23 Leukocyte recruitment in *Adrb2*$^{-/-}$ mice in inflammation 93
Figure 3.24 *Icam1* expression in *Adrb2*$^{-/-}$ mice 94
Figure 3.25 Sympathetic innervation in large vessels 95
Figure 3.26 Sympathetic innervation in microvasculature 96
Figure 3.27 Tyrosine hydroxylase levels in large vessels 96
Figure 3.28 NG2 expression in large vessels 97
Figure 3.29 NG2 expression in microvasculature 97
Figure 3.30 Leukocyte recruitment in *Ng2Cre+ Bmal1*$^{flox/flox}$ mice in inflammation 98

Figure 3.31 *Icam1* expression in *Ng2Cre+ Bmal1*$^{flox/flox}$ mice 99
Figure 3.32 L-selectin levels in adherent cells from arterioles and venules..... 100
Figure 3.33 Platelet-neutrophil interactions in arterioles and venules 101
Figure 3.34 Circadian thrombosis in venules and arterioles..... 102
Figure 3.35 Circadian thrombosis in venules and arterioles from *Ng2Cre+ Bmal1*$^{flox/flox}$ mice 103

List of tables

Table 2.1 PCR reaction mix for genotyping. 49
Table 2.2 PCR primers used for genotyping.....49
Table 2.3 Primer sequences used for quantitative real time PCR 67
Table 2.4 Antibody list 69
Table 2.5 Reagents list.....70

Abbreviations

6-OHDA	6-hydroxydopamine
ACTH	Adrenocorticotropic hormone
ANOVA	Analysis of variance
ANS	Autonomic Nervous System
APC	Allophycocyanin
AR	Adrenergic Receptors
ARNTL	Aryl hydrocarbon receptor nuclear translocator-like protein
BMAL1	Brain and muscle Arnt-like protein 1
cAMP	Cyclic adenosine monophosphate
CAR	CXCL12-abundant reticular
CCL	C-C chemokine ligand
CCR	C-C chemokine receptor
CD	Cluster of differentiation
cDNA	Complementary deoxyribonucleic acid
CFSE	Carboxyfluorescein succinimidyl ester
CLOCK	Circadian locomotor output cycles kaput
CNS	Central Nervous System
CRY	Cryptochrome
CT	Circadian time
CXCL	C-X-C chemokine ligand
CXCR	C-X-C chemokine receptor
DC	Dendritic cell
DMSO	Dimethyl sulfoxide
DNA	Deoxyribonucleic acid
DNase	Deoxyribonuclease
DβH	Dopamine beta (β)-hydroxylase
EC	Endothelial cell
EDTA	Ethylenediaminetetraacetic acid

ESAM	Endothelial cell-selective adhesion molecule
ESL-1	E-selectin ligand-1
FACS	Fluorescence activated cell sorting
FEV	Forced expiratory volume
FITC	Fluorescein-5-isothiocyanate
FLS	Fibroblast-like synoviocytes
GAPDH	Glyceraldehyde-3-phosphate dehydrogenase
GFP	Green fluorescent protein
GR	Glucocorticoid receptor
HEV	High endothelial venule
HSC	Hematopoietic stem cell
HSPC	Hematopoietic stem and progenitor cell
i.p.	Intraperitoneal
i.v.	Intravenous
ICAM	Intercellular adhesion molecule
IFN-ɣ	Interferon ɣ
IL	Interleukin
ILC	Innate lymphoid cell
JAM	Junctional adhesion molecule
KO	Knock-out
LFA-1	Lymphocyte function-associated antigen 1
LPS	Lipopolysaccharide
LXR	Liver X receptor
Ly6C	Lymphocyte antigen 6 complex, locus C
Mac-1	Macrophage antigen 1
MadCAM-1	Mucosal vascular addressing cell-adhesion molecule 1
MFI	Mean fluorescence intensity
MFIM	Multichannel fluorescence intravital microscopy
NE	Norepinephrine
NF	Neurofilament
NFκB	Nuclear factor kappa B

NK	Natural killer cell
NKT	Natural killer T cell
OCT	Optimal cutting temperature
OVA	Ovalbumin
PBS	Phosphate-buffered saline
PCR	Polymerase chain reaction
PE	Phycoerythrin
PECAM-1	Platelet/endothelial-cell adhesion molecule 1
PER	Period circadian protein
PI3K	Phosphoinositide 3-kinase
PNS	Parasympathetic Nervous System
PSGL-1	P-selectin glycoprotein ligand 1
qPCR	Quantitative polymerase chain reaction
RA	Rheumatoid arthritis
RNA	Ribonucleic acid
RNase	Ribonuclease
SCG	Superior cervical ganglion
SCN	Suprachiasmatic nuclei
SEM	Standard error of the mean
SMA	Smooth muscle actin
SMC	Smooth muscle cell
SNS	Sympathetic Nervous System
TAE	Tris-acetate-ethylenediaminetetraacetic acid
TCR	T cell receptor
TE	Tris-EDTA
Th	T helper cell
TH	Tyrosine hydroxylase
TLR	Toll-like receptor
TNF-α	Tumor necrosis factor-α
VCAM	Vascular cell-adhesion molecule
VLA4	Very late antigen 4 (also known as α4β1-integrin)

VPAC2	Vasoactive intestinal peptide receptor 2
WT	Wild type
ZT	Zeitgeber time
βAR	β-adrenergic receptor

1 Introduction

1.1 Cardiovascular system

1.1.1 General overview

The heart, blood and the vasculature (arteries, veins and capillaries) are the principal components of the cardiovascular system. Its most important function is to transport oxygenated blood, with nutrients, immune and other functional cells to the body's periphery and collect the poorly oxygenated blood and waste products. Through the pulmonary artery, blood is pumped from the right ventricle of the heart to the lungs, where it is oxygenated. Simultaneously, oxygenated blood from the lungs is pumped to the periphery of the body from the left ventricle of the heart through the aorta. Arteries are therefore the blood vessels that transport blood away from the heart, while veins transport blood back to the heart as we can see in the **Figure 1.1** where these processes are illustrated. Capillaries carry blood within tissues and are the exchange sites of nutrients, gases, and other products (Lilly, 2010).

The aorta is the main artery in the body and developmentally gives rise to the rest of the arteries, with the exception of pulmonary arteries. It branches to form large arteries and from these, smaller arteries are embedded in tissues. These finally branch into the small-diameter arterioles, the resistance vessels that are critical mediators of blood pressure. On the venous side, the narrowest vessels are venules. These vessels merge to form veins, which finally converge to create the two largest veins of the body: the venae cavae (superior and inferior). Capillaries are the smallest vessels of the body and form the connection between arterioles and venules. A simplified scheme of the artery-vein network is shown in **Figure 1.2**.

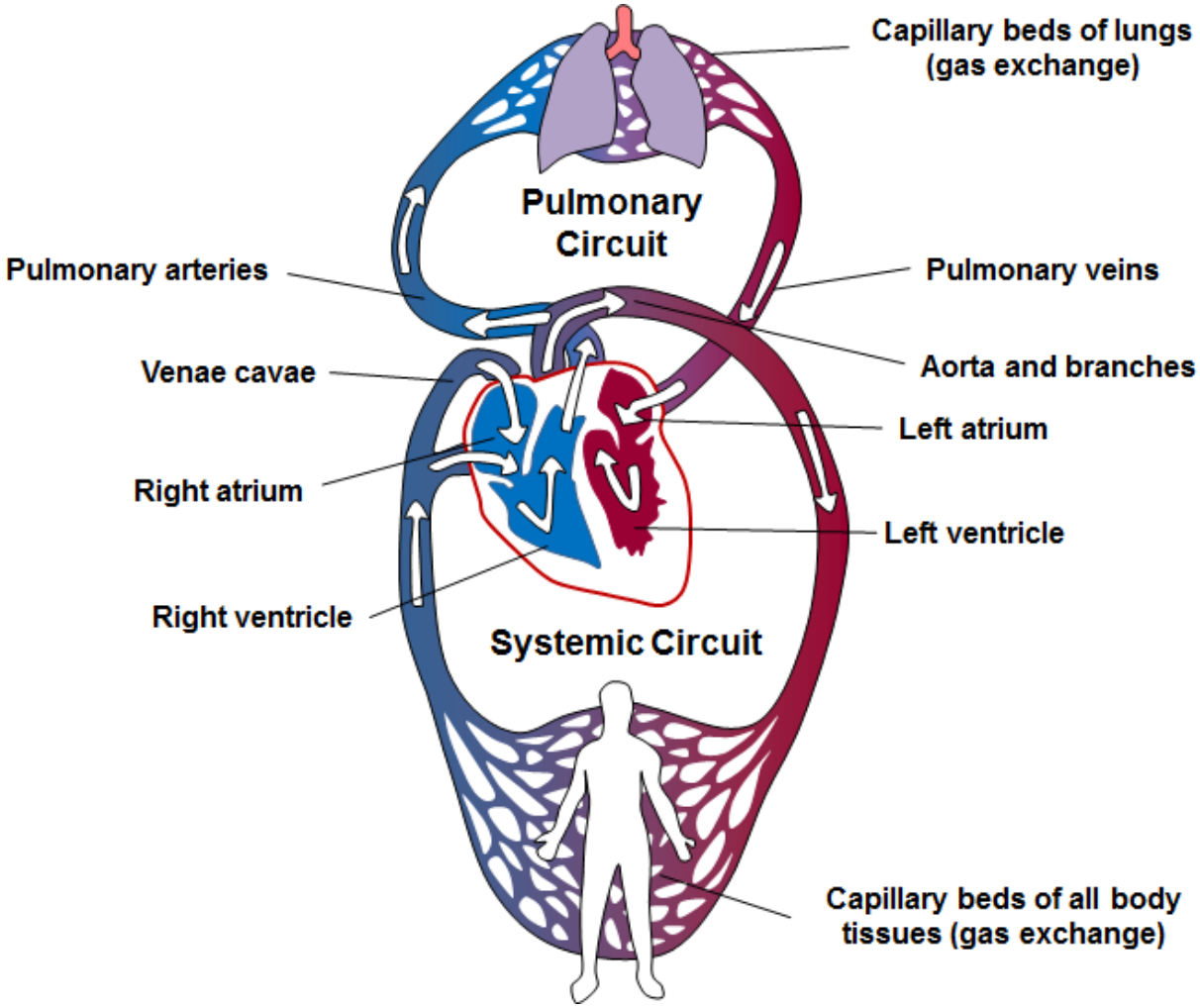

Figure 1.1 Cardiovascular System. Oxygenated blood from the lungs is pumped by the heart to the rest of the body through the aorta, which branches into smaller arteries, arterioles and finally into capillaries, where the gas exchange occurs. These capillaries merge and form venules and veins, to finally culminate in the superior and inferior vena cava that bring back poorly oxygenated blood to the heart. From here, the pulmonary arteries transport blood to the lungs to be re-oxygenated. Modified from (Pearson Education, 2011).

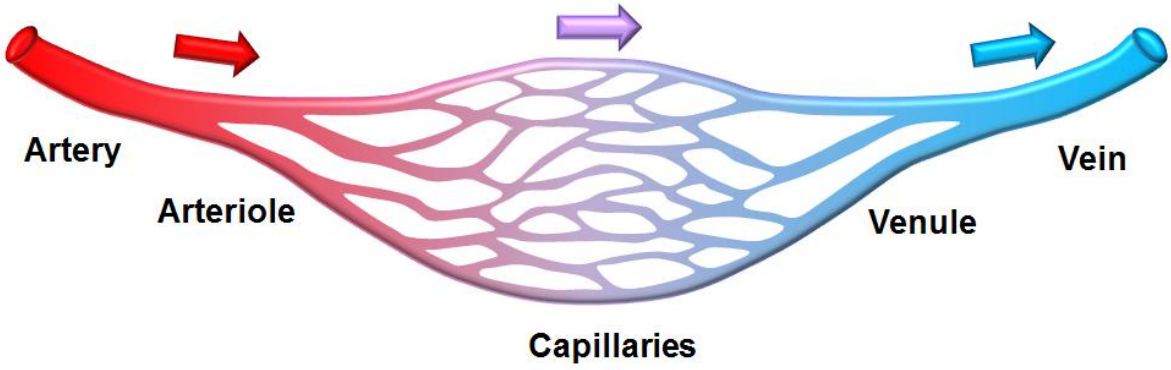

Figure 1.2 Artery-vein network. Arteries branch into smaller arteries and arterioles. On the contrary, venules merge into larger veins and then into the vena cava. Capillaries are the smallest vessels in the body and form the connection between arterioles and venules. Adapted from (Rogers, 2017).

With the exception of capillaries, all blood vessels share the same basic structure consisting of three layers: outer layer or *tunica externa*, middle layer or *tunica media* and inner layer or *tunica intima* (Fawcett, 1994). However, there are some remarkable differences between arteries and veins, as discussed below.

1.1.2 Vessels: differences between arteries and veins (structure and function)

In terms of structure, arteries and veins show several differences (**Figure 1.3**):

- Size: Arteries are smaller in diameter than veins but their walls are much thicker (dela Paz and D'Amore, 2009).
- *Tunica externa* (adventitia): This layer is composed of connective tissue, collagen and elastic fibers. In the case of large vessels, they even have their own blood supply (*vasa vasorum*). Smooth muscle cells (SMCs) are

orientated in a longitudinal fashion. While in veins the *adventitia* is the major part of the vessel wall, in arteries or arterioles it represents only half of the total thickness (dela Paz and D'Amore, 2009).

- *Tunica media*: Formed by circumferentially orientated SMCs that provide muscular support, in addition to some elastic fibers. In arteries, this layer is thicker and there is an additional external elastic lamina, which is not clearly defined in veins. As a consequence, walls in veins are thinner and less rigid. These conditions allow arteries to work at higher pressures than veins. On the other hand, due to their capacity to expand, veins hold a much larger proportion of the blood than arteries (dela Paz and D'Amore, 2009).
- *Tunica intima*: This layer is formed by the endothelium and a supportive matrix of connective tissue (collagen and elastic fibers). In the case of arteries, there is an additional internal elastic layer present between the intima and the media, which is absent in veins. In addition, the presence of valves that avoid the backflow of blood is an exclusive characteristic of large veins (dela Paz and D'Amore, 2009).
- Endothelial cells (ECs): These cells show different size and shape depending on the vascular bed they belong to. Arteriolar ECs are elongated and narrow compared to venous ECs, which are short and wide (Florey, 1966). In addition, the arteriolar ECs are thicker than venous ones with the exception of ECs from high endothelial venules (HEVs), situated within lymph nodes (Girard et al., 2012). Another difference is the shear stress they are exposed to, being higher in the case of the arteries and arterioles than in veins and venules.
- Intercellular junctions: Three different types can be defined, described as tight junctions (*zona occludens*), adherens junctions (*zona adherens*) and gap junctions (cell-cell communications) (Bazzoni and Dejana, 2004). These three structures are much tighter and are more highly organized in arteries than in veins.
- Lumen: Arteries have a much narrower lumen, which contributes to the maintenance of higher blood pressures in these vessels.

- Sympathetic innervation of vessels: Sympathetic innervation is present in all blood vessels except capillaries and post-capillary venules (Krams, 2017). In the case of rats, however, the peripheral nervous system follows a similar structure as the arteries, branching together. From these main nerve trunks, small branches emerge and connect with the network of varicosed adrenergic fibers, which surround the main artery. Contrary to the arteries, veins are lacking adrenergic innervation (Marshall, 1982).

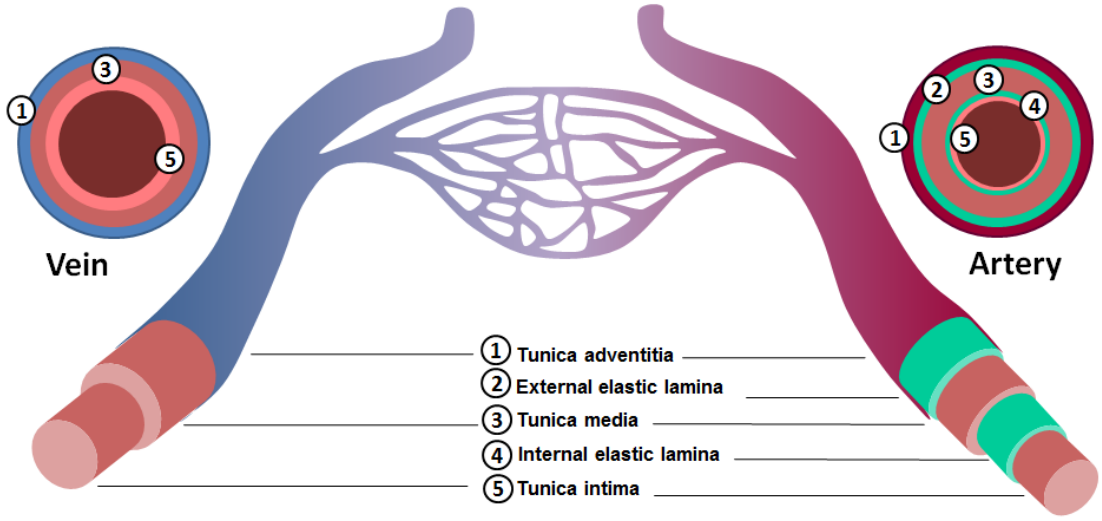

Figure 1.3 Structural features of the vasculature. With the capillaries as an exception, all blood vessels are composed of three layers: *tunica intima* (composed of endothelial cells), *tunica media* (SMCs and elastic fibers) and *tunica adventitia*, which contains elastic fibers, collagen and connective tissue. Whereas arteries and arterioles exhibit an internal and an external laminal layer, veins and venules are devoid of this structure. Modified from (dela Paz and D'Amore, 2009).

Additional differences between arteries and veins exist at the functional level:

- Blood direction: As previously described, arteries carry blood away from the heart while veins carry blood towards it.
- Blood oxygenation: Contrary to veins and with the exception of the pulmonary artery, arteries carry oxygenated blood from the heart towards the body.
- Function of the endothelium: Arteries and arterioles are able to modify their vascular tone through vasodilation and vasoconstriction (relaxation or constriction of the SMCs in the tunica media), changing their vascular resistance and blood pressure. On the other hand, veins, mainly post-capillary venules, are able to change their permeability during inflammation in response to agonists such as histamine and serotonin (Majno and Palade, 1961). Another factor that increases the permeability in veins is the lack of well-structured tight junctions.
- Leukocyte trafficking: Rolling, firm adhesion and transmigration are the main steps of the leukocyte adhesion cascade. This event is almost exclusive to post-capillary venules due to its lower flow rate, thinner walls, fewer tight junctions and higher expression of cell adhesion molecules. However, depending on the organ, leukocyte recruitment can also occur in capillaries, as is the case in the lung (Looney and Bhattacharya, 2014). The adhesion cascade will be discussed in the next part of this Introduction.

Apart from the structural and functional differences associated with blood flow, blood pressure or blood oxygenation, there is a diverse gene expression profile between arteries and veins. There is a molecular discrepancy between arterial and venous ECs, which appears to be intrinsic and not related to the environmental conditions. This suggests an early diversion in the development of both vascular beds, an event that has been linked to Notch signaling pathways and involving the Hey2 transcription factor (Chi et al., 2003).

1.1.3 The leukocyte adhesion cascade

Inflammation is a crucial process that occurs in the body in response to different stimuli such as infections or after injuries. Leukocyte recruitment to tissues is a critical event that takes place during the inflammatory response. Leukocytes become activated and extravasate from blood to tissues in a sequence of distinct steps known as the leukocyte adhesion cascade. Many studies have investigated this process, which can be summarized in the sequence of the following steps: the capture and rolling of leukocytes, their slow rolling, firm adhesion, crawling and transmigration (paracellular or transcellular) as shown in **Figure 1.4**.

- Capture/Rolling: This is the initial step in the cascade and occurs after endothelial cell activation, but in some vascular beds, such as the skin, this also takes place in steady-state conditions. Endothelial cells express E- and P- selectin. These proteins bind to their ligand on the leukocyte, P-selectin glycoprotein ligand-1 (PSGL-1), which was initially thought to interact uniquely with P-selectin. Apart from PSGL-1, E-selectin binds to CD44 and E-selectin ligand-1 (ESL-1) in neutrophils (Hidalgo et al., 2007).
- Slow rolling: This step requires the expression of E-selectin on endothelial cells (Jung and Ley, 1999) and CD18/β_2 integrins on the rolling leukocytes (Jung et al., 1998) and has been termed "slow rolling" to differentiate it from the much faster rolling that occurs without cytokine stimulation. There are different kinds of β_2 integrins, but the most relevant in this step are the lymphocyte function-associated antigen 1 (LFA-1) and the macrophage receptor 1 (Mac-1), whose ligand are ICAM-1, ICAM-2 and ICAM-3. Studies have described a change in the conformation of LFA-1 and therefore a higher ligand-binding affinity of the integrin under shear stress, suggesting the importance of LFA-1 in this step (Astrof et al., 2006). However, although this step of the cascade facilitates recruitment, it is not required, as high concentrations of chemoattractants are also able to arrest fast-rolling cells (Scharffetter-Kochanek et al., 1998).

- Firm adhesion: Due to the rolling step, leukocytes come in close contact with the endothelium and thus are able to interact with endothelial cell surface-bound chemokines, which are strongly induced by inflammatory mediators. As a consequence of the binding of chemokines to their receptors on leukocytes, an inside-out signaling cascade activates leukocyte integrins (Charo and Ransohoff, 2006). Studies in humans (Anderson and Springer, 1987) and mice (Wilson et al., 1993) suggest the importance of LFA-1 and Mac-1 in this process, since deficiencies in these β_2-integrins lead to impaired leukocyte recruitment and an associated increase in bacterial infections. However, *in vivo* studies showed that LFA-1 is the most important β_2 integrin in firm adhesion, while Mac-1 seems to be more relevant in neutrophil activation and phagocytosis (Lu et al., 1997). LFA-1 and Mac-1 bind to endothelial ICAM-1 and ICAM-2 (Hogg et al., 2002), which are constitutively expressed. ICAM-1 expression can additionally be strongly enhanced after endothelial cell activation (Dustin et al., 2011). In contrast, endothelial cell vascular cell-adhesion molecule 1 (VCAM-1) is recognized by β_1 integrins very late antigen 4 (VLA-4), particularly expressed by lymphocytes and monocytes (Elices et al., 1990).
- Transmigration: This is the final step in the leukocyte adhesion cascade and the one that is the least understood. In the case of lymphocytes, leukocyte transmigration has been shown *in vitro* to be initiated by dynamic interactions between adherent leukocytes and endothelial cells forming ‘docking structures’ consisting of VCAM-1 and ICAM-1 (Barreiro et al., 2002). Two different types of transmigration routes have been described: paracellular, if the leukocyte is migrating from blood to tissues between two endothelial cells, and transcellular, if the migration occurs through the body of endothelial cells.

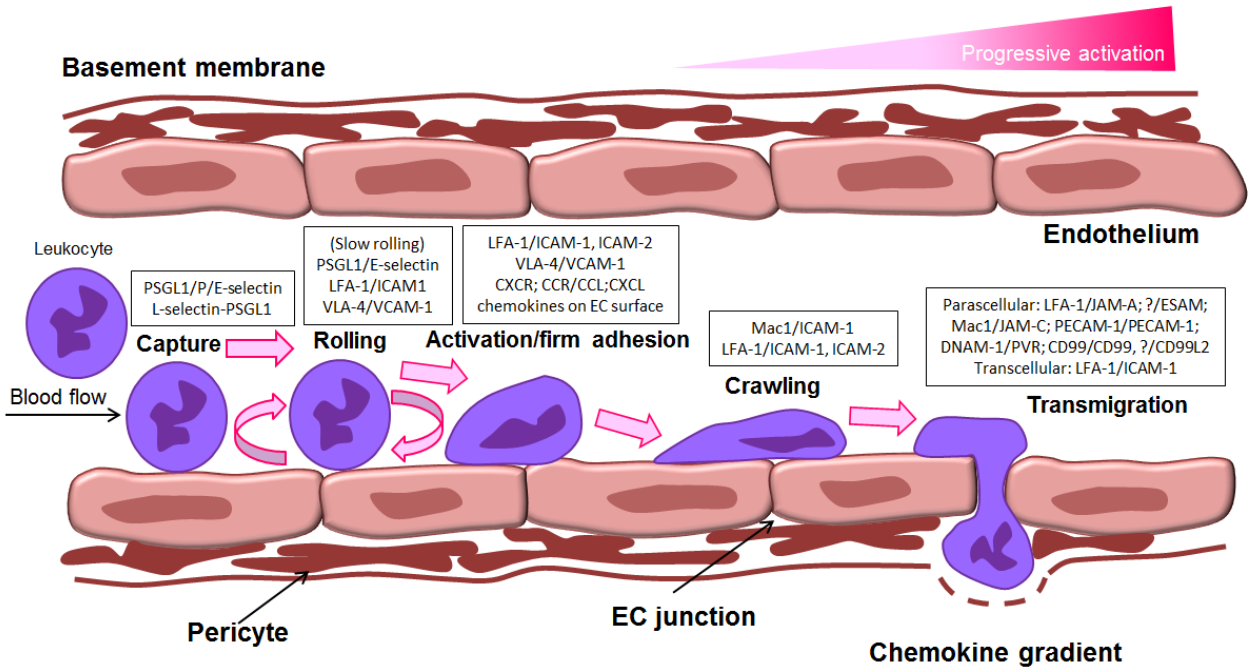

Figure 1.4 General scheme of the leukocyte adhesion cascade. Leukocytes are captured and start to roll along the endothelium due to the expression of selectins. Chemokines play an important role in firm adhesion and activation, whereas in the crawling step, integrins are the key molecules. Leukocytes transmigrate through the endothelium following a chemokine gradient. Crucial molecules involved in each stage are specified in boxes. ESAM, endothelial cell-selective adhesion molecule; ICAM, intercellular adhesion molecule; JAM, junctional adhesion molecule; LFA-1, lymphocyte function-associated antigen 1 (also known as $\alpha_L\beta_2$-integrin); Mac-1, macrophage antigen 1; MadCAM-1, mucosal vascular addressin cell-adhesion molecule 1; PSGL-1, P-selectin glycoprotein ligand 1; PECAM-1, platelet/endothelial-cell adhesion molecule 1; PI3K, phosphoinositide 3-kinase; VCAM-1, vascular cell-adhesion molecule 1; VLA-4, very late antigen 4 (also known as $\alpha_4\beta_1$-integrin). Adapted from Ley et al, (Ley et al., 2007).

Leukocyte recruitment is predominantly a venular process but some studies have reported that under inflammatory conditions barrier function is also altered in arterioles and adhesion molecules are upregulated in order to support leukocyte and platelet interactions. This indicates that arterioles can also contribute to

inflammatory responses in addition to their role in blood flow regulation (Sumagin and Sarelius, 2013). However, this process appears to be mostly restricted to intravascular events.

ICAM-1 is a very important molecule in leukocyte-endothelial interactions and, as for other adhesion molecules, the mechanism of its upregulation in veins is the same as the one in arteries (Nabah et al., 2005) but its distribution is different between the two vessels. While venular endothelium expresses higher ICAM-1 levels in steady-state conditions, contributing to leukocyte adhesion, arteriolar ICAM-1 was found to be present in lower amounts. This could be a potential reason for the lack of leukocyte adhesion in arterioles under normal situations. Another explanation for the reduced frequency of arteriolar adhesion may lie in the fact that the luminal surface area of arteriolar ECs is roughly twice that of venular ECs, so they might simply not reach sufficient surface density levels of ICAM-1 (Sumagin and Sarelius, 2006).

However, Sumagin and colleagues showed that ICAM-1 could support rolling but not adhesion in arterioles, suggesting an important role in the initial phases of the inflammatory cascade. They also hypothesized that in arterioles, both leukocyte rolling and increased levels of ICAM-1, rather than leading to adhesion and transmigration, might have a different functional outcome (Sumagin and Sarelius, 2007). Another study has linked the rolling step in arterioles with P-selectin (Nabah et al., 2005). Together, it seems that the contribution of arterioles to inflammatory responses is restricted to the initial steps of the process.

1.2. Circadian rhythms

1.2.1 General overview

Organisms have acquired biological clocks during evolution as time-keeping mechanism in order to adapt to their rhythmic environment. Depending on frequency, there are different categories of rhythms in mammals: ultradian, which last from seconds to hours, like blood circulation, pulse and hormonal secretions (Tannenbaum and Martin, 1976); circadian, of about 24 hours; and infradian, which exhibit longer periods than 24h, such as menstruation cycles, breeding or seasonal rhythms (Hoppensteadt and Keller, 1976).

Circadian rhythms are endogenous oscillations of about 24h (from the Latin, *circa* = about, *diem* = day) that operate in all light-sensitive organisms (Mauvoisin et al., 2015). They are involved in diverse biological functions such as physiology, behavior and metabolism and can be found at multiple levels, from the whole organism to different tissues and also at the molecular level, as virtually every cell carries an intrinsic molecular clock. There are different external cues, known as *Zeitgebers*, for the organism to synchronize their internal clock to the environment, such as food, temperature or light. For a rhythm to be termed circadian, one important characteristic is that it must oscillate in a constant environment (i.e. devoid of zeitgebers like light-dark cycles, also known as free-running conditions). The other two criteria are that they must be entrainable and exhibit temperature compensation (Golombek and Rosenstein, 2010). In addition, there is a distinction between the terminology zeitgeber time (ZT) and circadian time (CT). ZT is a unit of time based on the period of a zeitgeber, for instance, the light:dark cycle. In a light:dark cycle, for diurnal organisms ZT0 (lights on) is the time of activity onset and ZT12 (lights off) defines activity onset for nocturnal animals. On the other hand, CT refers to a standard unit of time based on the endogenous free-running period of a rhythm. By agreement, in free-running, constant conditions, the

beginning of activity of day-active organisms is circadian time zero (CT0) and the start of activity of night-active organisms is CT12 (Karatsoreos and Silver 2017).

1.2.2 Entrainment and synchronization of the clock

As mentioned above, different external cues (*Zeitgebers*) are able to synchronize the clock. The most important of these cues is light (Aschoff, 1960). Light additionally indirectly affects food intake as it sets the wake-sleep cycle. In the case of mammals, which are opaque individuals, light detection by the eye is essential to transmit the lighting information to the central pacemaker in the brain. Light is processed through the retina and this signal is transduced via the retinohypothalamic tract to the central (or master) clock of the organism, located in the suprachiasmatic nuclei (SCN) of the hypothalamus (Golombek and Rosenstein, 2010). The SCN are composed of about 20.000 neurons, which together are considered the pacemaker of the organism (Ralph et al., 1990). From here, signals can be relayed to the rest of the body via different routes: humoral or neural. On the one hand, adrenocorticotropic hormone (ACTH), released by the pituitary gland, targets the adrenal glands, leading to a circadian release of glucocorticoids and catecholamines (noradrenaline and adrenaline). On the other hand, the sympathetic nervous system (SNS) directly innervates peripheral organs and tissues and may orchestrate their clocks via local noradrenaline secretion from nerve varicosities (Dickmeis, 2009) (**Figure 1.5**).

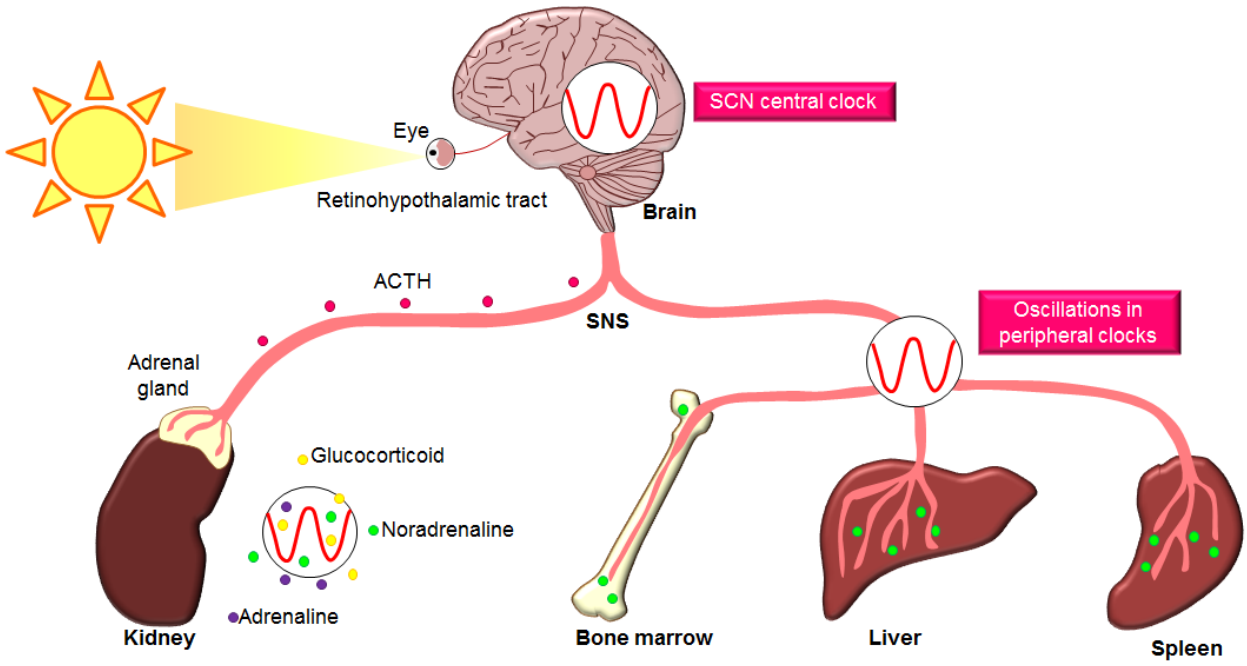

Figure 1.5 Entrainment and synchronization of the clock. Light is the most important external cue used to synchronize the organism with its rhythmic environment. It is sensed through the eye, which signals via the retinohypothalamic tract to the suprachiasmatic nuclei (SCN), where the central clock is located. From here, there are two ways of transmitting the signal, hormonal or via direct innervation of the SNS. Adrenocorticotropic hormone (ACTH) is released from the pituitary gland and targets the adrenal gland, which secretes other hormones such as glucocorticoids, adrenaline and noradrenaline in a circadian manner. The SNS innervates directly organs such as the bone marrow, liver and spleen and through its varicosities can secrete noradrenaline. Modified from Scheiermann et al., 2013.

1.2.3 The molecular clock

At the molecular level, the clock is a highly complex machinery consisting of multiple transcription factors that together produce auto-regulatory transcription-translation feedback loops, where photic input plays a role in synchronizing the transcription of the clock genes.

The core clock genes are *Clock* (circadian locomotor output cycles kaput) and *Bmal1* (brain and muscle Arnt-like protein 1, encoded by *Arntl*), which encode for the proteins CLOCK and BMAL1. These proteins dimerize in the cytoplasm and this heterodimer is then translocated to the nucleus where it binds to canonical enhancer-boxes (E-box) of the negative regulators of the clock (*Per1/2, Cry1/2, Nr1d1/2*). In addition, the heterodimer BMAL1-CLOCK controls the transcription of clock-controlled genes such as *Dbp*, which binds D-boxes and thus can influence additional downstream genes (Bunger et al., 2000). Period circadian protein (PER) and cryptochrome (CRY) form a heterodimer to repress their own expression, forming the negative branch of the auto-regulatory feedback loop (Shearman et al., 2000). A second loop includes the circadian regulation of *Bmal1* transcription by the transcription factors REV-ERBα/β (encoded by *Nr1d1* and *Nr1d2*) (Preitner et al., 2002) and ROR (Alvarez et al., 2003), where BMAL1 transcription is indirectly inhibited (**Figure 1.6**).

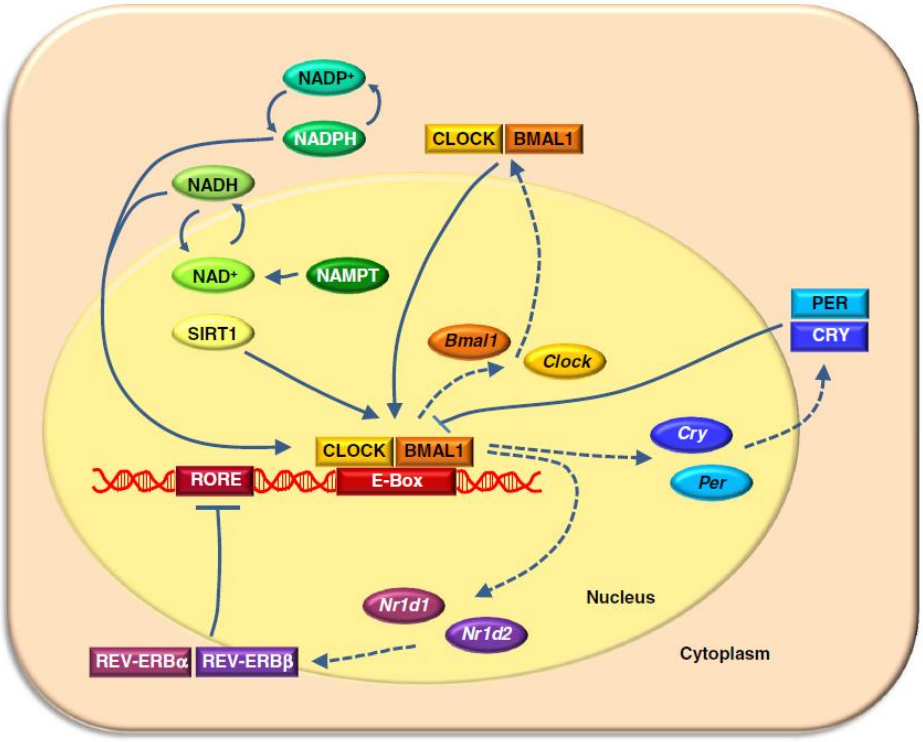

Figure 1.6 The molecular clock. Core clock genes *Bmal1* (brain and muscle aryl hydrocarbon receptor nuclear translocator (ARNT)-like 1) and *Clock* (circadian locomotor output cycles kaput) are transcribed to BMAL1 and CLOCK transcription factors, which form a heterodimer that binds E-box sequences of clock-controlled genes. This system is auto-regulated through negative feedback loops, as BMAL1 and CLOCK inhibit the transcriptional activity of CLOCK and BMAL1 (Druzd et al., 2014).

1.2.4 Clock genes links to immunology

From an immunological perspective, there are a number of examples that link the clock with the immune system. Deficiencies in clock genes can lead to anti- or pro-inflammatory properties as shown in diverse immune phenotypes of clock gene knock-out mice.

‘Anti-inflammatory’ clock genes:

- *Bmal1:* The absence of this core clock gene results in a complete loss of circadian rhythmicity in constant darkness and also under light-dark conditions (Bunger et al., 2000). In another publication, it was shown the lack of oscillations in either CXCR4 or CXCL12 in bone marrow (Lucas et al., 2008) (Mendez-Ferrer et al., 2008). In addition, reduced numbers of B cells in peripheral blood, spleen and bone marrow (Sun et al., 2006). When lack of *Bmal1* was restricted to myeloid cells, using *LysM-Cre x Bmal1*$^{flox/flox}$ mice, the time-dependent response to lipopolysacchadire (LPS) IL-6 expression was not rhythmic and high (Gibbs et al., 2012). This was accompanied by an increase of inflammatory cytokines and chemokines (IL-1β, IL-6, INF-γ and CCL2). In the case of the study conducted by Nguyen and colleagues, a higher number of Ly6^{hi} monocytes was noticed when targeting specifically myeloid cells (Nguyen et al., 2013).

- *Cry:* Increased levels of the pro-inflammatory cytokines IL-6, TNF-α as well as iNOS, enhanced NFκB activation and a stronger response to LPS have been reported in the double knock out mice for both CRY proteins (*Cry1*$^{-/-}$ *Cry2*$^{-/-}$ mice) (Narasimamurthy et al., 2012). In the single Cry1 KO mice (*Cry1*$^{-/-}$ mice), increased joint swelling in an arthritis model was observed (Hashiramoto et al., 2010). Another evidence of the anti-inflammatory role of Cry was described in an article related to rheumatoid arthritis (RA), where they used fibroblast-like synoviocytes (FLS) cells, crucial effector cells in this disease. FLS cells from the double KO mice showed a significantly enhanced inflammatory response, at both the gene (*Il6, Cxcl5,* and *Il1β*) and protein (CXCL1, IL6, and CXCL5) level after TNFα stimulation (Hand et al. 2016).

- *Rora:* A defect in T and B cell development has been shown in *Rora*$^{-/-}$ mice and, in response to LPS stimulation, mast cells showed a stronger IL-6 and TNF-α production (Dzhagalov et al., 2004).

- *RevErbα: Nr1d1*$^{-/-}$ mice showed a loss of circadian IL-6 expression in response to LPS stimulation (Gibbs et al., 2012). However, Th17 cell differentiation was shown

to be promoted in these mice, which would have an anti-inflammatory effect, suggesting a role for this gene in pro-inflammatory responses as well (Yu et al., 2013).

‘Pro-inflammatory’ clock genes:

- *Clock: Clock*$^{-/-}$ mice showed reduced nuclear accumulation of p65 associated with reduced NF-κB activation (Spengler et al., 2012). In addition, Bellet and colleagues reported a lower response to LPS in mouse embryonic fibroblasts (Bellet et al., 2012) and bone marrow derived macrophages (Bellet et al., 2013) as well as a reduction in the gut colonization of *Salmonella enterica*.

- *Per:* In the case of *Per1*$^{-/-}$ mice, an altered circadian expression of cytokines such as IFN-γ and cytolytic factors in splenic natural killer (NK) cells were described (Logan et al., 2013). In *Per2* mutant mice there was a decreased serum concentration of IFN-γ during the day (Arjona and Sarkar, 2006), as well as reduced production of IL-1β in response to LPS challenge due to a defect in NK and NKT cell function (Liu et al., 2006).

1.2.5 Circadian rhythms and the immune system

As mentioned above, there is a strong link between clock genes and inflammation as many mice deficient in clock genes show alterations in immune phenotypes. In addition, different immuno-modulatory parameters such as cytokines, chemokines, chemokine receptors and cell adhesion molecules fluctuate according to the time of the day. This is also the case for the numbers of circulating leukocytes. Oscillations in the immune system will be discussed in the next section.

1.2.5.1 Circadian control of inflammatory mediators

- Cytokines: several cytokines have been reported to oscillate in a rhythmic manner in response to an inflammatory stimulus. For instance, IL-1β peaks at ZT8 and drops at ZT12 in peritoneal fluid (Nguyen et al., 2013), IL-5 has its acrophase at ZT3 and its trough 12h later in serum (Nussbaum et al., 2013), and IL-6 and IL-12 are mostly released at CT12 (Gibbs et al., 2012) in mice. In a study analyzing human serum from healthy individuals, fluctuations in IL-2, IL-10, GM-CSF and TNF-α were reported (Young et al., 1995), suggesting that, even in steady-state conditions, there are oscillations of these pro-inflammatory mediators.
- Chemokines: Gibbs and colleagues have described peaks at CT12, with the same pattern, in the levels of CCL2, CCL5 and CXCL1 in serum from mice injected with LPS (Gibbs et al., 2012). Expression of CXCL12, a chemokine important for HSCs homing to the bone marrow, was shown to be higher during the active phase of mice (Mendez-Ferrer et al., 2008).
- Chemokine receptors: CXCR4, the receptor for CXCL12, has been reported to oscillate - peaking at ZT13 in circulating HSCs (Lucas et al., 2008) and at ZT17 in murine neutrophils (Casanova-Acebes et al., 2013) during homeostasis. Similar observations for CXCR4, but at inverted times, were found in human T cells, as well as for CX_3CR1 in CD8 T cells (Dimitrov et al., 2009).
- Adhesion molecules: L-selectin expression changes over 24h in neutrophils (Casanova-Acebes et al., 2013). ICAM-1 peaks at the onset of the activity phase in muscle endothelial cells, as well as E-Selectin, P-Selectin and VCAM-1 in endothelial cells from bone marrow (Scheiermann et al., 2012).

1.2.5.2 Circadian control of immune cell trafficking

In contrast to circulating erythrocytes and platelets, whose numbers do not oscillate, leukocyte counts follow a 24h pattern in blood. Higher numbers are found

during the behavioral rest phase of the organism which in rodents is during the day and for humans occurs at night (Druzd et al., 2014).

Among cells of the innate immune system, monocytes have been shown to oscillate in murine blood across the day. In a study performed by Nguyen and colleagues, Ly6C^{HI} inflammatory monocytes exhibited diurnal variation, controlling their trafficking to places of inflammation. These oscillations were regulated by the repressive activity of the circadian gene *Bmal1* and this conferred an advantage against *Listeria monocytogenes* infection (Nguyen et al., 2013).

Similar to monocytes, the number of neutrophils in blood is higher during the day than during the night. CD62^{HI} neutrophils represent young cells that have just been released into blood from the bone marrow and, as the day passes, these become CD62^{LO} CXCR4^{HI} (aged neutrophils). Aged neutrophils migrate back to the BM towards the end of the day where they are phagocytosed by macrophages. This leads to the activation of the macrophages and liver-X-receptors (LXR), which reduce the number of niche cells and the quantity of CXCL12, thereby promoting the release of HSCs to the blood circulation (Casanova-Acebes et al., 2013). This suggests neutrophil migration is closely linked to HSC biology.

The number of circulating eosinophils is also rhythmic. Circadian cycling of eosinophils has been shown to be due to oscillatory IL-5 secretion by innate lymphoid cells (ILC2) from peripheral tissues. A circadian intestinal peptide stimulates ILC2 cells through the vasoactive intestinal peptide receptor (VPAC2) receptor and increasing IL-5 release, thus linking eosinophil levels to metabolic cycling (Nussbaum et al., 2013).

Among cells of the adaptive immune system, T lymphocyte numbers in human blood have been shown to depend on circulating cortisol and catecholamines, which are rhythmically secreted. Naïve T cell numbers were lower during the day, and thus negatively correlated with cortisol levels. These cells though showed the highest CXCR4 expression. Actually, a recent publication described the importance of glucocorticoid regulation in diurnal CXCR4 oscillations (Shimba et al. 2018). In

contrast, the number of CD8 T cells was directly correlated with adrenaline rhythms (Dimitrov et al., 2009).

A study conducted by Fortier and colleagues demonstrated that the T cell response to a T cell receptor (TCR) stimulus varies in a circadian manner. These differences were not due to the daily variation in the number of T cell subsets either in the lymph nodes or the expression levels of the TCR. The authors demonstrated instead that a circadian variation exists in the protein levels of the TCR-associated kinase ZAP70. In addition, they showed *in vivo* that the antigen-specific response of T cells is influenced by the timing of immunization (Fortier et al., 2011).

Day-night differences in the response of $CD4^+$ T cells to immunization have also been reported, where mice were immunized with ovalbumin (OVA) in the presence of CpG oligodeoxynucleotides, a ligand for Toll-like receptor 9 (TLR9). This receptor is expressed at high levels during the active phase of the mice (night), which leads to a stronger response of T cells due to an enhanced activation of antigen presenting cells expressing TLR9 (Silver et al., 2012). A summary with different examples of rhythms in immune parameters can be visualized in the **Figure 1.7**, modified from a Review from Druzd and colleagues (Druzd et al., 2014).

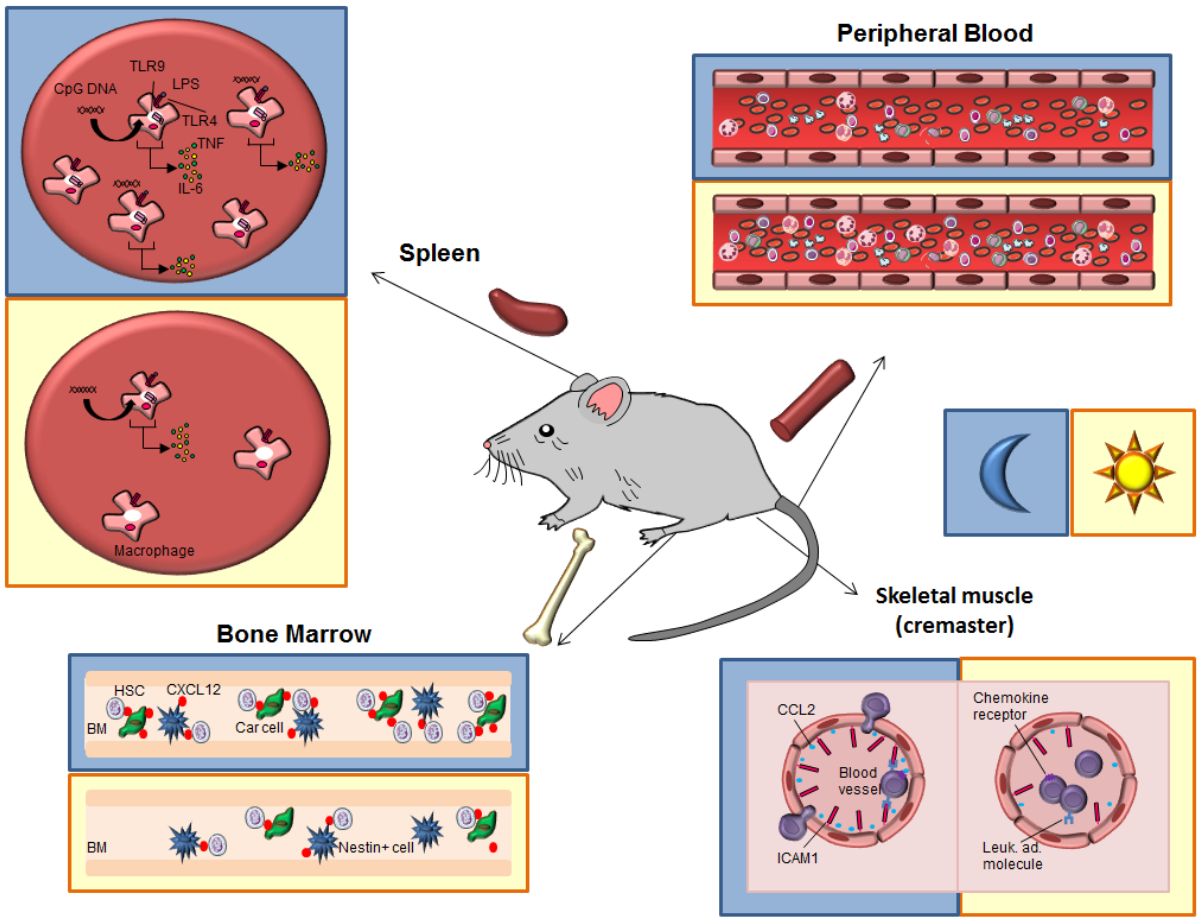

Figure 1.7 Rhythms in immune parameters. There are oscillations in the number of leukocytes and their activation status in different immune tissues according to the phase of activity (active during the night and resting during the day in mice). In the spleen, the number of macrophages is higher at night and those macrophages express more TLR9 receptors, which, in response to stimuli such as bacterial DNA, secrete larger quantities of pro-inflammatory molecules such as TNF-α and IL-6. In blood, all hematopoietic progenitors and leukocyte subsets are more abundant during the day whereas erythrocytes and platelets do not strongly oscillate. In bone marrow, there is higher hematopoietic stem cell (HSC) recruitment due to a higher number of CXCL12-abundant reticular (CAR) and Nestin^{+} cells, which release CXCL12 in a circadian manner. In skeletal muscle (cremaster muscle), there is a higher expression of ICAM-1 and CCL2 during the active phase that leads to an enhanced leukocyte infiltration to this tissue. Modified from (Druzd et al., 2014).

1.2.6 Diseases associated with circadian rhythms

Several diseases show circadian rhythmicity, meaning that their symptoms differ across the day. This is the case for diverse chronic inflammatory diseases, such as rheumatoid arthritis (RA), asthma or allergic reactions. Patients with RA show an increase in joint pain and stiffness between 05:00 and 08:00am, which has been linked to higher serum levels of the pro-inflammatory cytokines IL-6 and TNF-α (Straub and Cutolo, 2007; Cutolo, 2012). In healthy subjects, serum levels of TNF-α and IL-6 have already begun to decrease at 6:00 and 9:00am respectively, whereas in RA patients these levels remain elevated until 10:00 and 11:00am (Straub and Cutolo, 2007). IL-6 has also been linked to a predisposition to thrombosis, as the highest prevalence occurs at the same time, from 6:00 to 9:00am in the morning, coinciding with a higher activation status of functional platelets (Undar et al., 1999). Another reason could be the role of IL-6 as coagulation stimulator (Stouthard et al., 1996).

Similarly, cardiovascular diseases such as myocardial ischemia (Mulcahy et al., 1988; Parker et al., 1994) and infarction (Muller et al., 1985) present a higher risk during the morning. This has been associated with changes in adrenergic activity, systemic arterial pressure, heart rate, vascular tone and coagulability (Tofler et al., 1995). However, leukocytosis is also associated with thrombotic events and some studies have linked the importance of leukocyte recruitment to vaso-occlusive crises in a mouse model of sickle cell disease (Hidalgo et al., 2009; Scheiermann et al., 2012).

In addition, later work shows that there are more infarcts in the morning and that the infarct sizes were found to be larger at that particular time of the day, suggesting a contributing role for a circadian leukocyte infiltration in these events (Suarez-Barrientos et al., 2011). Another observation that supports this hypothesis is that the number of leukocytes in blood correlates with an increased morbidity and mortality of ischemic vascular disease (Coller, 2005). In fact, in a recent publication by Schloss and colleagues, the authors described how CCR2 surface

expression on Ly6C^{HI} monocytes fluctuates in a rhythmic manner, significantly influencing cardiac monocyte recruitment after an acute ischemic event (Schloss et al., 2017).

In contrast, nocturnal asthma reaches its climax at night, at around 04:00am, when symptoms such as cough, dyspnea, airflow limitation, airway hyper-responsiveness and sudden death are exacerbated. Although lung function fluctuates over the 24h period in healthy individuals, these fluctuations are greatly exaggerated in patients with nocturnal asthma, with differences in forced expiratory volume (FEV) and expiratory flow rate between wakefulness and sleep. In addition, alveolar tissue from patients with nocturnal asthma showed a greater number of eosinophils and macrophages at 04:00am as reviewed in this publication by (Litinski et al., 2009).

Taking into consideration the specific occurrences of these events would be useful in the field of chronopharmacology, the time-of-day-dependent administration of drugs, in order to improve the existing therapies of inflammatory diseases or incorporate the possibility of time-dependent treatments.

1.2.7 Shift workers and health complications

Over the last few decades, the importance of the maintenance of circadian rhythms in health has been elucidated. Alterations in these rhythms can lead to a malfunction of the immune system. This has been suggested to be an important reason why shift workers are more prone to develop certain diseases such as cancer or cardiovascular problems.

Risk of multiple types of cancer has been reported to be increased due to shift work. For instance, colorectal cancer is more prevalent in nurses (Schernhammer et al., 2003) and shift workers (Mormont et al., 2000). Similar associations were observed with respect to breast cancer in premenopausal nurses (Schernhammer

et al., 2006) and women who worked at night (Hansen, 2001), as well as prostate cancer in working men in Japan (Kubo et al., 2006).

Regarding cardiovascular complications, coronary heart disease also shows a higher prevalence in shift workers, in combination with other adverse lifestyle factors (Tenkanen et al., 1998). Atherosclerosis and myocardial infarction can also be exacerbated by shift work (Haupt et al., 2008).

Taken together, these studies provide evidence for a negative effect of shift work upon health, due to a dysregulation in the alignment of workers' internal clocks.

1.3 Sympathetic Nervous System

1.3.1 General overview

The sympathetic nervous system (SNS), together with the parasympathetic nervous system (PNS), is part of the autonomic nervous system (ANS), responsible for the involuntary actions of the body such as control of heart rate, intestinal/glandular activity and smooth muscle relaxation/contraction. The SNS and PNS act in a complementary manner: while the PNS is in charge of the "rest-and-digest" or "feed-and-breed" response, the SNS activates the "fight and flight" response.

The SNS originates in thoracic and lumbar regions of the spinal cord and, among other activities, controls the body's response during a perceived threat. Its neuronal pathways are very fast, composed of two different sets of neurons: those that have their cell bodies within the spinal cord, called pre-synaptic, and those whose soma resides in ganglia outside the central nervous system (CNS), called post-synaptic. Pre-synaptic neurons release acetylcholine that targets post-synaptic neurons.

Through an electrochemical impulse along the axons of the latter, there is a secretion of noradrenaline at nerve varicosities close to the peripheral target. One of the targets of pre-synaptic neurons is the adrenal gland, responsible for the release of adrenaline, noradrenaline and glucocorticoids into the bloodstream.

1.3.2 Role of the SNS in the vasculature

SNS innervation is much more predominant around arteries than veins as shown in **Figure 1.8**. In fact, sympathetic neurons and arteries are associated during embryonic development, when these neurons differentiate into ganglia alongside the main embryonic artery, the dorsal aorta (Eichmann and Brunet, 2014).

The SNS is involved in the vasoconstriction of arteries and arterioles through the release of noradrenaline at the varicosities that are in close contact with smooth muscle cells (SMCs) of arteries that lie along the axon. The activation mechanism consists of the stimulation of adrenergic receptors expressed by the SMCs (Westcott and Segal, 2013). A defective arterial innervation and vasoconstriction response is associated with cardiovascular disease. Increased SNS activity is responsible for heart complications such as infarction, transient ischemia or stroke. These diseases follow a circadian rhythmicity, having the highest number of events in the morning, which may also be due to the fact that the SNS has a higher activity at this time of the day in humans (Malpas, 2010).

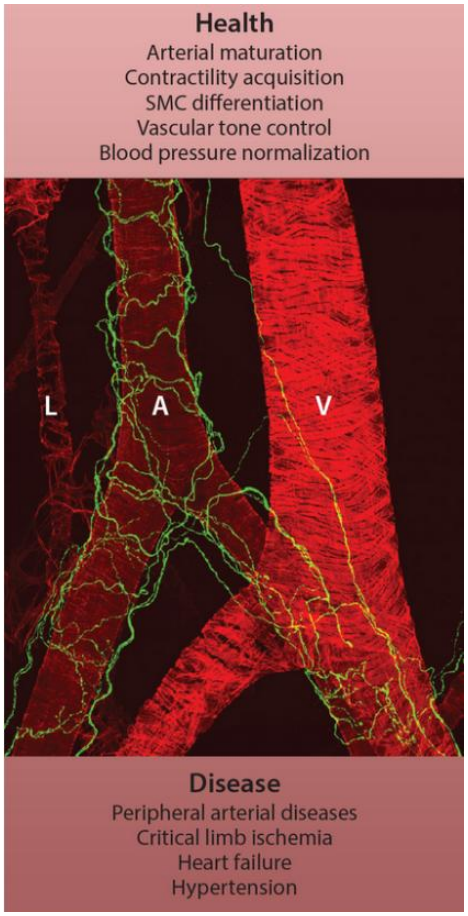

Figure 1.8 Innervation status of the vasculature by SNS. Adrenergic input seems to have different roles in physiology and pathophysiology; however, the function of sympathetic nerve activity in vascular pathophysiology is still not completely understood. Tyrosine hydroxylase (TH) immunostaining (green) of a mouse artery (A) labeled with anti–smooth muscle antibody (SMA) (red). L, lymphatic vessel; V, vein (Eichmann and Brunet, 2014).

Apart from the role in arteriolar vasoconstriction, sympathetic nerves may be involved in post-ischemic revascularization processes though three different mechanisms: first, the release of catecholamines, particularly noradrenaline. In animals which lack catecholamines (dopamine-beta-hydroxylase (*Dbh*)$^{-/-}$ mice, deficient in dopamine beta-hydroxylase, the enzyme mediating the conversion from dopamine to noradrenaline), post-ischemic revascularization was reduced

(Chalothorn et al., 2005), as well as revascularization after the resection of the femoral artery in *Adrb2*$^{-/-}$ mice (Ciccarelli et al., 2011). Second, the SNS has been described to be a crucial modulator in hematopoietic stem and progenitors cell (HSPC) mobilization from bone marrow via the regulation of CXCL12 (Mendez-Ferrer et al., 2008). HSPC mobilization and homing to ischemic tissues seems to be crucial in arteriogenesis (Segers and Lee 2008), highlighting the importance of the SNS in this process. Third, regulation of inflammation by the SNS suggests that sympathetic nerves can influence the growth of large arteries through the communication with immune cells (Silvestre, 2008). *Dbh*$^{-/-}$ mice show a decrease in the number of leukocytes accumulated in the wall of bypass collateral arteries and reduced revascularization, suggesting the link between sympathetic nerve–derived adrenergic activation and arterial growth via effects on immune cells (Chalothorn et al., 2005)

1.3.3 Adrenergic receptors

The adrenergic receptors (AR) are a class of G-protein-coupled receptors that are targeted by the catecholamines noradrenaline and adrenaline. Although similar in structure, different receptors regulate the diverse physiological processes by controlling the synthesis or release of a variety of second messengers or the activity of ion channels. Each major type of receptor shows preference for a particular class of G-protein (e.g., α_1 to G_q; α_2 to G_i) (Westfall, 2009).

There are two classes of adrenergic receptors: alpha (α_1 and α_2) and beta (β_1, β_2 and β_3). α-ARs (1 and 2 subtypes) are found in some cells such as alveolar and peritoneal macrophages or under certain pathologic conditions (Heijnen et al., 1996).

At the tissue level, β-adrenergic receptors are found in all organs which are related with growth such as skeletal muscle, adipose tissue and some neuro-endocrine organs (Yang and McElligott, 1989). They also play an important role in modulating cardiovascular responses. From a therapeutic perspective β_1ARs in the heart (the target for β-blockers), and β_2ARs in the lungs (the target for β_2 agonists), are the most important (Stein, 2012).

1.3.4 Adrenergic control of the immune system

Signals from the CNS are sent via the SNS to peripheral tissues by catecholamines through adrenergic receptors. Noradrenaline and adrenaline target cells through the two groups of adrenergic receptors described above (Elenkov et al., 2000). Both receptors are found in innate immune cells, whereas T and B cells appear to only express β_2 adrenergic receptors (Nance and Sanders, 2007). As mentioned above, in general, the most abundant receptor in leukocytes is the β_2 adrenergic receptor. The highest density is found on natural killer cells (NKs) and the lowest in T helper (Th) cells. In fact, no β_2 adrenergic receptors were observed in the case of Th2 cells (Elenkov et al., 2000). This reduced expression of β_2 adrenergic receptors in adaptive cells of the immune system could be due to the fact that the nervous system is perfectly located to regulate immediate nonspecific inflammatory responses (Sternberg, 2006).

It has been reported that the SNS exerts an inhibitory role in inflammation, through a direct innervation of immune organs. Noradrenaline can drastically inhibit the production and secretion of TNF-α in response to LPS (Ignatowski et al., 1996). In addition, SNS targeting of the adrenal gland releases glucocorticoids, which have been described to suppress maturation, differentiation and proliferation of all immune cells, including dendritic cells (DCs) and macrophages. They are also involved in the inhibition of NFκB, which, after its translocation to the nucleus, is

responsible for the upregulation of other pro-inflammatory molecules (Ghosh et al., 1998). Glucocorticoids are also involved in the decrease in expression of cell adhesion molecules, such as ICAM-1, E-Selectin (Cronstein et al., 1992) and VCAM-1 (Atsuta et al., 1999), as well as of the chemokines CC-chemokine ligand 2 (CCL2) and CXC-chemokine ligand 8 (CXCL8) (Miyamasu et al., 1998).

As previously mentioned, the relation between the SNS and circadian rhythms in terms of immunity lies in the ability of the SNS to synchronize the circadian release of pro-inflammatory mediators with the external environment. Once environmental information is processed in the master clock (SCN), the signal is sent via two different methods: via direct innervation of the SNS to peripheral organs (e.g. bone marrow, liver or spleen) along the arterial tree, or via hormones, targeting the adrenal gland and secretion of noradrenaline, adrenaline and glucocorticoids. The level of noradrenaline exhibits a daily rhythmicity reaching its peak during the active phase (Maestroni et al., 1998). This leads to different effects on leukocyte migration, proliferation and function. In addition, apart from adrenaline and noradrenaline, the adrenal medulla contains and secretes a high quantity of IL-6 and TNF-α in response to inflammatory stimuli, such as LPS and IL-1 (α and β) (Papanicolaou et al., 1996).

Rhythmic leukocyte recruitment to tissues is also regulated by the SNS. Mice deficient in the β_2 or β_3 adrenergic receptors (*Adrb2*$^{-/-}$ and *Adrb3*$^{-/-}$) showed no more oscillations in their recruitment to either bone marrow or skeletal muscle. In line with these observations, administration of β_2 or β_3 adrenergic receptor agonists (clenbuterol or BRL37344, respectively) enhanced bone marrow engraftment after transplantation, through upregulation of cell adhesion molecules such as P-Selectin, E-Selectin and VCAM-1 (Scheiermann et al., 2012).

Recent work has described an interaction of Nestin$^+$ cells with the SNS. Nestin, which is an intermediate filament protein known as a neural stem/progenitor cell marker, is expressed in undifferentiated CNS cells during development (Suzuki et al., 2010). Nestin$^+$ cells located in the bone marrow are sympathetically innervated alongside arteries and express β_3 adrenergic receptors on their surface. In bone

marrow, they are involved in the regulation of the hematopoietic stem cell niche via expression of CXCL12 and other niche factors (Mendez-Ferrer et al., 2008).

These studies all point to an important role of the SNS in the control of the immune system and in the circadian rhythmicity of leukocyte recruitment. Since post-capillary venules, where this phenomenon usually takes place, are devoid of adrenergic innervation, the purpose of this thesis was to try to elucidate how these adrenergic stimuli reach veins to regulate leukocyte infiltration to tissues.

2 Materials and Methods

2.1 Animals

2.1.1 Mouse strains

Bmal1$^{flox/flox}$ and *Icam1*$^{-/-}$ mice were obtained from Jackson Laboratories. *Ng2Cre* mice were a gift from Konstantin Stark. These lines were crossed to generate mice, which lack *Bmal1* specifically in arteriolar pericytes (*Bmal1*$^{flox/flox}$x*Ng2Cre*). *LyE*-GFP mice, which express GFP fluorescence in the myeloid lineage, were a gift from Markus Sperandio. *Cx3cr1*$^{GFP/+}$ mice were a gift from Christoph Reichel. These mice express GFP fluorescence in monocytes, dendritic cells, NK cells, and microglia under control of the endogenous *Cx3cr1* locus.

7-8 week old wild-type C57BL6/N control mice were acquired from Charles River. Mice were housed under a 12h:12h light-dark cycle with *ad libitum* access to food and water. All experimental procedures were performed according to German legislation and approved by the Regierung of Oberbayern.

2.1.2 Genotyping

Ear samples were digested in 200µl lysis buffer (5mM EDTA, 200mM NaCl, 0.2% SDS in 100mM Tris-HCl, pH 8.5) containing proteinase K (1µl, 1,5U per sample) at 55°C overnight. After centrifugation (10 min RT at 14000rpm), the supernatant was transferred to an Eppendorf tube containing 200µl isopropanol to induce DNA precipitation. Tubes were then inverted and centrifuged 10 min at 14000 rpm. Supernatant was carefully discarded and DNA pellets were resuspended in 100µl Tris-EDTA (TE) buffer and incubated for 1h at 37°C before being used in the PCR reaction mix (see **Table 2.1**).

Component	Volume (µl)
Water	8.6
Master Mix (2X)	10
Forward primer (10µM)	0.2
Reverse primer (10µM)	0.2
DNA	1

Table 2. 1 PCR reaction mix for genotyping.

Samples were initially denatured at 94°C for 3 minutes, followed by 35 amplification cycles of DNA denaturation (94°C, 30 sec), primer annealing (55°C for *Bmal1*$^{flox/flox}$, 30 sec) and DNA polymerization (72°C, 30 sec), with a final extension step (72°C, 2 minutes). Assessment of the *Cre* gene was performed by a denaturation at 95°C for 3 minutes, followed by 38 cycles of DNA denaturation (95°C, 20 sec), primer annealing (62°C, 30 sec), and DNA polymerization (72°C, 30 sec), with a final extension step (72°C, 10 minutes). Primer sequences were used as shown in the following table (**Table 2.2**):

Primer	Sequence (5' → 3')
Bmal1 (*Arntl*) FW	ACT GGA AGT AAC TTT ATC AAA CTG
Bmal1 (*Arntl*) RV	CTG ACC AAC TTG CTA ACA ATT A
Generic *Cre* FW	GCG GTC TGG CAG TAA AAA CTA TC
Generic *Cre* RV	GTG AAA CAG CAT TGC TGT CAC TT

Table 2. 2 PCR primers used for genotyping

PCR products were run on a 1% agarose-TAE gel, using GelRed in order to visualize the bands with an ultraviolet light on a Gel iX20 Imager (Bioolympics). A DNA ladder (ThermoFisher Scientific) was used to check the band size from the products (**Figure 2.1**).

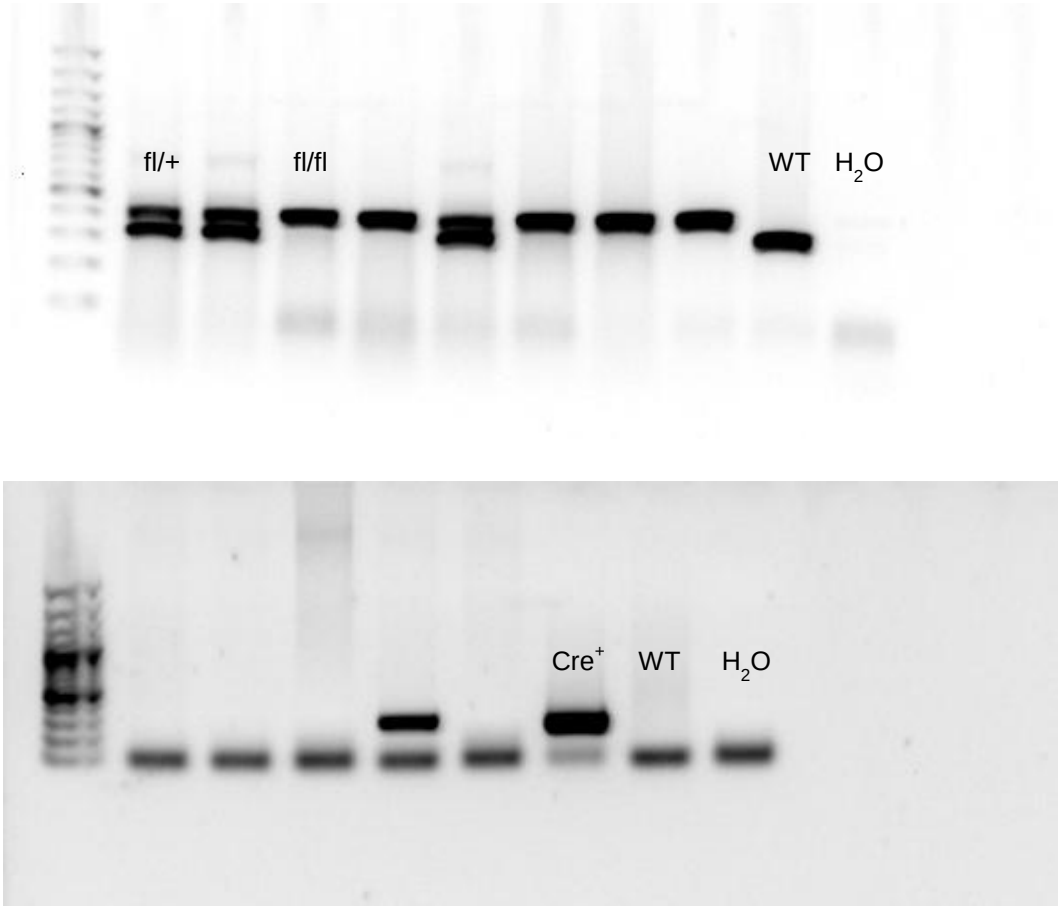

Figure 2.1 PCR genotyping gels. Examples from *Bmal1* and *Cre* amplification. Heterozygous (*Bmal1flox*/wt; bands 327bp and 431bp) and homozygous for the *Bmal1flox/flox* (431bp), as well as Cre^{+} bands (324bp) were detected.

2.1.3 Tamoxifen preparation and treatment

To induce recombination in the *CreERT2* mice (*Cdh5* and *Bmx*), 8-10 week old mice were injected i.p. with tamoxifen daily for 5 consecutive days, changing injection site left/right every day. Tamoxifen was dissolved in corn oil (20mg/ml) with incubation at 37°C for 1h. Any remaining crystals were dissolved by incubating a further 3-4h at room temperature on a rotator to constantly invert the tube.

2.2 Multichannel fluorescence intravital microscopy (MFIM)

2.2.1 Carotid artery and jugular vein imaging

Mice were anesthetized by i.p. injection of ketamine (100mg/kg), xylazine (20mg/kg) and acepromazine (1%). A ventral incision was made in the neck and the carotid artery and jugular vein were exposed. A knot was tied around the sternocleidomastoid muscle and the muscle was pulled to the side. Surgical knots were placed above (short suture thread) and below (long suture thread) the tendon and a cut was made in the middle, to sever the tendon. Two knots were then tied around the bone and used to pull it to the side. A similar model was described in the paper by Chevre and colleagues (Chevre et al. 2014). After this preparation, the neck and the underlying vessels were treated topically with TNF-α (150µg in 100ml PBS) for 2h prior to imaging (**Figure 2.2A**).

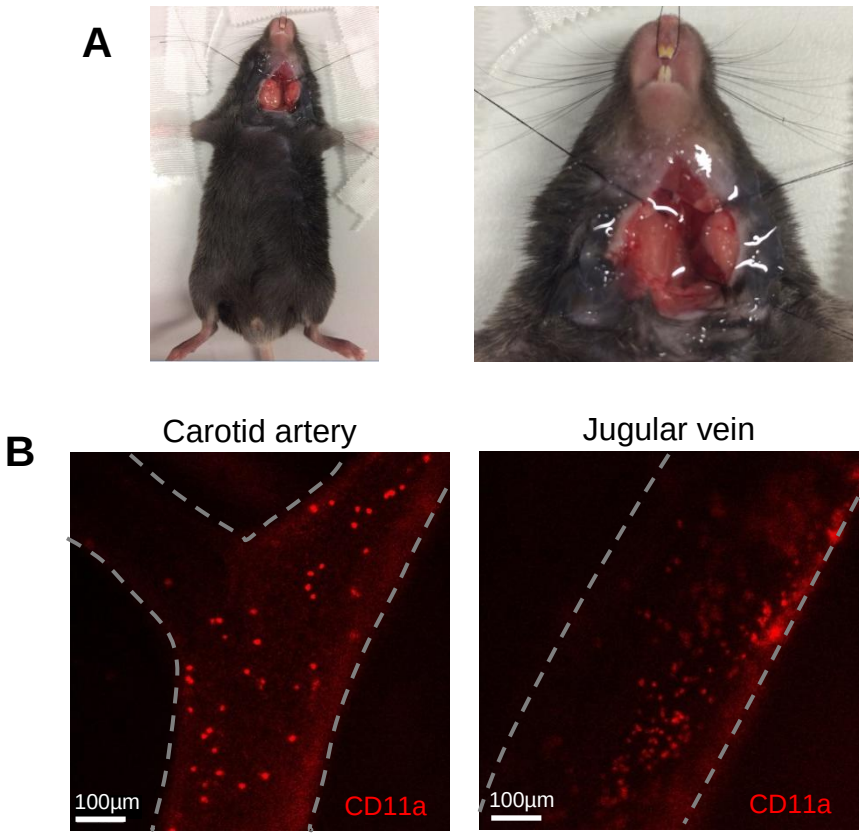

Figure 2.2 Carotid artery/jugular vein *in vivo* imaging. (A) Carotid artery/jugular vein preparation. (B) Epifluorescence microscopy images from carotid artery (left) and jugular vein after 2h topical TNF-α stimulation and intra-arterial injection of anti-CD11a-PE antibody.

A catheter was inserted in the femoral artery for administrating fluorescence-conjugated antibodies (1µg). Images were acquired on a fixed-stage microscope Axio Examiner.Z1 for bright field, inclined illumination, DIC-IR/VIS and epifluorescence, with motorized objective and condenser focusing as well as motorized reflector turret, in combination with a Colibri LED excitation system (Zeiss) (**Figure 2.3**).

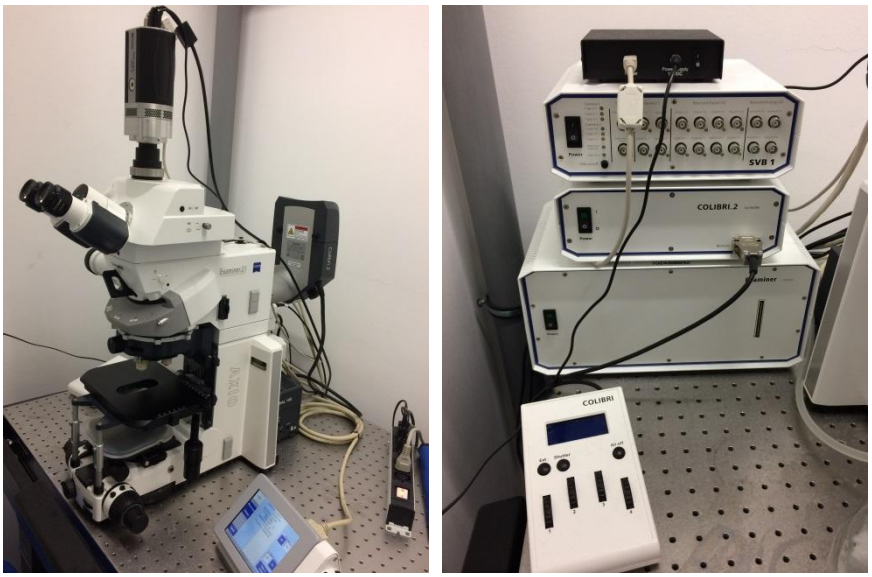

Figure 2.3 Epifluorescence microscope set-up. Axio Examiner.Z1 microscope (left). Colibri light system (right).

Quantification of adherent cells (defined as no obvious movement for at least 30s) in the carotid artery and jugular vein was performed manually and plotted per vessel. Since the size was not always constant, cells per area were calculated with the formula for the lateral surface area of a cylinder ($2\pi r$ x length), divided by two as only one side of the vessel was visualized. In the case of the carotid, two cylinders were considered for the calculation due to the branching of the vessel.

In order to measure the mean fluorescence intensity (MFI) from adherent cells, the Zeiss Blue Zen software was used. Circular masks were drawn on the cells (aprox. 10 cells per vessel) and by selecting the maximum threshold value, area and intensity were calculated, as shown in **Figure 2.4**.

A

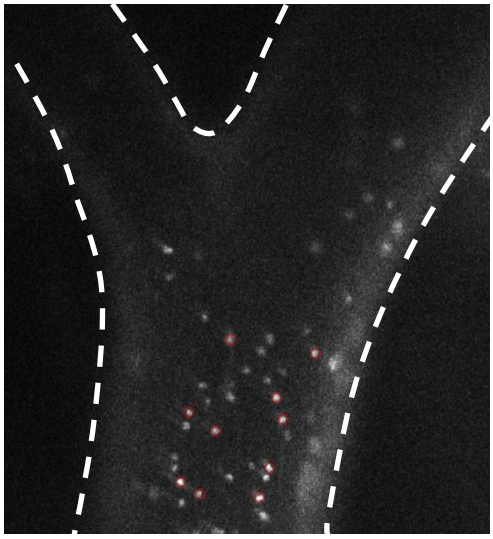

B

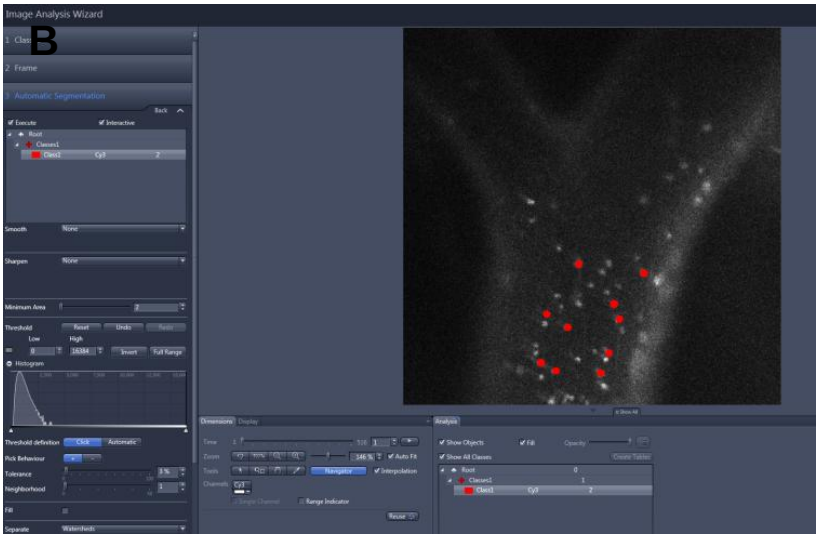

C

	ID	Area[µm²]	Intensity...
	A	B	C
1	2	199.680	1,478.308
2	3	212.480	1,551.880
3	4	212.480	1,645.627
4	5	186.880	1,396.644
5	6	197.120	1,564.260
6	7	197.120	1,468.584
7	8	197.120	1,697.948
8	9	212.480	1,663.518
9	10	192.000	1,385.160
10	11	192.000	1,832.613

Figure 2.4 Representative example of mean fluorescence intensity measurement in adherent cells. (A) Circular masks were drawn around the area of interest (red line) and those areas were colored in red (B). (C) Cell areas with ID number (column A), size in µm^2 (column B) and mean intensity (arbitrary units) (column C).

The intensity values given by the software were used as the mean fluorescent intensity for each cell.

2.2.2 Cremaster muscle imaging

Mice were anesthetized with Fentanyl (0,5mg/kg), Midazolam (5mg/kg) and Medetomidine (0,5mg/kg) via i.p. injection. Cremaster preparation was performed as explained in a previous publication (Scheiermann et al. 2012). Through a central incision of the scrotum, the right testis was exposed. The cremaster muscle surrounding the testis was opened ventrally in a zone with less vasculature, using careful electrocautery to cut the muscle and at the same time stop any bleeding, and spread over a plexiglas cube of a custom-made microscopy stage (**Figure 2.5**). Epididymis and testicle were detached from the cremaster muscle by electrocautery and placed back into the peritoneum. During the procedure as well as after surgical preparation, the muscle was superfused with warm buffered saline (0.9% NaCl). A catheter was inserted in the femoral artery for administration of antibodies. TNFα was injected i.p. or in the scrotum 3h before the imaging in order to visualize leukocyte adhesion in arterioles, since this phenomenon does not occur in steady-state conditions in these vessels.

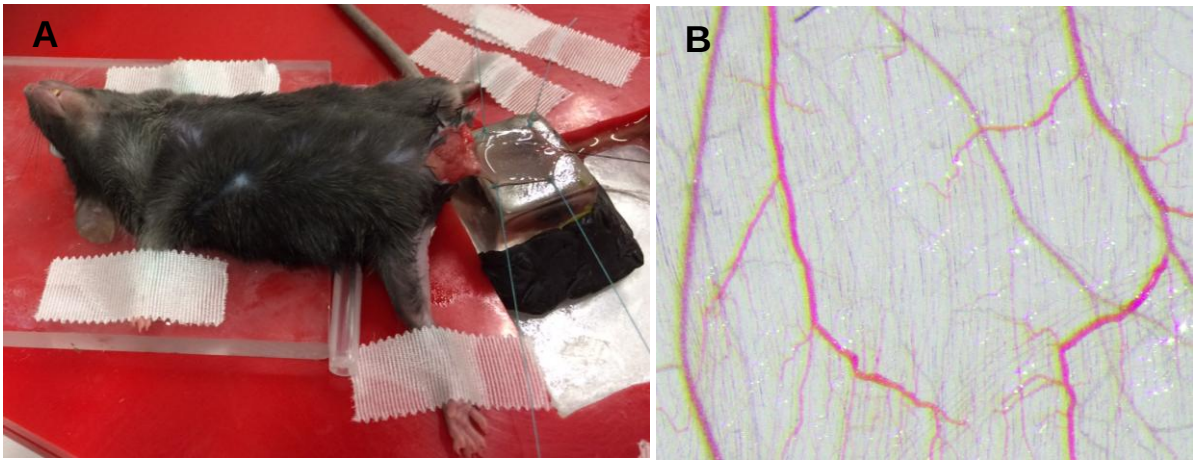

Figure 2. 5 Cremaster muscle preparation. Cremaster muscle preparation set-up (A). Blood flow in the cremaster microvasculature was checked using bigger magnification after surgery (B).

One of the advantages of the cremaster muscle in intravital microscopy is that it is very thin, which allows the use of transmitted light microscopy for imaging the microvasculature. Leukocyte migration can be visualized without using fluorescence imaging, as shown in the following picture (**Figure 2.6**). Another positive aspect of the cremaster muscle is that multiple vessels can be easily screened in the same mouse.

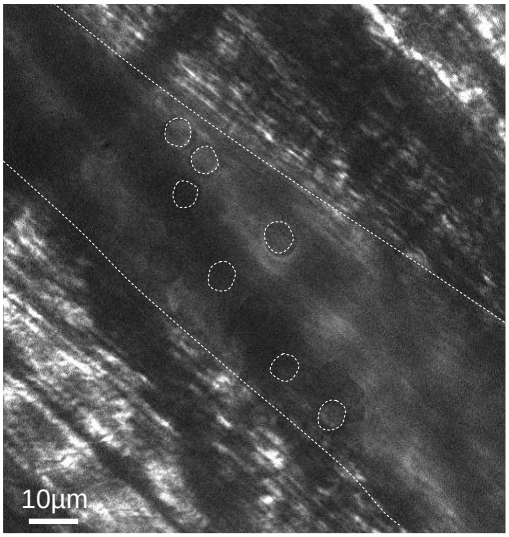

Figure 2.6 MFIM of the cremasteric microcirculation. Rolling leukocytes, surrounded by white lines, were visualized in the microvasculature using brightfield microscopy (63X).

Unlike the imaging of carotid artery or jugular vein, breathing is not an issue in the imaging process of the cremasteric microcirculation. In addition, using different fluorescently-conjugated antibodies, leukocyte phenotypes can be studied in more detail (**Figure 2.7A**). Results are reported as number of adherent cells/area, with the area defined as ($2\pi r \times l$) and where r is the radius (diameter/2) and l is the length of the vessels. Adherent cells were defined as cell with no obvious movement for at least 30s (**Figure 2.7B**).

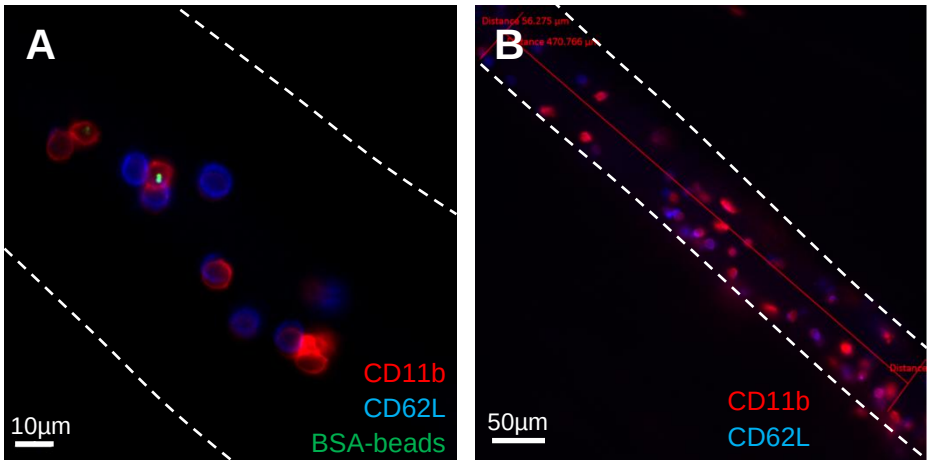

Figure 2.7 Cremaster muscle MFIM. (A) Microscope images of a cremasteric venule visualized with the 63x objective (Epifluorescence microscope). CD11b-PE was used as a myeloid marker, CD62L-APC for L-Selectin expression and BSA-coated fluorescent beads as a marker for cell activation. (B) Quantification of leukocyte adhesion (cremasteric venule), 20x objective.

2.3 Immunofluorescence on frozen sections

Carotid artery and jugular vein tissues were harvested without any perfusion after 2h topical stimulation with TNF-α, embedded in OCT (TissueTek) and frozen on dry ice. No method to stop the vessels collapsing was needed. 10µm cross-sections were cut on a cryostat (Leica) and stained with antibodies as detailed in **Table 2.4**. Methanol was used for fixation and goat serum (20% in PBS) for blocking in order to minimize unspecific antibody binding. Tissues were permeabilized by 0,5% Triton X-100. All images were acquired on an epifluorescence microscope (Axio Examiner.D1, Zeiss), equipped with 405, 488, 563 and 655 nm LED light sources. As example, a representative picture is shown in the **Figure 2.8**.

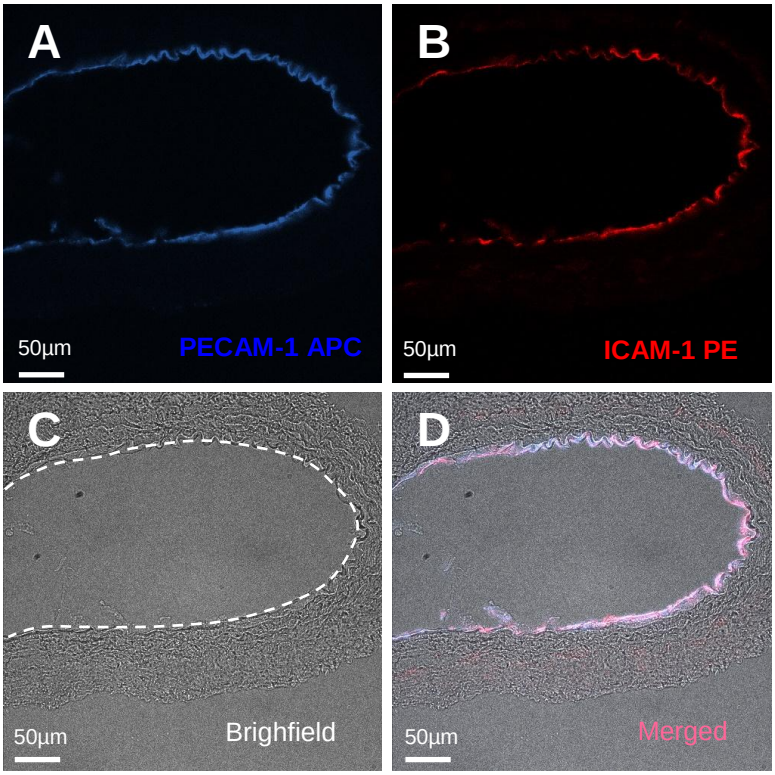

Figure 2.8 Representative fluorescence imaging picture. Picture from a jugular vein 10µm section stained with ICAM-1-PE (A), PECAM-1-APC (B). Brightfield (C) was obtained with transmitted light microscopy and merged (D) in order to visualize the whole structure.

To quantify protein expression levels, analyses were performed on immunostained sections using a mask based on PECAM-1 staining, in combination with other antibodies, with the help of the Zeiss Blue Zen software.

As shown in **Figure 2.9A**, a profile (red line) was drawn surrounding the area of interest (jugular vein, in this example). Positive areas for PECAM-1 (APC, shown in blue) were then used to generate a mask of the endothelium, shown in yellow (B). Within this PECAM-1 mask, mean fluorescence intensities of other fluorescently-stained adhesion molecules were quantified. In the **Figure 2.9C**, the mean intensity values for the areas positive for PECAM-1 and the antibody of interest (ICAM-1, conjugated to PE) are shown. Areas smaller than 10µm^2 were not considered in calculations as these often represented noise.

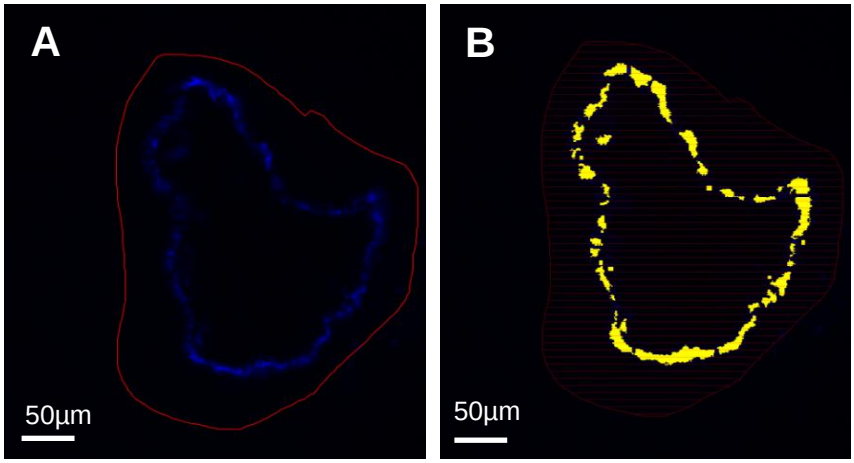

C

	ID	Area[µm²]	Intensity...	Intensity...
	A	B	C	D
1	55	351.692	2,029.843	3,610.174
2	31	200.239	1,653.182	2,880.560
3	5	176.938	1,820.519	3,554.601
4	52	167.472	1,824.330	3,072.478
5	54	160.191	1,841.309	3,147.968
6	24	120.143	1,574.861	2,208.139
7	3	117.231	2,071.839	4,714.528
8	11	114.318	1,964.567	3,164.720
9	4	112.862	1,415.071	1,989.568
10	48	99.755	1,914.788	2,716.482
11	2	86.649	2,653.311	4,660.050
12	14	82.280	1,503.354	2,292.363
13	43	64.805	1,525.708	2,344.022
14	49	60.436	1,703.651	2,897.831
15	7	59.708	1,683.963	2,173.451
16	8	45.873	1,184.286	1,681.476
17	26	45.145	1,685.887	3,196.306
18	29	42.960	1,446.136	1,485.068
19	13	41.504	1,358.684	2,321.439
20	20	38.591	1,573.604	3,516.151

Figure 2.9 Representative example of quantitative expression analyses. (A) A mask using PECAM-1 expression was drawn around the area of interest (red line) and PECAM-1 positive pixels were colored in yellow (B). (C) PECAM-1 areas with ID number (column A) and size in µm^2 (column B). The MFIs for each region are represented in column C (PECAM-1) and column D (ICAM-1). Areas smaller than 10 µm^2 were discarded.

2.4 Adoptive transfer and flow cytometry experiments

To investigate the recruitment of leukocytes from blood to the vessels, adoptive transfer experiments were performed and donor-labeled-cells recruited in the tissues were measured. In order to prepare donor cells, spleen and bone marrow from donor mice were harvested and donor cells isolated. Single cell suspensions were made by flushing bone marrow with cold PBS and smashing spleen gently through a 40 µm cell strainer (ThermoFisher Scientific). Cells were lysed with red cell lysis buffer for 5 min, then 5 ml PBS were added to stop the lysis reaction. Cells were spin down at 1300 rpm for 5 min and resuspended in cell incubation buffer (PBS, 0.2%BSA, 2mM EDTA) and counted on a cell counter (ProCyte DX cell counter). Bone marrow and spleen cells were mixed with a ratio of 50:50, and labeled with 1.5 µM CFSE for 20 min at 37 °C. After washing 3 times with PBS, cells were resuspended in PBS and $20X10^6$ cells were injected intravenously in each recipient mouse, which simultaneously were stimulated with TNFα topically on the carotid and the jugular. Two hours later, carotid and jugular were harvested from recipient mice and digested for performing flow cytometry.

For identifying different leukocyte subsets in blood, cells were gated from total white blood cells (WBC) counts, from which the different leukocyte subsets were distinguished by specific surface markers. Blood cells were gated from live cells and singlets. Then leukocyte subsets were identified by different combinations of antibodies. CD115 and Gr-1 for differentiation of neutrophils; inflammatory monocytes (IM) and non-inflammatory monocytes (NIM); CD4, CD8 and B220 for identifying lymphocytes; NK1.1 and CD3 for NK cells and NKT cells; Siglec-F and CCR3 were used for eosinophil.

2.5 Functional blocking of adhesion molecules and chemokine receptors

In order to investigate the role of ICAM-1, VCAM-1, CXCL1, CXCL2 and CCL2 in leukocyte adhesion in the macrovasculature, 200µg of blocking antibodies or 125 µg CXCR2 and CCR2 antagonists were injected i.v. per mouse 1h before stimulation with TNF-α and 3h before performing *in vivo* imaging analyses. In the case of chemokine receptor antagonists, 1% Tween80, 5% DMSO in PBS were used as vehicle.

2.6 Denervation techniques

2.6.1 Chemical sympathetic denervation (6-OHDA)

As indicated in the **Figure 2.10**, mice were injected twice before the experiment with 6-hydroxydopamine (6-OHDA), which is used to selectively destroy dopaminergic and noradrenergic neurons in the body. The initial dose consisted of 100mg/kg, followed two days later by a dose of 250mg/kg. The experiment was performed three days later. 6-OHDA was prepared in ascorbic acid solution at 20mg/ml (in PBS).

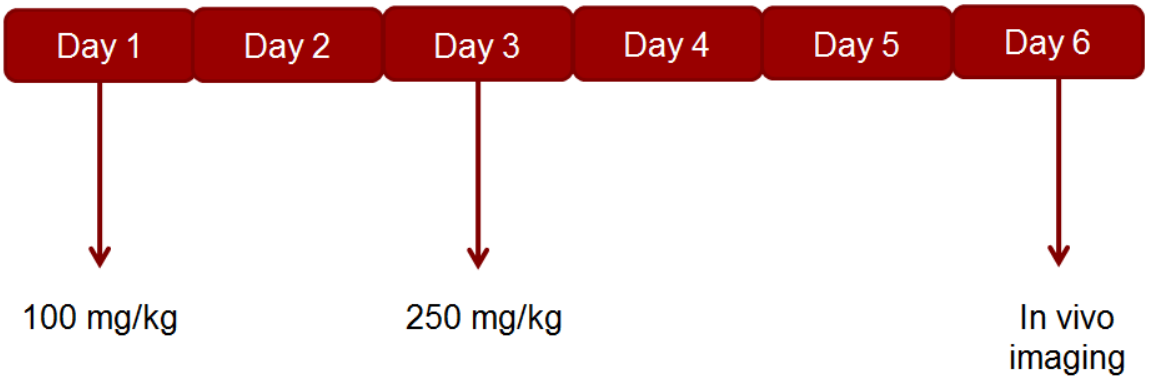

Figure 2.10 6-OHDA treatment scheme. 6-OHDA was administrated on day 1 (100mg/kg) and 3 (250mg/kg) and the analysis was performed on day 5.

2.6.2 Surgical sympathetic denervation (SCGx)

The superior cervical ganglion is located underneath the carotid bifurcation. Using forceps to carefully pull apart the carotid artery, the ganglion was identified and removed unilaterally by blunt dissection with the forceps. On the other side, an analogous manipulation was performed without transecting the ganglion (sham). Animals were sutured and left to recover for 4 weeks in order to re-establish blood leukocyte counts to steady-state levels, using the absence of inflammation as an indicator to proceed.

2.7 β_2 adrenergic receptor antagonist treatment

To block β_2 adrenergic receptor function, the antagonist butoxamine was administered via i.p. injection (5mg/kg); 2h prior to imaging for acute experiments or for five days in a row for chronic experiments.

2.8 Thrombosis assay

An initial dose of 100µl fluorescein isothiocyanate (FITC)-coupled dextran (2.5%) was administrated intravenously to mice and fluorescence was checked until it reached 1800 (arbitrary units, AU). Fluorescence was kept constant and to verify comparable intravascular FITC concentrations among experimental groups, digital images were taken from each vessel and the mean fluorescence intensity was measured (Bihari et al., 2010). As shown in **Figure 2.11**, FITC phototoxicity was induced using a 488nm epifluorescence excitation source. This leads to energy absorption by the dye locally within the vessel and to endothelial cell damage with the formation of a thrombus as a consequence. Occlusion time was quantified for multiple vessels in each mouse (3 venules and 3 arterioles of the same size, 60µm and 40µm respectively) at different time points.

Figure 2.11 Set-up of phototoxicity-induced thrombus formation. Fluorescence was measured in order to keep it constant during the experiment (left). 488nm light was used for inducing FITC phototoxicity and occlusion time was quantified.

2.9 RNA isolation

Tissue samples were homogenized in 200µl Trizol (QiAzol, QiAgen) in (innuSPEED Lysis Tubes. In particular, P model was used, which is a 0.5 ml tube with screwing cap (green) containing optimized ceramic beads (2.4 - 2.8 mm) from Analytik Jena) and a homogenizer (SpeedMill PLUS, Analytik Jena), which mechanically disrupts the tissue due to the up- and down movement of the beads. Homogenized samples were centrifuged at maximum speed of 14000 rpm for 10 min at 4°C. The supernatant was transferred to a new tube and 40µl chloroform was added. After shaking vigorously for 15 seconds, samples were incubated for 2-3 minutes and centrifuged at 12000 rpm for 15 minutes, 4°C. Following centrifugation, three layers were visible: a lower organic phase (proteins and lipids), middle phase (denatured proteins and genomic DNA) and an upper aqueous phase (RNA). The upper phase was transferred to a new tube. RNA precipitation was induced with 100µl isopropanol and incubation for at least 1h at -20°C. Following 30 minutes centrifugation at maximum speed at 4°C, the resulting pellet was washed with 75% ethanol. Samples were centrifuged for 15 min and resuspended in RNAse-free water in combination with 1U DNAse per sample (ThermoFisher Scientific). After 30 minutes incubation at 37°C, samples were purified using the RNeasy Mini Kit (Qiagen) according to the manufacturer's instructions. RNA samples were stored at -80°C.

2.10 Reverse transcription

RNA concentration and quality were measured using a NanoDrop LITE (Thermo Fisher Scientific). 100-200 ng RNA were reverse-transcribed into cDNA using the High Capacity cDNA Reverse Transcription Kit (Applied Biosystems), in accordance to the manufacturer's instructions. cDNA samples were stored at -20°C.

2.11 Quantitative real-time PCR

Q-PCR was performed with SYBR Green on a StepOnePlus Real-Time PCR System (Applied Biosystems). The primer concentration used was 0.5µM. The PCR protocol consisted of one cycle at 95 °C (10 min) followed by 40 cycles of 95 °C (15 s) and 60-64 °C depending upon primers used (1 min). Glyceraldehyde-3-phosphate dehydrogenase (GAPDH) was used as a housekeeping gene. The sequences of the oligonucleotides used can be found in the following table (**Table 2.3**).

Primers	Sequence	Annealing(°C)
Adrb2_F	GTA CTG TGC CTA GCC TTA GCGT	60
Adrb2_R	GGT TAG TGT CCT GTC AAG GAGG	
Adrb3_F	TCT AGT TCC CAG CGG AGT TTT CAT CG	60
Adrb3_R	CGC GCA CCT TCA TAG CCA TCA AAC C	
Bmal1_F	AGA GGT GCC ACC AAC CCA TA	62
Bmal1_R	TGA GAA TTA GGT GTT TCA GTT CGT CAT	
Bmal1_F	CCT AAT TCT CAG GGC AGC AGA T	60
Bmal1_R	TCC AGT CTT GGC ATC AAT GAG T	
Ccl2_F	TCTCTTCCTCCACCACCATGC	60
Ccl2_R	AGCTTCTTTGGGACACCTGCTG	
c-fos_F	ATG GGC TCT CCT GTC AAC ACA C	60
c-fos_R	ATG GCT GTC ACC GTG GGG ATA AAG	
Clock_F	CAA AAT GTC ACG AGC ACT TAA TGC	62
Clock _R	ATA TCC ACT GCT GGC CTT TGG	
Cry1_F	CTC GGG TGA GGA GGT TTT CTT	62
Cry1_R	GAC TTC CTC TAC CGA GAG CTT CAA	
Cxcl1_F	GCTGGGATTCACCTCAAGAA	60
Cxcl1_R	TGGGGACACCTTTTAGCATC	

Cxcl2_F	AGTTTGCCTTGACCCTGAAGC	60
Cxcl2_R	AGGCTCCTCCTTTCCAGG	
Dbh_F	GAT CTC ATC ATG CTC TGG ACT G	60
Dbh_R	CTG GTA GTC TTG CTG GGA ATC	
Gapdh_F	TGT GTC CGT CGT GGA TCT GA	60
Gapdh_R	CCT GCT TCA CCA CCT TCT TGA	
GRa_F	GAA GGA AAC TCC AGC CAG AA	60
GRa_R	CAG CTA ACA TCT CGG GGA AT	
Icam1_F	GGA CCA CGG AGC CAA TTT C	60
Icam1_R	CTC GGA GAC ATT AGA GAA CAA TGC	
Nr1d1_F	GAT AGC TCC CCT TCT TCT GCA TCA TC	60
Nr1d1_R	TTC CAT GGC CAC TTG TAG ACT TC	
Nr1d2_F	TCA TGA GGA TGA ACA GGA ACC	60
Nr1d2_R	GAA TTC GGC CAA ATC GAA C	
Per1_F	TGA GAG CAG CAA GAG TAC AAA CTC A	60
Per1_R	CTC GCA CTC AGG AGG CTG TAG	
Per2_F	GTC CAC CTC CCT GCA GAC AA	60
Per2_R	TCA TTA GCC TTC ACC TGC TTC AC	
Rora_F	CTC GAG ATG CTG TCA AGT TTG G	60
Rora_R	CGG CGT ACA AGC TGT CTC TCT	
Rory_F	CTC AGC GCC CTG TGT TTT TC	60
Rory_R	TGA GAA CCA GGG CCG TGT AG	
Sele_F	CCC TGC CCA CGG TAT CAG	60
Sele_R	CCC TTC CAC ACA GTC AAA CGT	
Selp_F	GGT ATC CGA AAG ATC AAC AAT AAG TG	60
Selp_R	GTT ACT CTT GAT GTA GAT CTC CAC ACA	
Th_F	GGT ATA CGC CAC GCT GAA GG	60
Th_R	TAG CCA CAG TAC CGT TCC AGA	
Tnfr1_F	GGG CAC CTT TAC GGC TTC C	60
Tnfr1_R	GGT TCT CCT TAC AGC CAC ACA	

Tnfr2_F	CAG GTT GTC TTG ACA CCC TAC	60
Tnfr2_R	GCA CAG CAC ATC TGA GCCT	
Vcam1_F	GAC CTG TTC CAG CGA GGG TCT A	60
Vcam1_R	CTT CCA TCC TCA TAG CAA TTA AGG TG	

Table 2.3 Primer sequences used for quantitative real time PCR

2.12 Statistical analyses

Statistical analyses were performed using GraphPad Prism 6 software. All data are represented as mean ± SEM. An unpaired student's t-test was used for comparisons between two groups. One-way ANOVA followed by Tukey's post hoc test or two-way ANOVA followed by Bonferroni's post hoc test were used for three or more groups. Statistical significance was assessed as *$p<0.05$, **$p<0.01$, ***$p<0.001$ and ****$p<0.0001$.

2.13 Antibody list

Antibody	Dye	Clone	Reactivity	Company	Quantity	Use
CD106 (VCAM-1)	PE	429 MVCAM.A	anti-m	Biolegend	1:50	IH
CD106 (VCAM-1)		M/K-2.7	anti-m	BioxCell	200µg/ mouse	Blocking
CD115	PE	AFS98	anti-m	Biolegend	1:100	FACS
CD11a	PE	M17/4	anti-m	Biolegend	1µg	*In vivo* imaging
CD11b	PE	M1/70	anti-m	Biolegend	1µg	*In vivo* imaging
CD3	PE/DZL594	17A2	anti-m	Biolegend	1:100	FACS
CD31 (PECAM1)	Alexa Fluor647	Mec13.3	anti-m	Biolegend	1:100	Immuno-histochem
CD4	Brilliant Violet 570™	RM4-5	anti-m	Biolegend	1:50	FACS
CD45R/B220	PE/Cy7	RA3-6B2	anti-m/h	Biolegend	1:300	FACS
CD54 (ICAM-1)	PE	YN1/1.7.4	anti-m	Biolegend	1:50	IH
CD54 (ICAM-1)		YN1/1.7.4	anti-m	BioxCell	200µg/ mouse	Blocking
CD62L (L-Selectin)	APC	MEL-14	anti-m	Biolegend	1µg	*In vivo* imaging
CD62L (L-Selectin)	PE	2PH1	anti-m	Biolegend	1:50	IH
CD62P (P-Selectin)	PE	Psel.KO2.3	anti-m/h	Biolegend	1:50	IH
CD8a	APC/Cy7	53-6.7	anti-m	Biolegend	1:500	FACS
DAPI				Biolegend		FACS
Gr-1	PerCP/Cy5.5	RB6-8C5	anti-m	Biolegend	1:300	FACS
Isotype		LTF-2	Rat IgG2b	BioxCell	200µg/ mouse	ICAM-1 isotype
Isotype		HRPN	Rat IgG1	BioxCell	200µg/ mouse	VCAM-1 isotype

Ly6-G	PE	1A8	anti-m	BD Biosciences	1µg	*In vivo* imaging
NF H		Polyclonal	anti-h/r/m	Millipore	1:200	IH
NF M		Polyclonal	anti-h/r/m	Millipore	1:200	IH
NK1.1	Alexa Fluor700	PK136	anti-m	ebioscience	1:100	FACS
Siglec-F	Alexa Fluor647	E50-2440	anti-m	BD bioscience	1:100	FACS
TH		Polyclonal	anti-m	Millipore	1:1000	IH
α-Smooth Muscle	Cy3	1A4	anti-m	Sigma Aldrich	1:200	IH

Table 2. 4 Antibody list. (h-human, m-mouse, r-rat).

2.14 Reagents

Compound	Company	Quantity	Use
Isopropanol	Sigma-Aldrich	1:3/1:2	DNA/RNA precipitation
6-OHDA	Sigma-Aldrich	100mg/kg (1st day) 250mg/kg (3rd day)	Chemical sympathetic denervation
Acid Ascorbic	MERCK	20mg/ml	6-OHDA antioxidant
Butoxamine (β_2 antagonist)	Sigma-Aldrich	5mg/kg	β_2 adrenoreceptor blocking
CCR2 antagonist	Tocris	5mg/kg	CCR2 blocking
Chloroform	Sigma-Aldrich	1:5	RNA isolation
Corn oil	Sigma-Aldrich	50µl/injection (5 days)	Cre recombination induction
CXCR2 antagonist	Tocris	5mg/kg	CXCR2 blocking
DMSO	Sigma-Aldrich	5%	Chemokine receptor block. (vehicle)
DNA ladder	Nippon genetics europe	5 µl	Electrophoresis gel
DNAse	ThermoFisher Scientific	1:50	DNA digestion (RNA isolation)

Fluorescein isothio-cyanate-dextran	Sigma-Aldrich	2,5% (in saline)	Thrombosis assay
gelRed	Biotium	1:20.000	Electrophoresis gel
Goat serum	Abcam	20%	Antigen blocking (immunohist.)
Methanol	Sigma-Aldrich	200µl	Fixation (immunohistochemistry)
OCT	Tissue-Tek	Manufact. instructions	Specimen matrix (immunohistoc.)
PFA (4%)	Sigma-Aldrich	200µl	Fixation (immunohistochemistry)
Proteinase K	Thermo Scientific	600U/ml (20mg/ml)	Tail/ear digestion
QIAzol	Qiagen	200ul/sample	RNA isolation
Retrotranscription kit	Applied Biosystems	Manufact. instructions	RNA retrotranscription to cDNA
RNeasy Mini Kit	Qiagen	Manufact. instructions	RNA purification
SYBR green	Thermo Fisher Scientific	1:2 (5µl/well)	qPCR
Tamoxifen	Sigma-Aldrich	1mg/injection (5 days)	Cre recombination induction
TNF-α	R&D Systems	0.15µg carotid/jugular 0.5µg cremaster	Induction of inflammation
Triton X100	Sigma-Aldrich	0,5%	Permeabilization (immunohistoc.)
TWEEN80	Sigma-Aldrich	1%	Chemokine receptor block. (vehicle)

Table 2. 5 Reagents list

3 Results

3.1. Differences in leukocyte adhesion between arteries and veins

Recent studies provide a molecular link between circadian rhythms and the immune system. Leukocyte counts oscillate according to the phase of physical activity of the organism. For instance, in blood, the peak is observed during the behavioral resting phase, while the recruitment of leukocytes to tissues occurs preferentially during the active phase of the organism (Scheiermann et al., 2013). In order to fully understand this phenomenon in large calibre vessels, we performed quantitative *in vivo* fluorescence microscopy of the carotid artery and the jugular vein after 2h tumor necrosis factor (TNF)-α stimulation, every 4h over the whole day (from ZT1 until ZT21; Zeitgeber Time, time after the onset of light). Using very low, non-blocking, doses of CD11a (LFA-1)-PE conjugated antibody we quantified the number of adherent cells to the endothelium in both vessels (**Figure 3.1A**). Clear diurnal rhythmicity in cell adherence was observed in both vessels, but with different phases. While the cell number was higher at ZT1 (8:00 am) in the carotid artery, the peak was significantly delayed in the jugular vein and appeared at ZT17 (midnight) (**Figure 3.1B**). In contrast, the lowest recruitment in the carotid artery was found at ZT17, the time of peak adhesion in the jugular. To facilitate comparison between the two vessels, data were plotted by fold change with respect ZT1 adhesion in carotid (**Figure 3.1C**) and the biggest discrepancies were found at ZT1 and ZT17. Therefore all subsequent experiments were focused on these two time points.

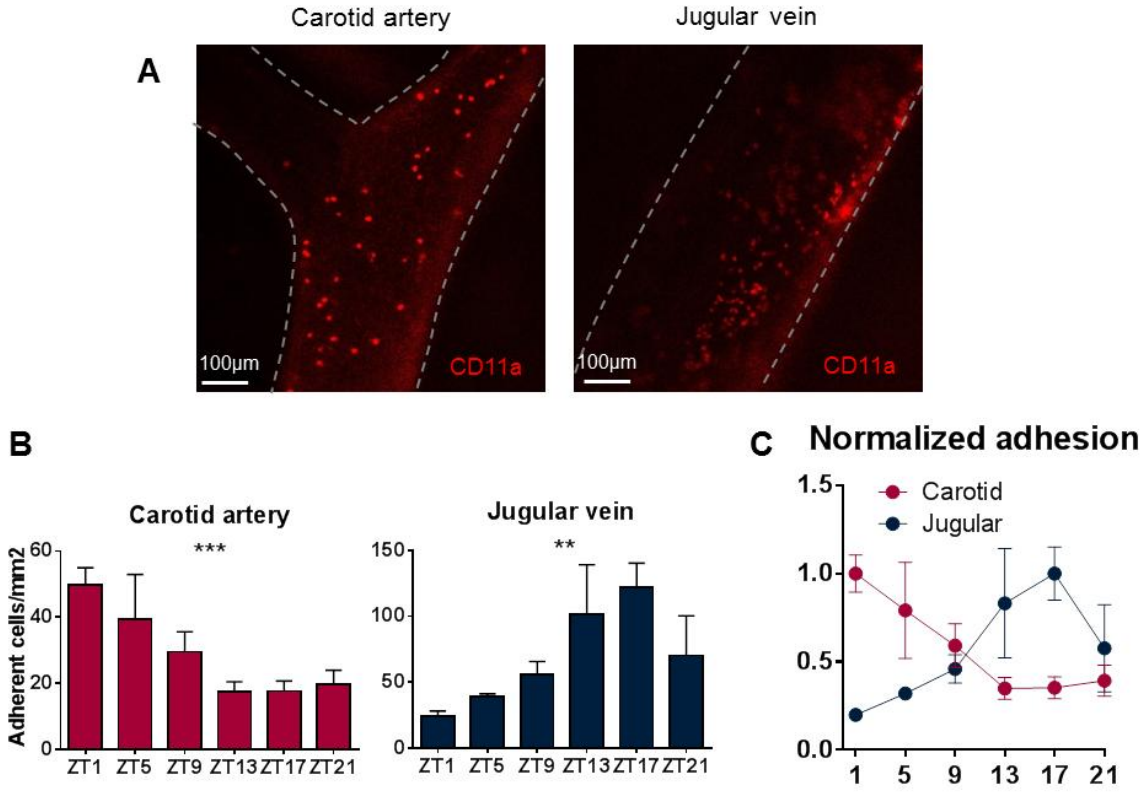

Figure 3.1 Diurnal oscillations in leukocyte adhesion in large vessels. (A) Epifluorescence microscopy images from carotid artery (left) and jugular vein (right) after 2h TNF-α stimulation. Cells were labeled with CD11a-PE antibody and adherent cells classed as those that did not move for 30s. (B) Quantification of adherent cells at different time points of the day in intervals of 4h (n= 4-13 mice), one-way ANOVA **p < 0.01, ***p < 0.001. (C) Normalized carotid and jugular adhesion data.

In order to validate these observations without antibody labeling to rule out potential off-target effects, we performed the same *in vivo* imaging approach of the carotid and jugular vein after 2h TNF-α stimulation in LyE-GFP mice (**Figure 3.2A**). These mice express GFP in myeloid cells, and we could report comparable results: higher leukocyte recruitment in the carotid artery in the morning (ZT1), and in the jugular vein at ZT17 (**Figure 3.2B**).

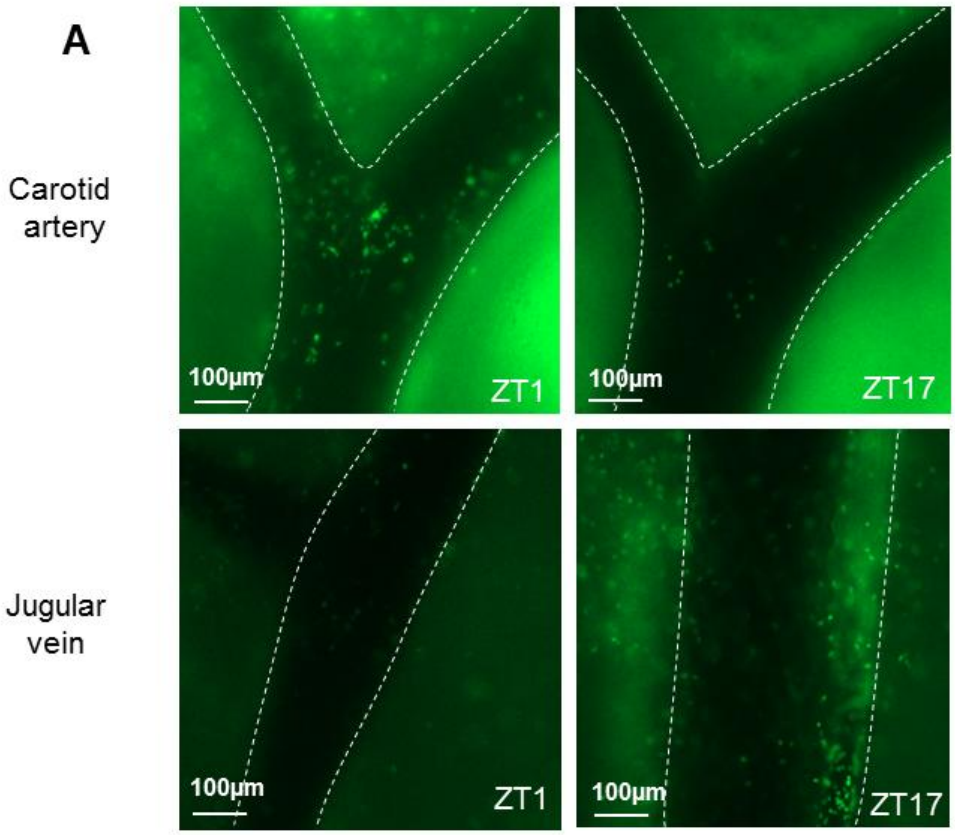

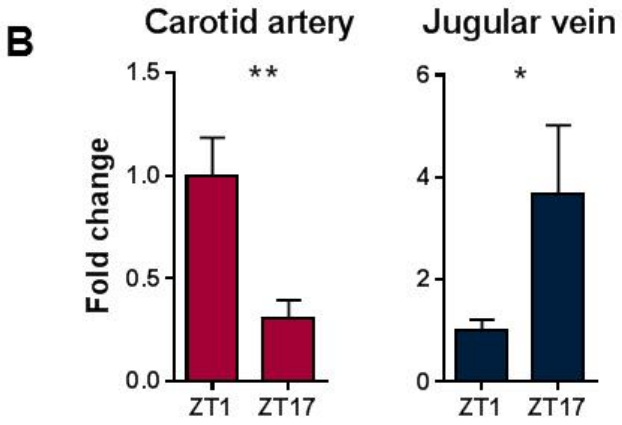

Figure 3.2 Differences in leukocyte recruitment in LyEGFP mice between morning and night. (A) Epifluorescence microscopy images from carotid artery (upper row) and jugular vein at ZT1 and ZT17 after TNF-α stimulation in mice that express GFP in myeloid cells. (B) Cell adhesion quantification in carotid artery and jugular vein (n = 4-7 mice), t-test *$p < 0.05$, **$p < 0.01$.

To confirm if this phenomenon was exclusive to the macrovasculature, or was representative of a broader tissue context, we next imaged the cremaster muscle microvasculature, where venules and arterioles are located side by side in the same tissue. TNF-α was injected into the scrotum 3h before the *in vivo* imaging procedure. We observed similar results as in the macrovasculature (**Figure 3.3A**); a higher recruitment in the arterioles in the morning and the opposite pattern in the venules (**Figure 3.3B**). This was thus indicative of a mechanism of broader relevance for the whole vasculature.

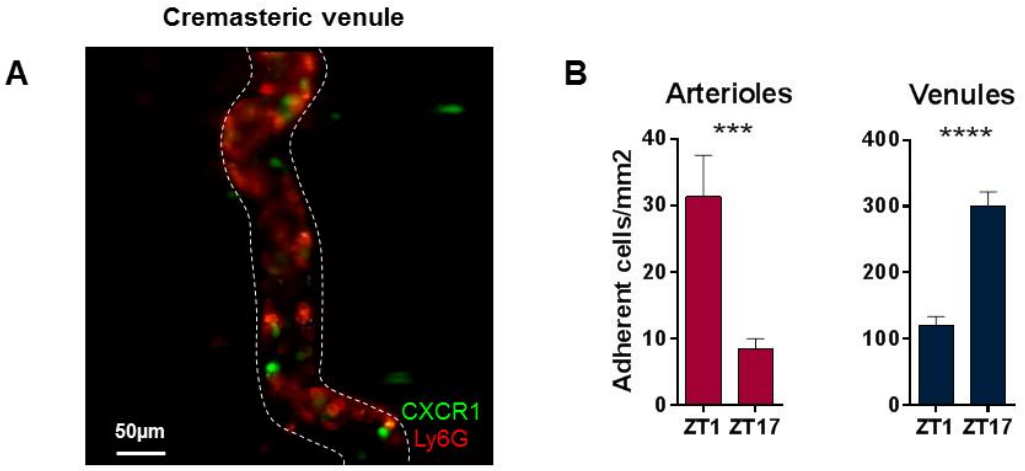

Figure 3.3 Differences in leukocyte adhesion in microvasculature. (A) Epifluorescence microscopy image from a venule in the cremaster muscle after 3h TNF-α stimulation. CXCR1-GFP mice showed GFP labeled inflammatory monocytes and neutrophils were labeled with Ly6G-PE. (B) Cell adhesion quantification in arterioles and venules (n = 5 mice), t-test ***p < 0.001, ****p< 0.0001.

We next quantified the surface expression levels of the integrins LFA-1 (CD11a) and Mac-1 (CD11b) on the adherent cells in the large caliber vessels *in situ*. No oscillation was observed for LFA-1 expression in either vessel (**Figure 3.4**). Mac-1, in contrast, oscillated but in the same manner for carotid and jugular, suggesting

that the differences observed in leukocyte adhesion were not due to the leukocyte phenotype but the microenvironment.

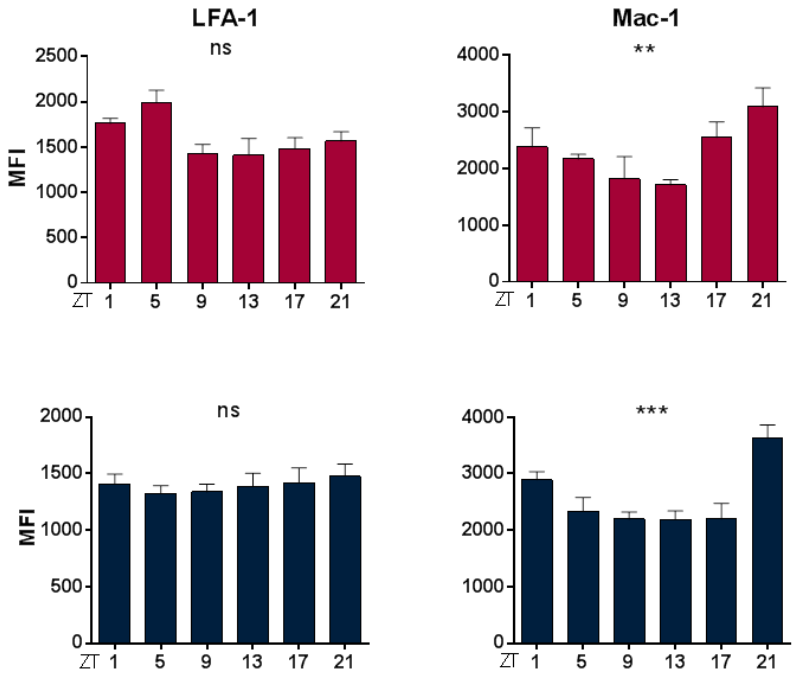

Figure 3.4 Differences in β2-integrins expression on adherent leukocytes. LFA-1 and Mac-1 mean fluorescence intensity from adherent leukocytes (CD11a+ or CD11b+ cells) in carotid artery (red) and jugular vein (blue) at different times of the day, after 2h TNF-α stimulation (n= 5-8 mice), one-way ANOVA **p < 0.001, ***p < 0.0001, ns, not significant.

To verify if these differences were driven by the microenvironment, we performed adoptive transfer assays where we injected donor cells - harvested from bone marrow and spleen and labeled with CFSE - from mice kept at the same time simultaneously into recipients that were phase-shifted to ZT1 and ZT17. Labeled cells were injected 2h prior to harvesting the vessels and mice were stimulated simultaneously with TNF-α as described before. Carotid artery and jugular vein were harvested and digested in order to perform flow cytometry (**Figure 3.5A**). We observed oscillations in the numbers of CFSE+ recruited cells in artery and vein and with the same peaks as before; higher numbers of cells in the morning in the

carotid artery and the opposite for the jugular vein (**Figure 3.5B**), even though the leukocytes were from the same time point. This confirmed the important role of the microenvironment in this phenomenon.

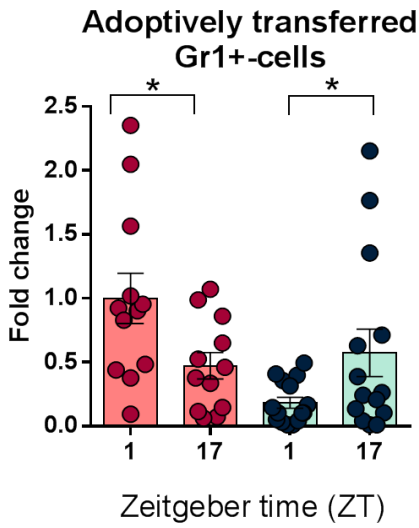

Figure 3.5 Relevance of the microenvironment in CFSE+ cells homing. Gr1+ cells from CFSE+ injected cells found in carotid artery (red) and jugular vein (blue) at ZT1 and ZT17 after 2h TNF-α stimulation (n =12-15 mice), t-test *$p < 0.05$.

3.2 Involvement of cell adhesion molecules and chemokines in diurnal leukocyte recruitment

Endothelial cells play a critical role in leukocyte adhesion, since they are physically located between tissues and blood, where this process occurs. Leukocyte recruitment is mediated by cell adhesion molecules and chemokines, some of which are expressed by endothelial cells in a circadian manner (Scheiermann et al., 2013). To address if critical molecules involved in adhesion were oscillatory over the day, we harvested the whole vessels after TNF-α stimulation for 2h at different time points and isolated RNA. qPCR analyses showed a 24h oscillation in

Icam1, Vcam1, Sele and *Selp*, which peaked at night in the jugular vein (**Figure 3.6**). In the case of the carotid artery, only *Icam1* expression oscillated significantly.

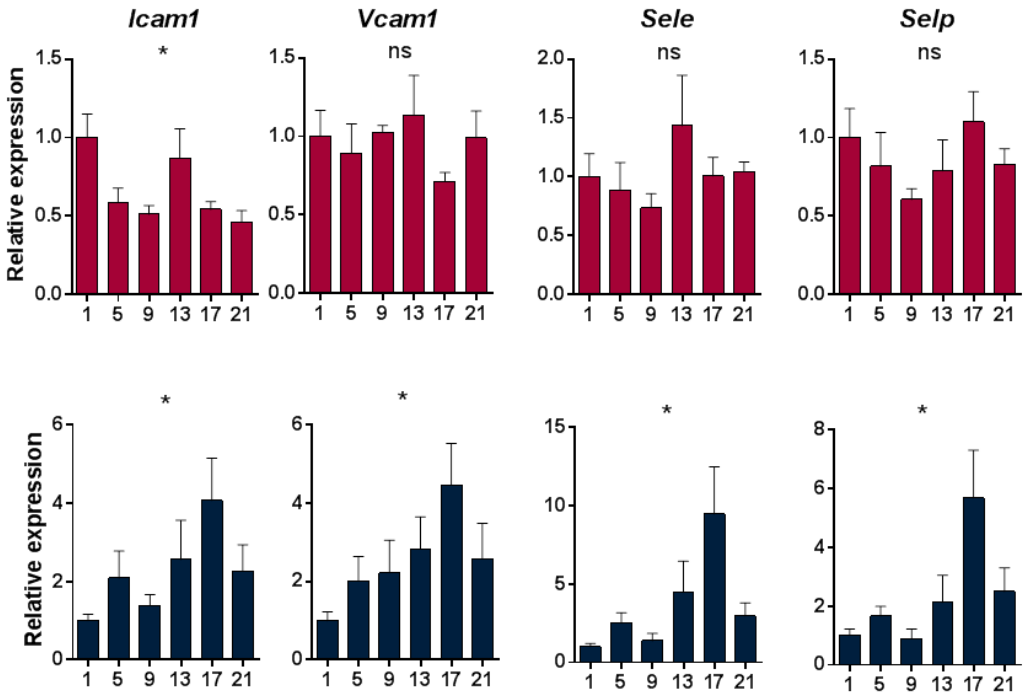

Figure 3.6 Cell adhesion molecule oscillations after inflammation. qPCR results of cell adhesion molecules from whole vessels, carotid (red) and jugular (blue), after 2h TNF-α stimulation at different time points during the day (n =3-6 mice), one-way ANOVA *p < 0.05.

In addition, we could report daily oscillations of the chemokines *Cxcl1, Cxcl2* and *Ccl2*, involved in myeloid cells trafficking in both vessels as well, with inverted phases in the carotid artery and the jugular vein (**Figure 3.7**). This suggests that the inflammatory response between arteries and veins dramatically differs over 24h.

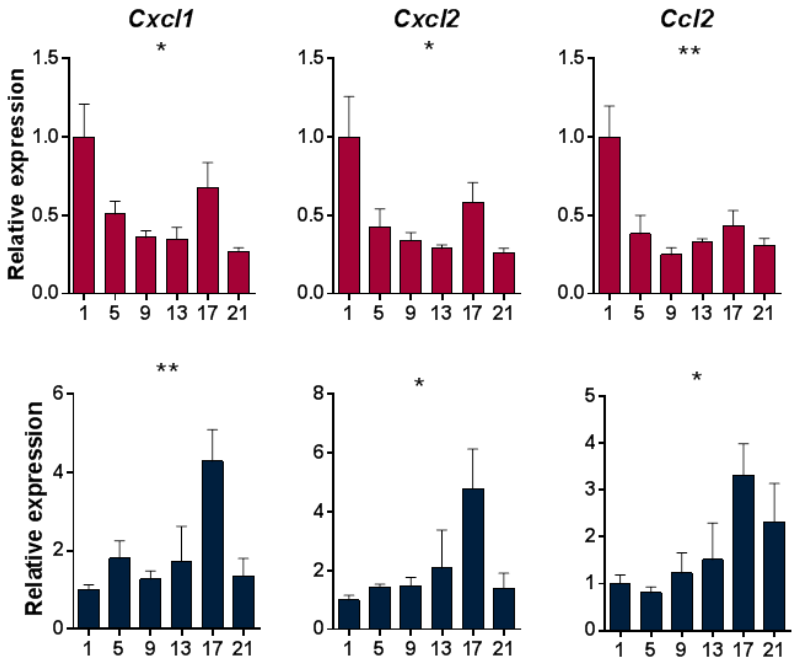

Figure 3.7 Chemokine oscillations over 24h in an inflammatory scenario. qPCR results of chemokine expression from whole vessels, carotid artery (red) and jugular vein (blue), after 2h TNF-α stimulation at different time points during the day (n =3 mice), one-way ANOVA *p < 0.05.

We next investigated whether changes in RNA levels of cell adhesion molecules correlated with protein levels. For that, we used OCT frozen sections of isolated vessels after TNF-α stimulation. Using staining for PECAM-1 (CD31), as a marker for endothelial cells, in combination with other antibodies for cell adhesion molecules, we detected corresponding protein oscillations for ICAM-1 and VCAM-1 specifically in endothelial cells (**Figure 3.8**).

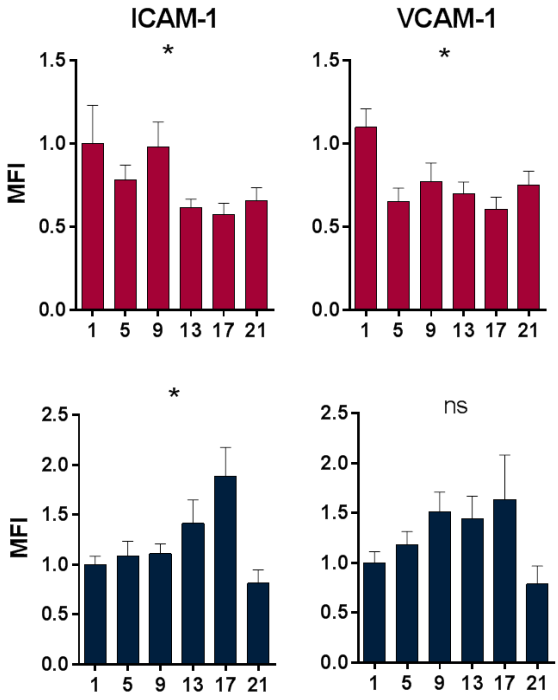

Figure 3.8 ICAM-1 and VCAM-1 protein oscillations over 24h during inflammation. ICAM-1 and VCAM-1 mean fluorescence intensities (MFI) in endothelium from carotid artery (red) and jugular vein (blue), at different time points during the day after 2h TNF-α stimulation (n = 3-6 mice), one-way ANOVA *p < 0.05.

Since ICAM-1 oscillatory expression phase-matched with the number of adherent leukocytes, we then performed *in vivo* quantitative imaging of cell adherence in *Icam1*$^{-/-}$ mice. When imaging the carotid artery of these mice at ZT1 and ZT17 (**Figure 3.9**), numbers of CD11a^{+} adherent cells no longer oscillated. Comparable observations were noticed in the jugular vein, where we could not detect differences between ZT1 and ZT17 as we did in the control mice, indicating the importance of this molecule in the time-of-day-dependent recruitment of leukocytes in both vessels.

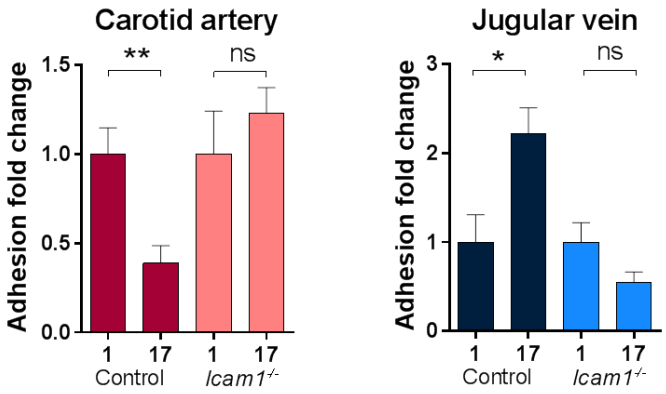

Figure 3.9 Leukocyte recruitment to large vessels in *Icam1*$^{-/-}$ mice. *In vivo* quantitative imaging of CD11a+ cells in carotid artery and jugular vein from *Icam1*$^{-/-}$ mice after 2h TNF-α stimulation at ZT1 versus ZT17 (n= 8-9 mice), t-test *p < 0.05, **p < 0.01, normalized to ZT1 levels.

We next blocked ICAM-1 or VCAM-1 with antibodies and performed the same procedure of imaging after 2h TNF-α stimulation in both vessels. In agreement with the *Icam1*$^{-/-}$ data, the oscillations were not seen any more either in carotid artery or jugular vein with an antibody targeting ICAM-1. The same effect was observed when VCAM-1 was blocked (**Figure 3.10**)

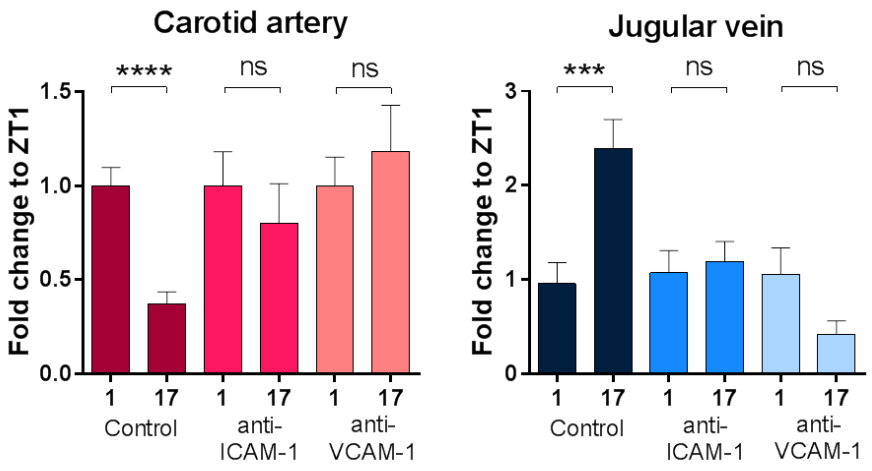

Figure 3.10 Importance of ICAM-1 and VCAM-1 in oscillatory recruitment in large vessels. *In vivo* quantitative imaging of CD11a+ cells in carotid artery and jugular vein after 2h TNF-α stimulation at ZT1 versus ZT17. ICAM-1 and VCAM-1 were blocked with anti-ICAM1 or anti-VCAM1 antibodies. (n= 4-16 mice), t-test ***p < 0.001, ****p<0.0001, normalized to ZT1 levels.

Similar results were obtained when we injected chemokine receptor antagonists against CXCR2 and CCR2 in the jugular vein but only for CCR2 in the carotid artery (**Figure 3.11**). This suggested the importance of the chemokines CXCL1 and CXCL2 in the vein, and CCL2 in both vessels. These results demonstrated that distinct rhythms in the expression of adhesion molecules and chemokines in arteries and veins were critical determinants for the different leukocyte adhesion patterns we observed.

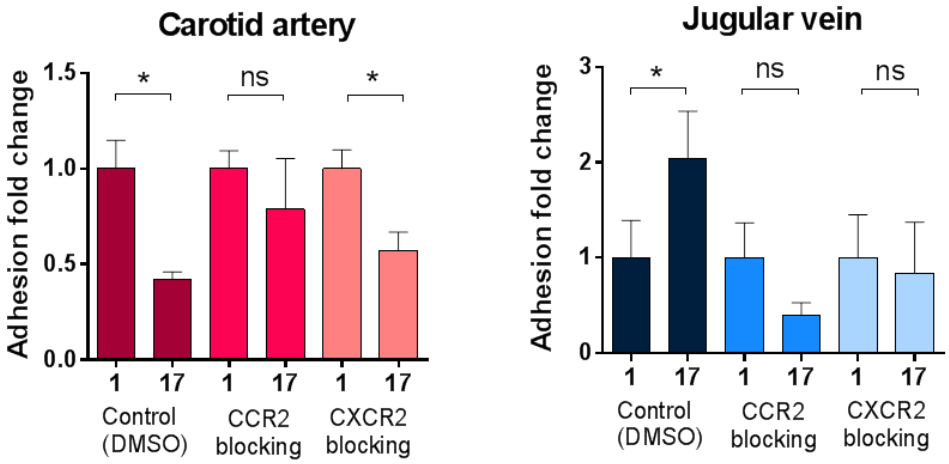

Figure 3.11 Functional role of chemokines in oscillatory leukocyte recruitment in large vessels. In vivo quantitative imaging of adherent CD11a+ cells in carotid and jugular vein after 2h TNF-α stimulation at ZT1 versus ZT17. CCR2 and CXCR2 were blocked with antagonists. (n= 4-6 mice), t-test *p < 0.05, normalized to ZT1 levels.

3.3 Similar circadian oscillations in arteries and veins

In collaboration with Prof. Dr. Henrik Oster, University of Lübeck, we examined whether overall circadian rhythms were different between arteries and veins. They used an *mPer2*^{Luc} mouse strain, in which a firefly luciferase gene has been knocked-in to the terminal exon of the clock gene *Per2,* producing a PER2::LUC fusion protein as described (Yoo et al. 2004). Using these animals, the aorta was harvested as a proxy for the arterial vascular bed and the vena cava as a proxy for the venular vascular bed. Both vessel segments were cultured for multiple days in tissue culture dishes. Luciferase expression exhibited noticeable circadian fluctuations in artery and vein, with a more pronounced rhythm in artery and differences in the peak times, peaking a few hours earlier in the vein than in the

artery (**Figure 3.12**). This indicated that underlying clock gene expression profiles in arteries and veins might be different.

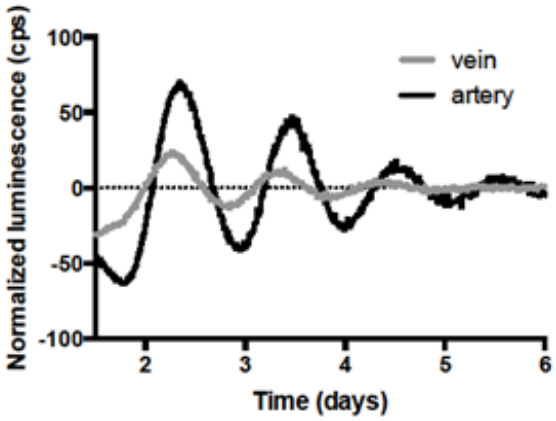

Figure 3.12 PER2 daily oscillations in arteries and veins. Differences in luminescence between samples from artery or vein (left). Peak time comparison between vein and artery (right).

However, when we checked the expression of core circadian genes in these tissues (*Bmal1*, *Clock*, *Per1*, *Per2* and *Cry1)* they all showed high overlap, peaking and troughing at the same times in the light cycle both in steady state (**Figure 3.13**) and TNF-α-induced inflammatory conditions (**Figure 3.14**). These data indicated that it was not the differences in the underlying rhythmicity of tissues that was driving the observed difference in oscillations but that an additional factor might regulate leukocytes differently in a timely manner between arteries and veins. In addition, TNF-receptor expression was not rhythmic in either arteries or veins (**Figure 3.15**).

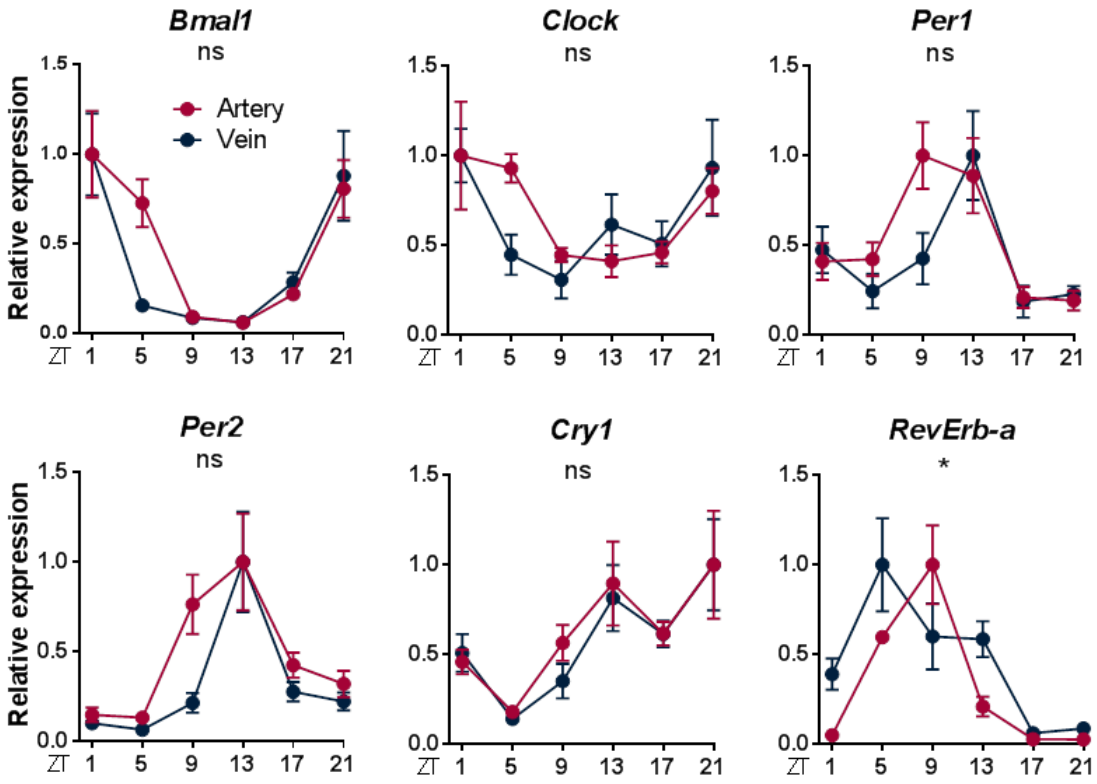

Figure 3.13 Circadian clock genes oscillations in arteries and veins in steady state conditions. Clock gene expression was analyzed by qPCR from RNA extracted from whole vessels, carotid artery (red) and jugular vein (blue), in steady state conditions at different time points during the day. A significant effect of time was observed for all genes, but only Rev-Erba showed a difference between vessels (n = 6 mice), two-way ANOVA *p < 0.05.

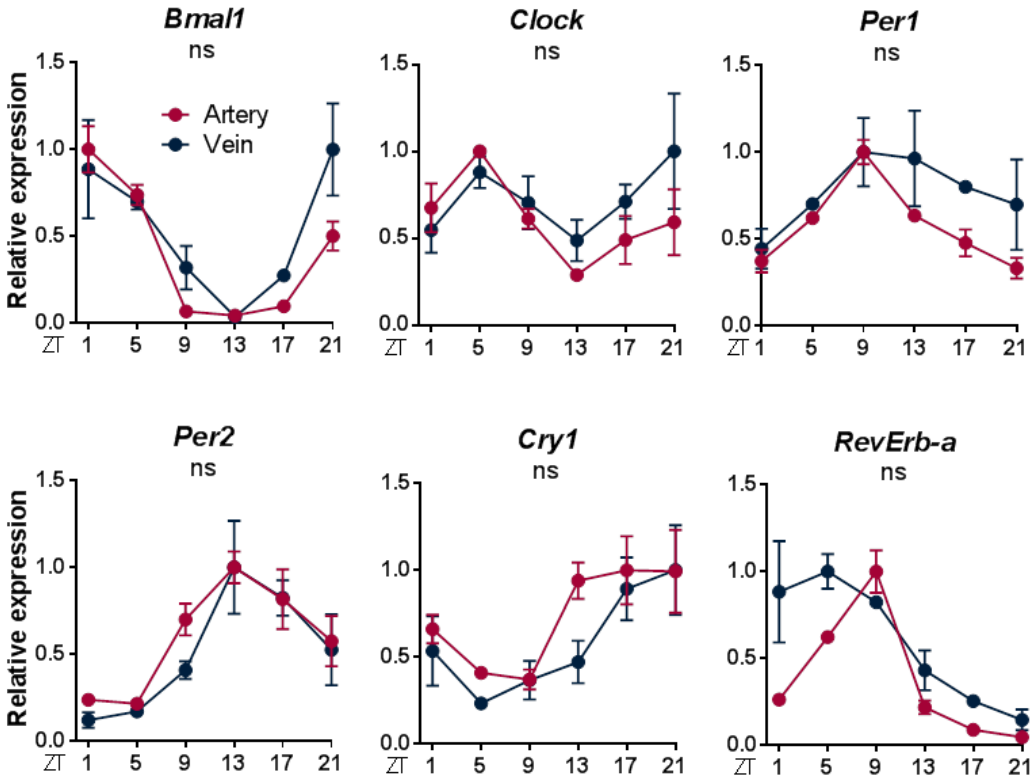

Figure 3.14 Circadian clock gene oscillations in arteries and veins in inflammatory conditions. Clock gene expression was analyzed by qPCR from RNA extracted from whole vessels, carotid (red) and jugular (blue), after 2h TNF-α stimulation at different time points during the day. Significant oscillations were observed for all genes, with no difference between vessels. (n = 3-4 mice), two-way ANOVA.

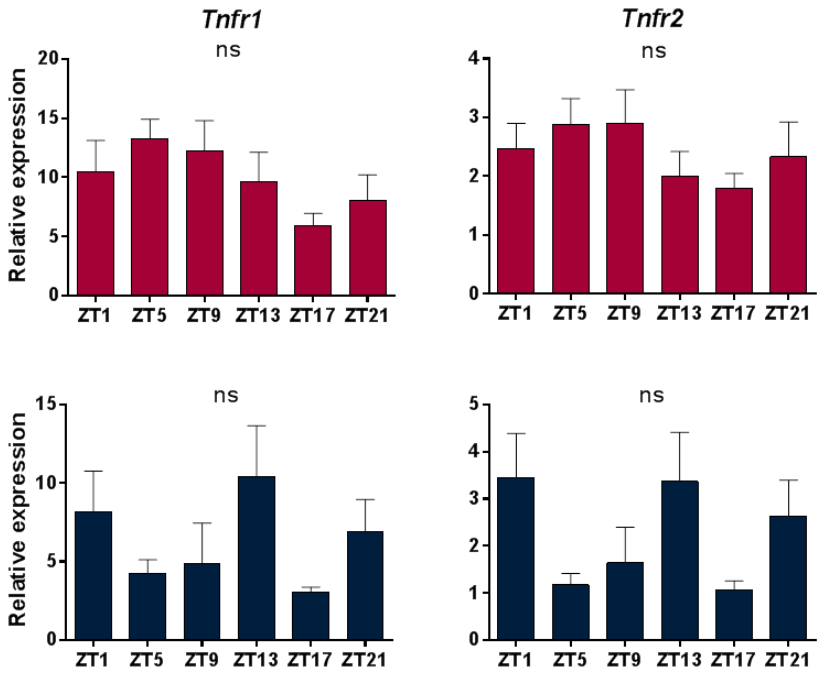

Figure 3.15 *Tnfr1* and *Tnfr2* oscillations in large vessels. TNF-α receptors 1 and 2 were measured by qPCR in steady state conditions from RNA from whole vessels every 4h during a day (n = 6 mice), one-way ANOVA.

3.4 Sympathetic control of circadian leukocyte recruitment in arteries and veins

The sympathetic nervous system (SNS) is an important orchestrator of rhythmicity in peripheral tissues, so we decided to investigate if its disruption at different levels could have an effect in leukocyte adhesion. First, we targeted the SNS systemically using a treatment with the compound 6-OHDA and performed *in vivo* imaging at ZT1 and ZT17 (**Figure 3.16**). This resulted in a lack of oscillation in adherent cell numbers in both vessels.

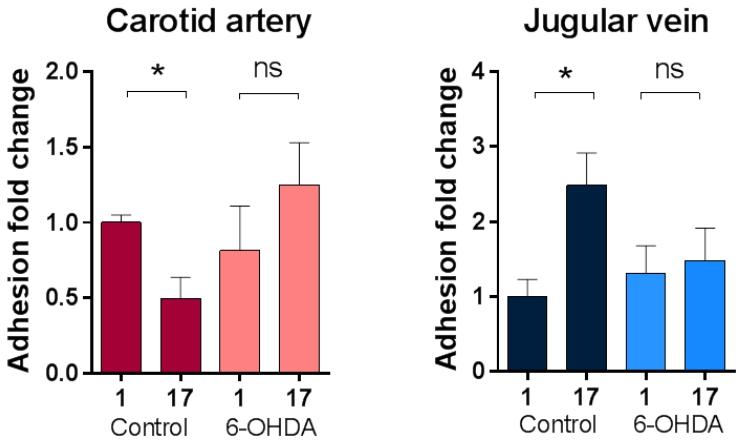

Figure 3.16 Leukocyte recruitment in animals with no sympathetic input. Mice were treated with 6-OHDA, a drug which disrupts sympathetic innervation, one week before the analysis. *In vivo* imaging was performed at ZT1 and ZT17, quantifying CD11a+ cells after 2h TNF-α stimulation (n = 5-8 mice), t-test *p < 0.05 normalized to ZT1 levels.

To assess the functional role of direct sympathetic innervation in this process, we surgically denervated the sympathetic contribution to vessels locally by cutting the superior cervical ganglion unilaterally. While the contralateral, nerve-intact, side still exhibited rhythmicity in leukocyte adhesion (**Figure 3.17**), local denervation resulted in a loss of oscillations.

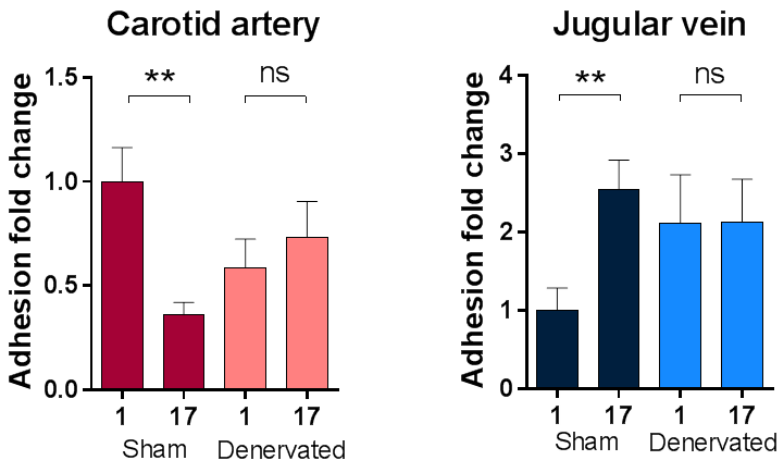

Figure 3.17 Leukocyte recruitment in animals after surgical denervation. Mice were unilaterally denervated by surgical removal of the superior cervical ganglion (SCG) one month before the analysis. *In vivo* imaging was performed at ZT1 and ZT17, quantifying adherent CD11a+ cells after 2h TNF-α stimulation (n = 5-12 mice), t-test **p < 0.01 normalized to ZT1 levels.

When measuring the cell adhesion molecule levels in these tissues (**Figure 3.18**), the differences between the expression at ZT1 and ZT17 were diminished in *Icam1* and *Vcam1* in the case of the carotid artery and in *Icam1, Vcam1, Sele,* and *Selp* in the jugular vein from denervated vessels.

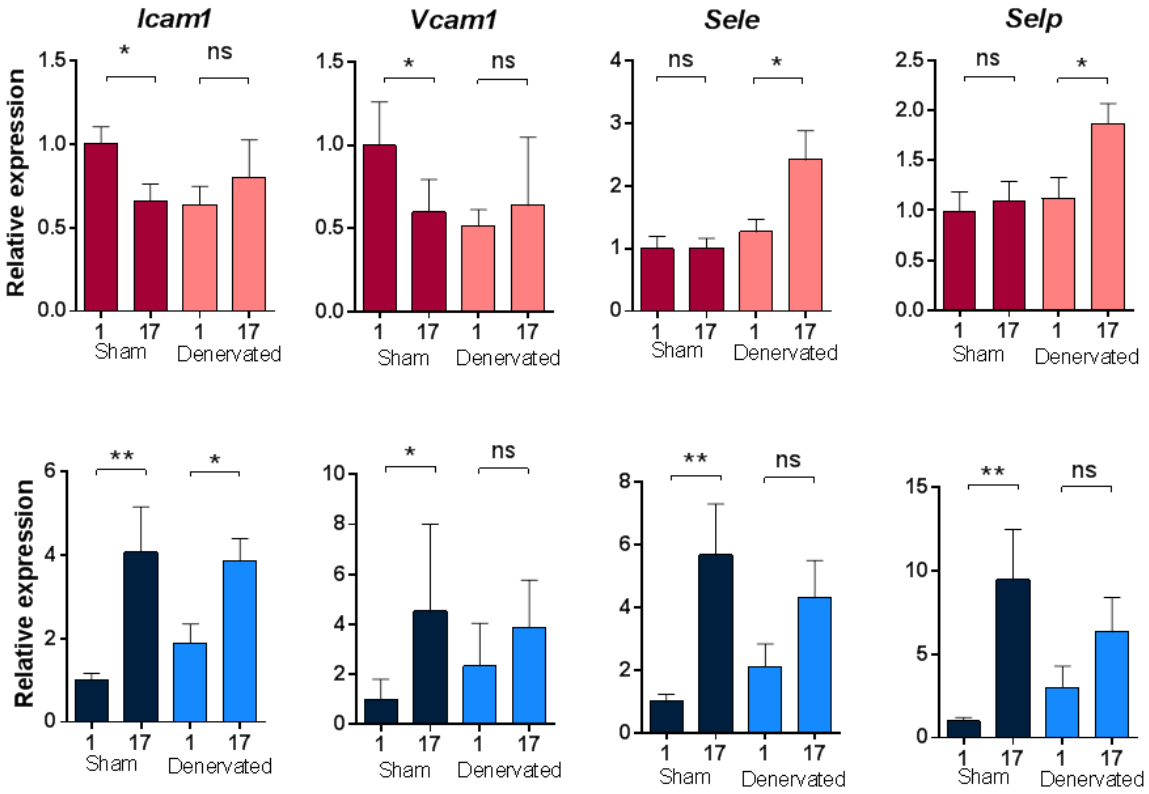

Figure 3.18 Cell adhesion molecule expression after surgical denervation. RNA from control and denervated vessels after 2h TNF-α stimulation was isolated and cell adhesion molecules checked by qPCR (n = 5-7 mice), t-test *p < 0.05, **p < 0.01.

We next wanted to determine which adrenergic receptors were involved in the rhythmicity observed in leukocyte recruitment in arteries and veins. For this, we injected the β2 antagonist butoxamine 2h before the imaging procedure. After blocking β2 adrenergic receptors pharmacologically, we observed an ablation in the time-of-day difference in leukocyte adhesion between ZT1 and ZT17 in the artery but not in the vein (**Figure 3.19**). This effect was restricted to ZT1, suggesting the importance of β2 adrenergic signaling in the early morning.

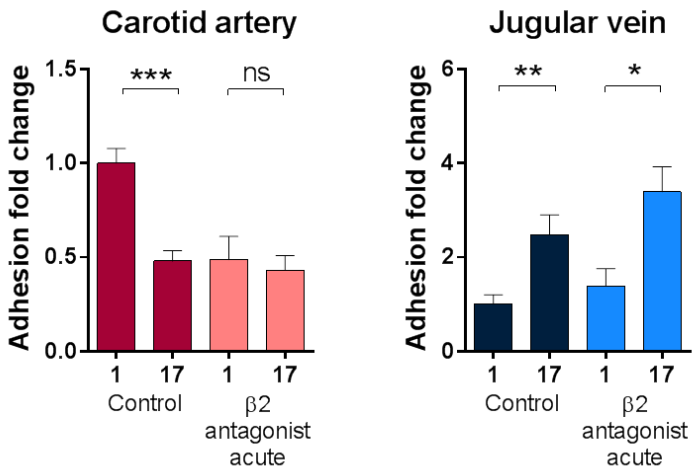

Figure 3.19 Leukocyte recruitment in animals after acute β2 adrenergic receptor blockade. β2 antagonist was injected i.p. 2h before the analysis. *In vivo* imaging was performed at ZT1 and ZT17, quantifying CD11a+ cells after 2h TNF-α stimulation (n = 6-11 mice), t-test, *p < 0.05, **p < 0.01, ***p < 0.001 normalized to ZT1 levels.

In order to link this observation with *Icam1* expression, we isolated RNA from vessels and performed qPCR analyses (**Figure 3.20**). There was a downregulation of *Icam1* after blocking β2 adrenergic receptors in the carotid artery at ZT1 but there was no effect in *Icam1* expression in jugular vein at any of the two time points, which correlated with the lower number of recruited cells found at this time in the artery but not in the vein.

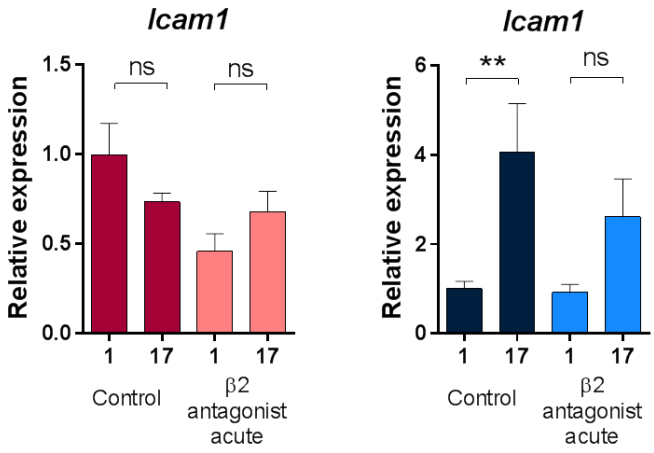

Figure 3.20 *Icam1* expression after acute β2 adrenergic receptor blockade. β2 antagonist was injected i.p. 2h before the analysis. Vessels were collected at ZT1 and ZT17, after 2h TNF-α stimulation and *Icam1* levels were checked by qPCR (n = 5-6 mice), t-test, *p < 0.05, **p<0.01 normalized to ZT1 levels.

Building on this data, we next tested the effects of chronic β2-adrenoreceptor antagonism, injecting the antagonist once a day, for 5 days in a row. After this chronic block of β2 adrenergic receptors, oscillatory recruitment was ablated in both vessels (**Figure 3.21**).

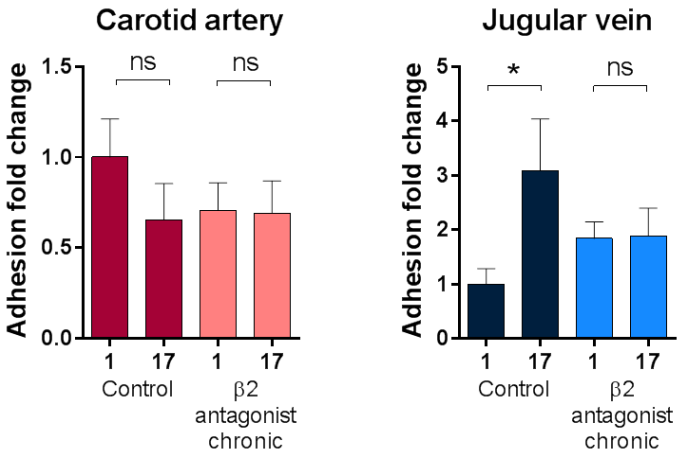

Figure 3.21 Leukocyte recruitment in mice after chronic β2 adrenergic receptor blockade. β2 antagonist was injected during 5 consecutive days before the analysis. *In vivo* imaging was performed at ZT1 and ZT17, quantifying adherent CD11a+ cells after 2h TNF-α stimulation (n = 4-7 mice), t-test *p < 0.05 normalized to ZT1 levels.

In this set of experiments, no oscillation in *Icam1* was observed with chronic antagonist treatment in both vessels (**Figure 3.22**).

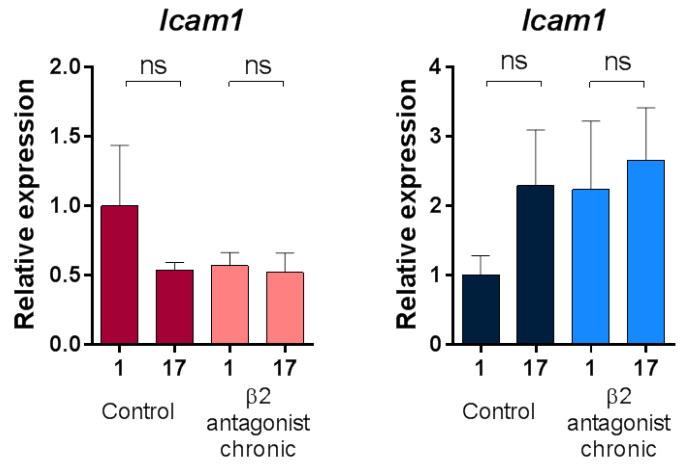

Figure 3.22 *Icam1* expression after chronic β2 adrenergic receptor blockade. β2 antagonists were injected i.p. during 5 consecutive days before the analysis. Vessels were collected at ZT1 and ZT17, after 2h TNF-α stimulation and *Icam1* levels were checked by qPCR (n = 3-4 mice), t-test *p < 0.05.

Finally, we validated the importance of the β2 adrenergic receptors genetically by using *Adrb2*$^{-/-}$ mice. When measuring numbers of adherent CD11a^{+} cells in these mice at ZT1 vs ZT17 after 2h TNF-α stimulation, oscillations were also lost in the artery but inverted in the vein (**Figure 3.23**).

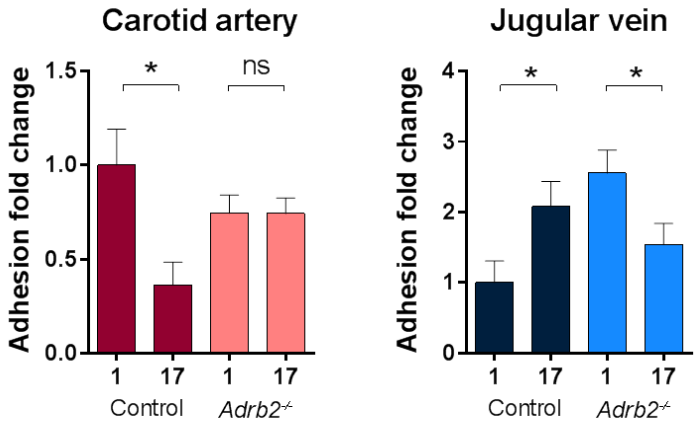

Figure 3.23 Leukocyte recruitment in *Adrb2*$^{-/-}$ mice in inflammation. *In vivo* imaging was performed at ZT1 and ZT17, quantifying adherent CD11a+ cells after 2h TNF-α stimulation (n = 7-9 mice), t-test *p < 0.05 normalized to ZT1 levels.

Icam1 expression in vessels obtained from the *Adrb2*$^{-/-}$ mice was also non-oscillatory (**Figure 3.24**) according with the lack of oscillations in recruited leukocytes in both vessels.

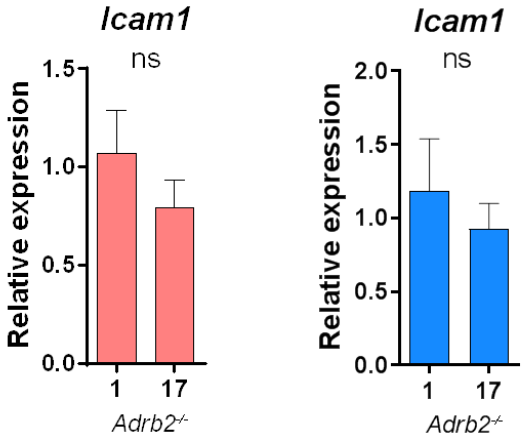

Figure 3.24 *Icam1* expression in *Adrb2*$^{-/-}$ mice. Vessels from *Adrb2*$^{-/-}$ mice were collected at ZT1 and ZT17, after 2h TNF-α stimulation and *Icam1* levels were checked by qPCR (n = 8-9 mice), t-test *p < 0.05.

3.5 Differences in adrenergic input between arteries and veins

Although the sympathetic nervous system (SNS) has been shown to regulate circadian leukocyte recruitment (Scheiermann et al. 2012) it is not understood how adrenergic signals are transduced to veins, the main site of leukocyte recruitment, since sympathetic innervation is present in arterioles but not in small venules. In this part, we aimed to elucidate the mechanisms of signal transduction and the cell types involved.

Tyrosine hydroxylase (TH) is the enzyme responsible for catalyzing the conversion of the amino acid L-tyrosine to L-3,4-dihydroxyphenalalanine (L-DOPA), which mediates neurotrophic factors release by the brain and CNS (Lopez et al. 2008). This factor is the precursor of catecholamines and TH is the rate-limiting enzyme in the catecholamine biosynthesis. TH is a thus a marker for adrenergic innervation, which can be combined with neurofilaments (NF) to label nerves. As shown in **Figure 3.25**, in the carotid artery we observed strong expression of both markers,

which was in stark contrast to the jugular vein, where the expression of these molecules was absent, indicating the lack of sympathetic innervation in this vein.

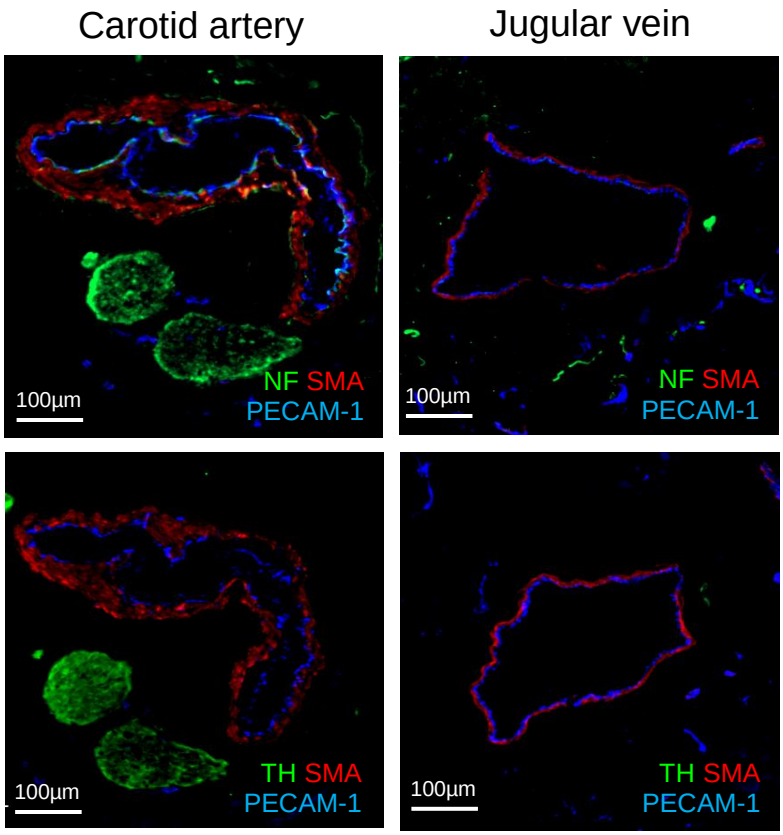

Figure 3.25 Sympathetic innervation in large vessels. Carotid artery (left) and jugular vein (right) were stained with CD31-APC (endothelial cells), SMA-PE (smooth muscle cells), and NF-488 (neurofilaments) or TH-AlexaFluor488 (tyrosine hydroxylase). Pictures were obtained with confocal microscopy (20x objective).

Similarly, when we measured tyrosine hydroxylase expression in the microvasculature of the cremaster muscle (**Figure 3.26**), we only detected its presence in arterioles but not venules.

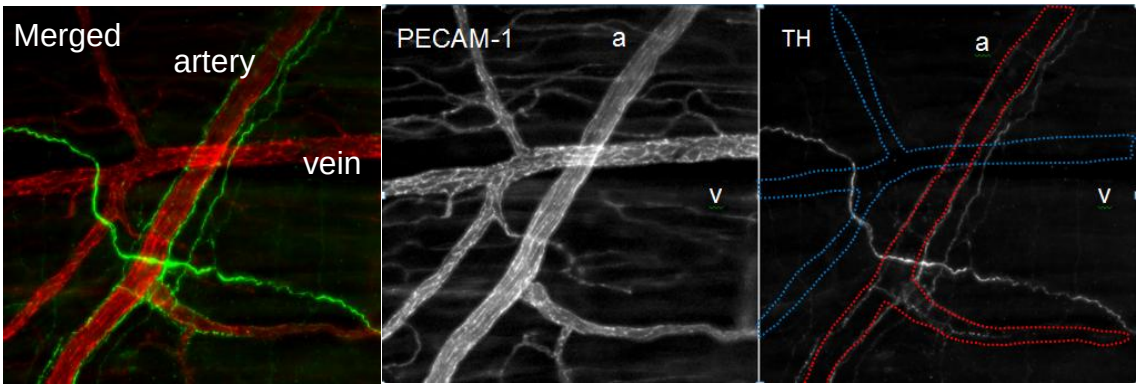

Figure 3.26 Sympathetic innervation in microvasculature. Confocal microscopy pictures from cremaster muscle vasculature (10x objective) were obtained after staining endothelial cells (PECAM-1 488) and tyrosine hydroxylase (TH-PE).

We confirmed TH expression analyses by qPCR in our model of denervation, where high expression of TH was detected at ZT1 in the carotid artery from the intact side (**Figure 3.27**). No TH was detected at ZT1 in carotid from the denervated side (data not shown) or in the jugular vein under all conditions tested.

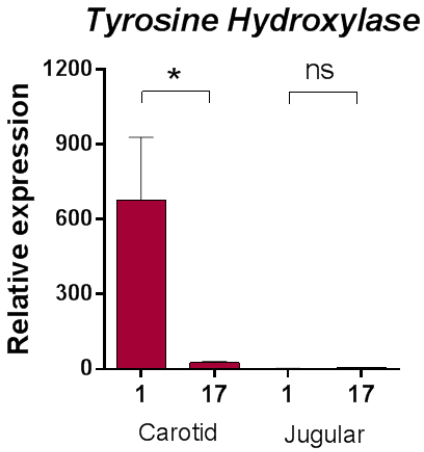

Figure 3.27 Tyrosine hydroxylase levels in large vessels. TH levels were measured by qPCR from RNA from carotid artery and jugular vein at ZT1 and ZT17 in steady state conditions. (n = 5-6 mice) t-test *$p < 0.05$.

Arterial innervation occurs at the level of $NG2^+$ mural cells, the expression of which is restricted to arteries (**Figure 3.28**).

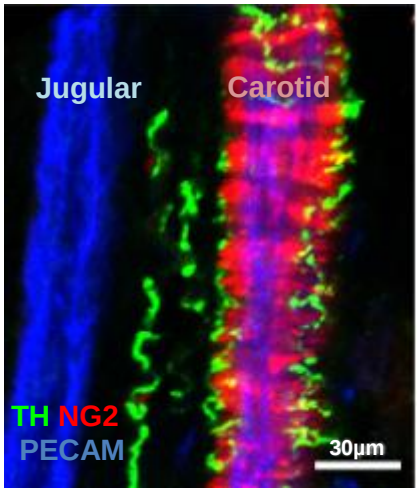

Figure 3.28 NG2 expression in large vessels. Confocal microscopy picture from jugular vein and carotid artery (10x objective). Tyrosine hydroxylase was stained with TH-488, arteriolar pericytes with NG2-PE and endothelial cells with PECAM-APC.

We could detect these mural cells in contact with TH fibers at the cremaster microcirculation level as well (**Figure 3.29**).

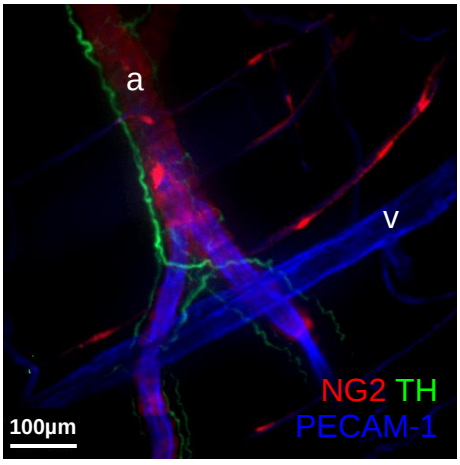

Figure 3.29 NG2 expression in microvasculature. Confocal microscopy image from jugular vein and carotid artery (10x objective). Tyrosine hydroxylase was stained with TH-Alexa488, arteriolar pericytes with NG2-PE and endothelial cells with PECAM-1-APC.

In order to investigate how the lack of rhythmicity could affect leukocyte trafficking, we combined *Bmal1*$^{flox/flox}$ animals with *Ng2Cre*-bearing animals, targeting arteriolar pericytes. Quantitative *in vivo* imaging with these mice after 2h TNF-α stimulation showed an ablation of the oscillations in adherent cells in the carotid artery. Surprisingly, oscillations in the jugular vein were altered as well, even though arteries were the genetic target of this approach (**Figure 3.30**).

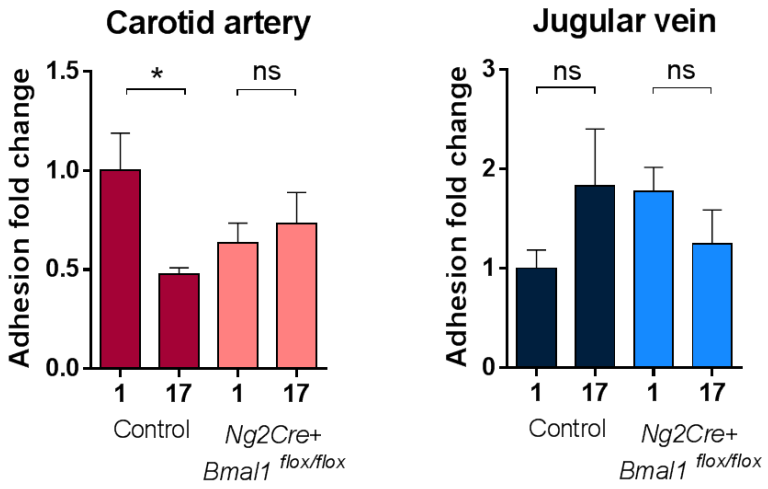

Figure 3.30 Leukocyte recruitment in *Ng2Cre+ Bmal1*$^{flox/flox}$ mice in inflammation. *In vivo* imaging was performed at ZT1 and ZT17, quantifying adherent CD11a+ cells after 2h TNF-α stimulation (n = 5-8 mice), t-test *p < 0.05 normalized to ZT1 levels.

To assess the reduction of *Bmal1* and *Icam1* in carotid artery and jugular vein, we harvested both vessels after TNF-α stimulation. *Bmal1* was reduced in both vessels, artery and vein (**Figure 3.31**), indicating that although the Cre was specific for arteriolar pericytes there was an effect in the vein. This was also seen for *Icam1* expression, which was reduced in both vessels.

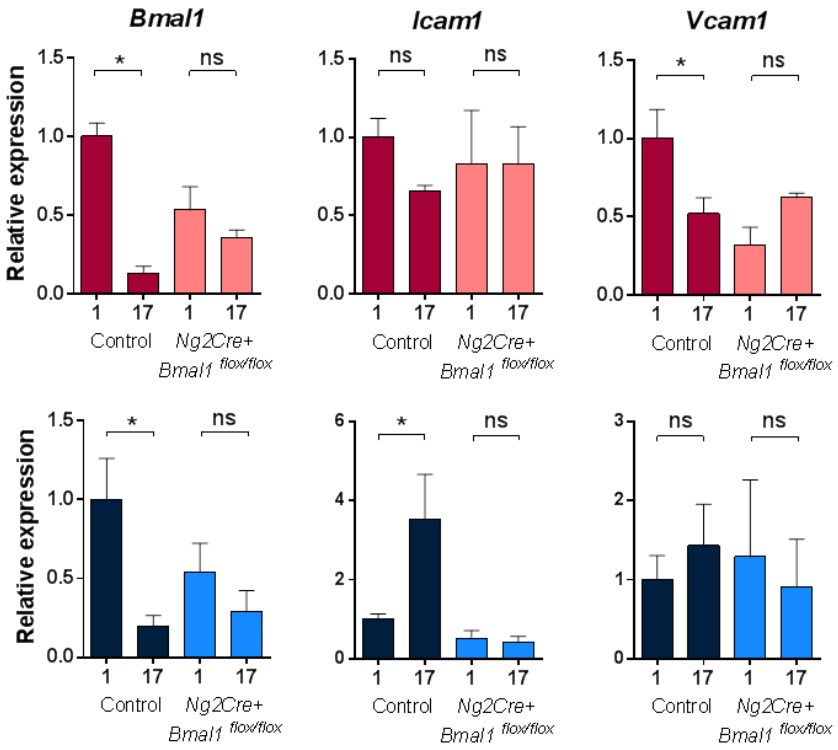

Figure 3.31 *Bmal1, Icam1* and *Vcam1* expression in *Ng2Cre+ Bmal1$^{flox/flox}$* mice. Carotid artery (red) and jugular vein (blue) from *Ng2Cre+ Bmal1$^{flox/flox}$* mice were collected at ZT1 and ZT17, after 2h TNF-α stimulation and *Bmal1, Icam1* and *Vcam1* levels were checked by qPCR (n = 3-7 mice), t-test *p < 0.05 normalized to ZT1 levels.

3.6 Clinical relevance: circadian thrombosis

In order to investigate if the activation status of adherent leukocytes was different between adherent cells in venules or arterioles, we used *in vivo* quantitative imaging and L-selectin expression (**Figure 3.32**). L-selectin can be used as an activation marker of neutrophils, the lower this protein is expressed, the more activated the cell is. As shown in the **Figure 3.32C**, $CD11b^{+}$ cells were more activated at ZT5 than at ZT17 in the arterioles and vice versa in the venules,

suggesting different activation states between the arteriolar and venular leukocytes at different time points over the day.

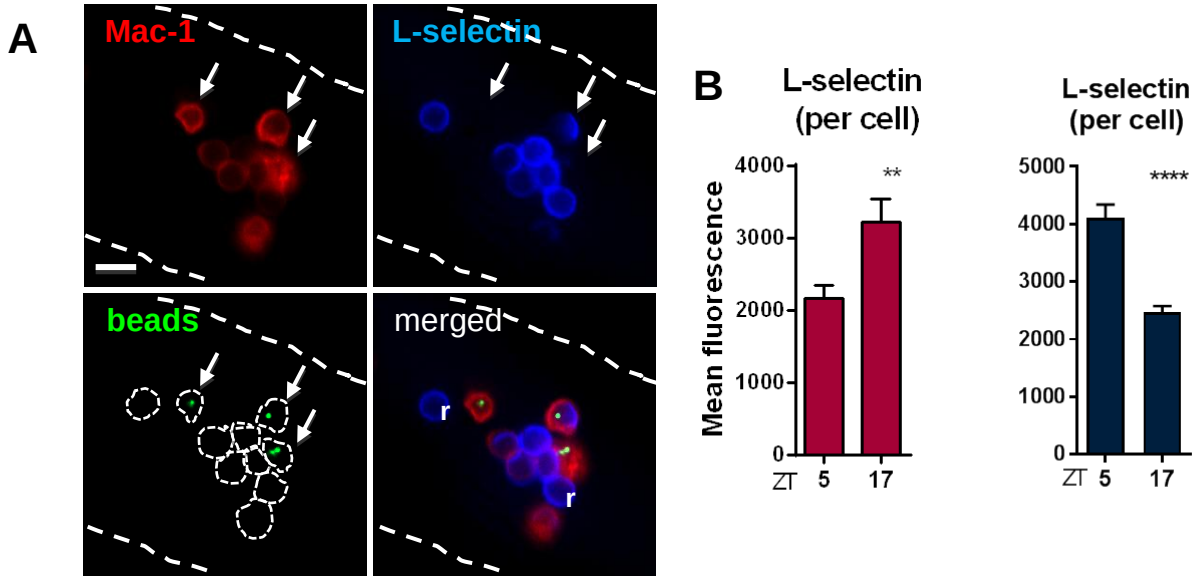

Figure 3.32 L-selectin levels in adherent cells from arterioles and venules. Epifluorescence microscope pictures (20x objective) from the cremaster microcirculation. Myeloid cells were stained with Mac-1-PE and L-selectin-APC. (A) Schematic example from recruited leukocytes in a cremasteric venule in which Mac-1, L-selectin and integrin activity through BSA-coated beads (488) were measured. (B) L-selectin levels were measured in adherent Mac-1+ cells in arterioles (red) and venules (blue) at ZT5 and ZT17 (mean fluorescence per cell), t-test **$p < 0.01$, ****$p < 0.0001$.

We focused next on the interactions produced between neutrophils and platelets in order to assess the relevance of different activation states of adherent neutrophils in arterioles and venules in the cremaster muscle after 3h TNF-α stimulation, using *in vivo* imaging. In contrast with the observations made in venules, the number of platelets-neutrophil interactions was higher at ZT1 and lower at ZT17 in arterioles

(**Figure 3.33**). This indicated a different phenotype in terms of activation in neutrophils or platelets found in arterioles and venules.

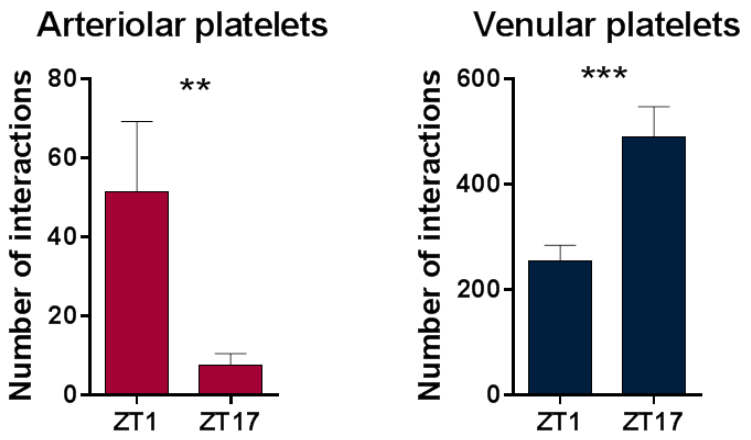

Figure 3.33 Platelet-neutrophil interactions in arterioles and venules. Interactions between platelets and adherent neutrophils were measured at ZT1 and ZT17 in arterioles and venules. (n = 6-21 vessels), t-test *p < 0.05, ***p < 0.001.

To test the relevance of our observations in pathology, we performed a thrombus formation model in the cremaster muscle. This method consists of injection of FITC-dextran i.v. to provoke phototoxicity of the compound after excitation with a laser of 488nm, which leads to damage in the endothelium and subsequent thrombus formation. The read-out was the occlusion time for the same-sized vessels we were targeting at different time points.

In the case of the venular side, a 24h oscillation was found in the time of occlusion, where ZT2 (2h after the onset of light, 9am) was the time point when the vessels took longer to be occluded compared to a shorter time at ZT8. The inverted case was observed in the arterioles, as the fastest occlusion time occurred at ZT2 and at ZT8 the longest (**Figure 3.34**). These results were in line with the activation status

data, indicating that a higher activation status of adherent leukocytes can lead to lower occlusion time in thrombosis.

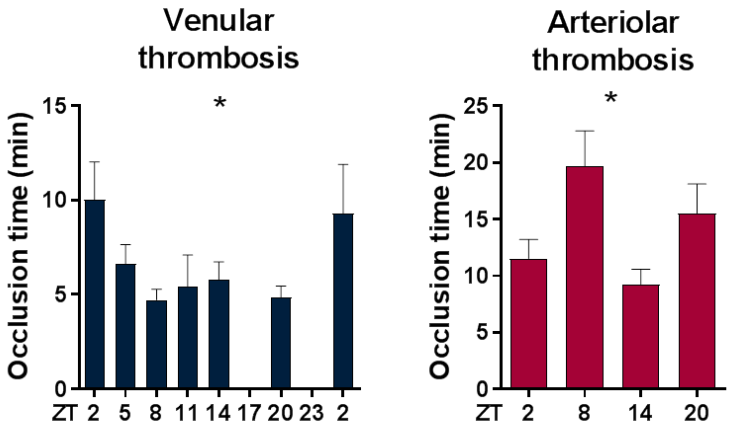

Figure 3.34 Circadian thrombosis in venules and arterioles. FITC-dextran phototoxicity was provoked by 488nm light in order to damage the endothelium and prompt thrombus formation in the cremaster microcirculation. Occlusion time was measured every 4h in venules and arterioles. ZT2 double-plotted in order to facilitate viewing, (n = 6-21 vessels), one-way ANOVA *$p < 0.05$.

When we performed these thrombosis experiments in *Ng2Cre Bmal1*$^{flox/flox}$ mice at ZT2 and ZT8, oscillations were ablated, suggesting the importance of rhythmicity in arteriolar pericytes in this process (**Figure 3.35**).

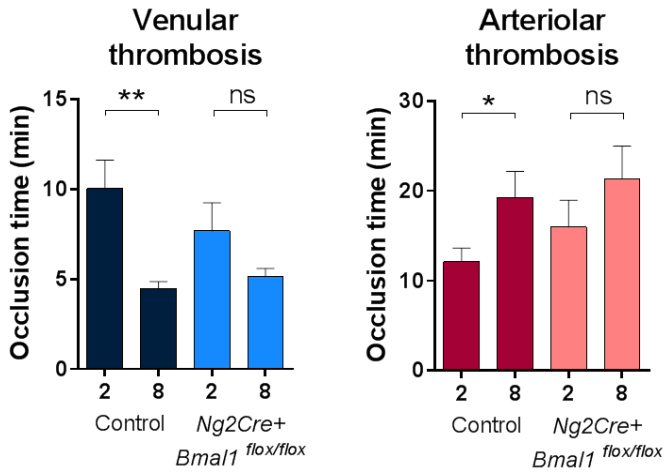

Figure 3.35 Circadian thrombosis in venules and arterioles from *Ng2Cre+ Bmal1$^{flox/flox}$* mice. Thrombus formation in the cremaster microcirculation from *Ng2Cre+ Bmal1$^{flox/flox}$* mice. Occlusion was measured at ZT2 and ZT8 (n = 6-21 vessels), t-test *p < 0.05, **p < 0.01.

4 Discussion

Circadian rhythms have helped organisms to adapt their body to their external environment. The recent link between circadian rhythms and the immune system has become a fast-growing field over recent years. Many primary research papers and a growing number of reviews have reported oscillations in the immune system, both innate and adaptive (Arjona et al. 2012; Scheiermann et al., 2013; Druzd et al., 2014; Curtis et al. 2014; Labrecque and Cermakian 2015; de Juan et al. 2016).

Of particular importance for this project is the role of the SNS in rhythmic leukocyte trafficking and acute inflammation. As the group of Prof. Paul Frenette showed previously, local adrenergic input was indispensable for circadian leukocyte recruitment to tissues (Scheiermann et al., 2012). Interestingly, as described in the literature, adrenergic innervation is generally only found in arteries but not in veins in rats (Marshall, 1982). In line with this publication, we did not detect sympathetic innervation in the jugular vein or smaller venules in mice. It is in these latter post-capillary venules where leukocyte recruitment predominantly occurs in most organs, so how local adrenergic input can influence leukocyte trafficking in veins is unknown. The purpose of this thesis was to clarify the diverse mechanisms involved in leukocyte recruitment to arteries and veins, with respect to similarities and differences between vascular beds, in an inflammatory scenario and in a circadian manner. After using pharmacological, surgical and genetic approaches, our data point to an important role of arteries and artery-associated sympathetic nerves in regulating rhythmic leukocyte recruitment to veins.

4.1. Circadian differences in leukocyte recruitment between arteries and veins

Rhythmic leukocyte trafficking has been previously shown to occur under steady state conditions (Scheiermann et al., 2012) and in inflammatory scenarios, where Nguyen and colleagues reported that Ly6C^{HI} inflammatory monocytes exhibit diurnal variation, controlling their trafficking to sites of inflammation (Nguyen et al., 2013). However, no study has ever distinguished between arteries and veins. There are several diversities when comparing arteries and veins, in terms of structure and function, as detailed in the introduction. In this study, we could show that leukocyte adhesion during inflammation follows circadian rhythmicity in both arteries and veins, but with opposite patterns. While the peak number of adherent cells was found at ZT1 (8:00h) in the carotid artery, and the trough at ZT17 (0:00h), the inverse was true for the jugular vein. Importantly, we could extend the relevance of these observations to the cremaster muscle microcirculation. This suggested that the phenotype was due to a vessel-intrinsic mechanism and not due to the tissue. Importantly, we detected similar time-of-day differences in arterial and venous blood, exhibiting higher leukocyte numbers at ZT1 compared to ZT13. This suggested that the differences observed in recruitment were not due to different numbers in circulating leukocytes in the arterial or venous compartments.

We investigated whether adherent cells showed different expression of leukocyte adhesion molecules among the day. LFA-1 and Mac-1 were measured *in situ* in cells adherent to veins and arteries. We detected no difference between cells from artery or vein, suggesting that a microenvironmental effect was responsible for the observations. This hypothesis was confirmed by performing an adoptive transfer assay, where we could observe that even if injected cells were coming from the same donor, there were still differences in the recruitment between arteries and veins when the recipients were at different timing regimes: whereas the highest recruitment was found for the artery at ZT1 and the lowest at ZT17, the opposite case was observed in the vein.

In summary, this data suggested the differences in leukocyte recruitment in arteries and veins were not due to the leukocyte but the microenvironment.

4.2. Cell adhesion molecules and chemokines are involved in circadian recruitment

Cell adhesion molecules and chemokines are crucial in the leukocyte recruitment process. A circadian expression of different pro-inflammatory mediators such as cytokines, chemokines or cell adhesion molecules has previously been reported. For example, CCL2 and CXCL1 have been found to oscillate in serum from mice (Gibbs et al., 2012), as well as CXCL12 in bone marrow (Mendez-Ferrer et al., 2008). In the case of cell adhesion molecules, ICAM-1 peaks at the onset of the activity phase in muscle endothelial cells, as well as E-selectin, P-selectin and VCAM-1 in endothelial cells from bone marrow (Scheiermann et al., 2012).

The mechanisms of cell adhesion molecule upregulation in veins and arteries are identical (Nabah et al., 2005), but the distribution of ICAM-1, for instance, is different between the two vessels. Compared with arteries, venular endothelium expresses higher ICAM-1 levels in steady-state conditions. In addition, the luminal surface area of arteriolar ECs is roughly twice that of venular ECs, so they simply cannot reach sufficient surface density levels of ICAM-1 to promote leukocyte adhesion (Sumagin and Sarelius, 2006). This evidence, together with the higher pressure and velocity of the blood in arteries, could explain the absence of leukocyte adhesion in arterioles under normal situations.

However, when we checked the expression *of Icam1, Vcam1, Selp* and *Sele* after induction of acute inflammation, a different upregulation profile between arteries and veins across the day was detected. In veins, there was a much higher expression of all of these transcripts at ZT17. In the case of artery, *Icam1* was the only transcript that showed an oscillation, although at the protein level, both ICAM-

1 and VCAM-1 matched our recruitment data. Additionally, we checked expression levels for the chemokines *Cxcl1*, *Cxcl2* and *Ccl2* and found they also oscillated in a completely different manner between arteries and veins; in phase with the adherent leukocytes and the cell adhesion molecules described previously. This indicated that arteries and veins have different oscillatory expression patterns in terms of cell adhesion molecules under inflammatory conditions.

Since the ICAM-1 expression profile matched best with the recruitment data, functional assays were performed using ICAM-1 blocking antibodies. As a result, there was a lack of oscillations in recruitment to both vessels, implying the relevance of ICAM-1 in rhythmic leukocyte recruitment. We could confirm this observation using *Icam1*$^{-/-}$ mice and obtaining similar results. Furthermore, functional blocking of VCAM-1, CXCR2, or CCR2 also reduced differences of adhesion and rendered them arrhythmic, with the exception of CXCR2 in the artery, confirming the importance in their oscillatory expression in mediating adhesion rhythmicity.

In conclusion, the diversity in the molecular signature of circadian expression of endothelial cell adhesion molecules and chemokines in arteries and veins are responsible for the shifted times in the recruitment process.

4.3. Differences in recruitment are independent of circadian clock gene expression

Clock genes are expressed in a rhythmic fashion in peripheral tissues, due to the existence of peripheral clocks that are entrained by humoral or neuronal cues from the SCN (central clock). Virtually every single cell has a molecular clock, which consists of auto-regulatory mechanisms of different transcription factors (Druzd et al., 2014).

Since clock genes are responsible for the circadian expression of clock controlled genes which can be differentially expressed in a tissue-specific manner (Motosugi et al. 2011), we wanted to verify if differences in clock genes expression could explain the differences in leukocyte recruitment to arteries and veins.

In order to investigate if overall clock gene expression was altered between arteries and veins over the course of the day, we established a collaboration with Prof. Henrik Oster and his group at the University of Lübeck. They used the expression of one of the core clock proteins, PER2, fused with a luciferase reporter as a bioluminescent readout of clock phase. They noticed differences in circadian fluctuations between the aorta and the vena cava. They detected a higher amplitude in the artery than in the vein and that the peak time came earlier in the vein than in the artery, suggesting that clock gene expression could be different between those vessels.

However, while we did observe a strong daily oscillation when we screened circadian clock gene expression (*Bmal1, Clock, Per1, Per2* and *Cry*), we did not detect phase differences in carotid artery or jugular vein in steady state conditions or in an acute inflammatory scenario. In fact, clock gene expression profiles were similar to a previous study performed in samples from lymph nodes where, for example, *Bmal1* was exhibiting its peak at ZT1 and ZT21, in antiphase with *Per1* and *Per2*, its negative regulators (Druzd et al., 2017). An exception was *Nr1d1 (Rev-Erb)* expression, which was slightly different in expression between artery and vein. It would be interesting to study this difference further.

This suggested that the differences reported in leukocyte recruitment were not due to differences in underlying clock gene expression but to additional factors.

4.4 SNS controls rhythmic leukocyte recruitment in arteries and veins

The SNS is involved, among other activities, in different involuntary physiological processes associated with the body's response during a perceived threat. With respect to its role related to the vasculature, it plays a major part in the arteriolar control of vasoconstriction and blood pressure and post-ischemic revascularization.

Of particular relevance for our study is the role of the SNS in the control of the immune system. Peripheral tissues are targeted by the SNS by the release of catecholamines (adrenaline and noradrenaline) acting on adrenergic receptors of the α and β subtype (Elenkov et al., 2000). Both types of adrenergic receptors are found in innate immune cells, whereas T and B cells appear only to express β2 adrenergic receptors (Nance and Sanders, 2007). In fact, the β2 adrenergic receptor is the most abundant receptor in leukocytes. However, this receptor is not exclusively expressed in leukocytes but has a very broad distribution pattern. It can be found in other cells, such as endothelial cells (Howell et al., 1988).

Previous studies have linked the SNS with rhythmicity in the immune system. In the case of circulating HSCs and their progenitors in the bone marrow, oscillations were described to be inversely correlated with the expression of the chemokine CXCL12, involved in homing. It was shown that *Cxcl12* expression, as well as the release of HSCs, are under circadian control due to noradrenaline secretion by the SNS. Adrenergic input was described to locally target stromal cells ($Nestin^{+}$) present in the bone marrow through their β3-adrenergic receptors. As a consequence, the transcription factor SP1 was decreased, leading to a quick downregulation of *Cxcl12* (Mendez-Ferrer et al., 2008).

In the case of T cells, neural signals through β2-adrenergic receptors are involved in a reduction in the egress of lymphocytes from lymph nodes causing an increase of lymphocyte numbers in LNs at night in mice (Suzuki et al., 2016). Another complementary publication described that by deleting *Bmal1,* rhythmic expression

of *S1pr1* was abolished in T cells leading to non-oscillatory egress of lymphocytes (Druzd et al., 2017).

In addition, leukocyte recruitment to tissues is under adrenergic control. *Adrb2*$^{-/-}$ and *Adrb3*$^{-/-}$ mice that express no β2- or β3-adrenergic receptors, respectively, show no more oscillations in recruitment to either BM or muscle tissue. According to these results, administration of β2- or β3-adrenergic receptor agonists (clenbuterol or BRL37344, respectively) was found to significantly improve BM engraftment after transplantation (Scheiermann et al., 2012).

These studies are in line with our observations, as we could demonstrate that oscillations in leukocyte recruitment to arteries and veins were abolished after targeting the SNS. After chemical and surgical sympathetic denervation, differences in leukocyte recruitment between day and night, as well as in ICAM-1 expression, were ablated, confirming the important role of the SNS in rhythmic recruitment in arteries and veins. Furthermore, we could demonstrate that β2 adrenergic receptors were relevant in this phenomenon since administration of β2 adrenergic receptor antagonists lead to a lack of oscillations in leukocyte recruitment in arteries and veins. These results correlated with the abolished rhythmicity in ICAM-1 expression. We could observe the same phenotype when we used *Adrb2*$^{-/-}$ mice. In summary, we could demonstrate the importance of the SNS, specifically β2 adrenergic receptors, in circadian leukocyte recruitment to arteries and veins.

4.5 Arteries drive rhythmic recruitment in arteries and veins

As shown with our previous experiments, there is a critical role of the SNS in leukocyte recruitment to arteries and veins in an inflammatory scenario. However, it appears that veins are not directly innervated by this system as we saw no sympathetic innervation of the jugular vein or in venules from the microvasculature.

Another indication of the absence of this adrenergic input was observed in the jugular vein, where tyrosine hydroxylase expression was not detected.

Sympathetic nerves are in direct contact with smooth muscle cells in arterioles, so we hypothesized that pericytes were critical in receiving and transmitting local SNS signals to venules. In order to verify this idea, we made use of the differential expression profile of NG2 (neural/glial antigen 2), a marker of arteriolar pericytes, which is absent from veins (Murfee et al., 2005). We employed Ng2-cre targeted mice to ablate the core circadian gene *Bmal1* in arterial $Ng2^{+}$-mural cells (*Ng2Cre x Bmal1*$^{flox/flox}$). Surprisingly, even if the lack of rhythmicity was induced only in the artery, we could no longer detect oscillations in leukocyte recruitment between day and night in both arteries and veins. According to these results, when checking the expression of *Bmal1, Icam1* and *Vcam1*, we could detect a downregulation of these molecules in both vessels. This indicated that rhythms in the vein were affected by the artery.

4.6 Different susceptibility in circadian thrombosis between arteries and veins

Acute cardiovascular complications are the major cause of death in developed countries. Some cardiovascular diseases such as myocardial ischemia or infarction represent a higher risk during the morning in humans. In a study from Muller at al. they reported the highest number of infarcts was found between 10:00 and 12:00 in the morning (Muller et al., 1985). Leukocyte recruitment is of critical importance in vaso-occlusive crises, as shown in a model of sickle cell disease (Hidalgo et al., 2009). Furthermore, there is a critical role of circadian leukocyte adhesion events in the onset of acute cardiovascular diseases (Scheiermann et al., 2012). Actually, in a recent publication, it has been described how CCR2 surface expression on $Ly6C^{HI}$ monocytes oscillates in a rhythmic manner, influencing cardiac monocyte recruitment after an acute ischemic event (Schloss et al., 2017).

L-selectin expression can be used as an activation marker on neutrophils, as it is shed over 24h in these cells (Casanova-Acebes et al., 2013). The lower expression of this protein is, the more activated the leukocyte has become (Zhang et al. 2015). Using *in vivo* quantitative imaging, we could measure the levels of L-selectin in adherent cells from arteries and veins, in phase with our previous observations. L-selectin levels were lower in adherent cells in arteries in the morning and higher during the night, indicating that cells in the morning were more activated. Opposite results were obtained from the cells adherent in the venular side. This correlated with the data from neutrophil-platelet interactions. While the highest number of interactions was found in the morning in arteries, it was the opposite case for the veins, coinciding with the time of higher activation of the adherent cells in both vessels, respectively. Taken together, the intravascular activation status of the cells was in line with the leukocyte recruitment in arteries and veins.

In order to test the relevance of these findings in our study, we checked the occlusion time in a thrombosis assay at different times of the day, comparing arterioles and venules. We observed a 24h oscillation in the venular side. The peak was found at ZT2 (09:00h) and the trough at ZT8 (15:00h). However, when checking the arteriolar side, the observations were completely the opposite. The time of the day when the arterioles occluded most quickly was ZT2 and the most slowly was ZT8. There was a second peak at ZT20 (03:00), agreeing with a previous publication by Westgate and colleagues in which they were performing the experiments in the femoral artery (Westgate et al. 2008) reporting similar results as ours in the arterioles. When using different core clock gene knock-out mice, this oscillatory pattern was abolished. Of special interest, a disruption in the diurnal variation in occlusion time but not in systemic blood pressure was noticed in *Tie2Cre x Bmal1*$^{flox/flox}$ mice, in which *Bmal1* was specifically eliminated in endothelial cells. This suggested the importance of the microenvironment in the heightened susceptibility to vaso-occlusion at different times.

When we used *Ng2Cre x Bmal1*$^{flox/flox}$ mice, a specific Cre for arteriolar mural cells, in order to induce lack of rhythmicity specifically in arteries, we could report an

ablation of the differences of occlusion time in both vessels, arteries and veins. This result suggested an influence from the artery to the vein in terms of rhythmicity. However, we do not know the mechanism, yet. We presume this effect is not dependent on humoral factors since adrenergic receptors were not oscillating significantly in artery or vein. Our hypothesis is that this arterial influence of the vein might be due to a physical transduction of a signal via connexins, for instance.

Overall, the results from our experiments point to an important and previously unrecognized role of arteries in regulating rhythmic leukocyte recruitment to veins, which could have potential implications in driving time-of-day-dependent cardiovascular complications.

5 References

Alvarez, J.D., Chen, D., Storer, E., and Sehgal, A. (2003). Non-cyclic and developmental stage-specific expression of circadian clock proteins during murine spermatogenesis. Biology of reproduction *69*, 81-91.

Anderson, D.C., and Springer, T.A. (1987). Leukocyte adhesion deficiency: an inherited defect in the Mac-1, LFA-1, and p150,95 glycoproteins. Annual review of medicine *38*, 175-194.

Arjona, A., A. C. Silver, W. E. Walker, and E. Fikrig. 2012. 'Immunity's fourth dimension: approaching the circadian-immune connection', *Trends Immunol*, 33: 607-12.

Arjona, A., and Sarkar, D.K. (2006). The circadian gene mPer2 regulates the daily rhythm of IFN-gamma. Journal of interferon & cytokine research : the official journal of the International Society for Interferon and Cytokine Research *26*, 645-649.

Aschoff, J. (1960). Exogenous and endogenous components in circadian rhythms. Cold Spring Harbor symposia on quantitative biology *25*, 11-28.

Astrof, N.S., Salas, A., Shimaoka, M., Chen, J., and Springer, T.A. (2006). Importance of force linkage in mechanochemistry of adhesion receptors. Biochemistry *45*, 15020-15028.

Atsuta, J., Plitt, J., Bochner, B.S., and Schleimer, R.P. (1999). Inhibition of VCAM-1 expression in human bronchial epithelial cells by glucocorticoids. American journal of respiratory cell and molecular biology *20*, 643-650.

Barreiro, O., Yanez-Mo, M., Serrador, J.M., Montoya, M.C., Vicente-Manzanares, M., Tejedor, R., Furthmayr, H., and Sanchez-Madrid, F. (2002). Dynamic interaction of VCAM-1 and ICAM-1 with moesin and ezrin in a novel endothelial docking structure for adherent leukocytes. The Journal of cell biology *157*, 1233-1245.

Bazzoni, G., and Dejana, E. (2004). Endothelial cell-to-cell junctions: molecular organization and role in vascular homeostasis. Physiological reviews *84*, 869-901.

Bellet, M.M., Deriu, E., Liu, J.Z., Grimaldi, B., Blaschitz, C., Zeller, M., Edwards, R.A., Sahar, S., Dandekar, S., Baldi, P.*, et al.* (2013). Circadian clock regulates the host response to Salmonella. Proceedings of the National Academy of Sciences of the United States of America *110*, 9897-9902.

Bellet, M.M., Zocchi, L., and Sassone-Corsi, P. (2012). The RelB subunit of NFkappaB acts as a negative regulator of circadian gene expression. Cell cycle (Georgetown, Tex) *11*, 3304-3311.

Bihari, P., Holzer, M., Praetner, M., Fent, J., Lerchenberger, M., Reichel, C.A., Rehberg, M., Lakatos, S., and Krombach, F. (2010). Single-walled carbon nanotubes activate platelets and accelerate thrombus formation in the microcirculation. Toxicology *269*, 148-154.

Bunger, M.K., Wilsbacher, L.D., Moran, S.M., Clendenin, C., Radcliffe, L.A., Hogenesch, J.B., Simon, M.C., Takahashi, J.S., and Bradfield, C.A. (2000). Mop3 is an essential component of the master circadian pacemaker in mammals. Cell *103*, 1009-1017.

Casanova-Acebes, M., Pitaval, C., Weiss, L.A., Nombela-Arrieta, C., Chevre, R., N, A.G., Kunisaki, Y., Zhang, D., van Rooijen, N., Silberstein, L.E.*, et al.* (2013). Rhythmic modulation of the hematopoietic niche through neutrophil clearance. Cell *153*, 1025-1035.

Chalothorn, D., Zhang, H., Clayton, J.A., Thomas, S.A., and Faber, J.E. (2005). Catecholamines augment collateral vessel growth and angiogenesis in hindlimb ischemia. American journal of physiology Heart and circulatory physiology *289*, H947-959.

Charo, I.F., and Ransohoff, R.M. (2006). The many roles of chemokines and chemokine receptors in inflammation. The New England journal of medicine *354*, 610-621.

Chevre, R., J. M. Gonzalez-Granado, R. T. Megens, V. Sreeramkumar, C. Silvestre-Roig, P. Molina-Sanchez, C. Weber, O. Soehnlein, A. Hidalgo, and V. Andres. 2014. 'High-resolution imaging of intravascular atherogenic inflammation in live mice', *Circ Res*, 114: 770-9.

Chi, J.T., Chang, H.Y., Haraldsen, G., Jahnsen, F.L., Troyanskaya, O.G., Chang, D.S., Wang, Z., Rockson, S.G., van de Rijn, M., Botstein, D.*, et al.* (2003). Endothelial cell diversity revealed by global expression profiling. Proceedings of the National Academy of Sciences of the United States of America *100*, 10623-10628.

Ciccarelli, M., Sorriento, D., Cipolletta, E., Santulli, G., Fusco, A., Zhou, R.H., Eckhart, A.D., Peppel, K., Koch, W.J., Trimarco, B.*, et al.* (2011). Impaired neoangiogenesis in beta(2)-adrenoceptor gene-deficient mice: restoration by intravascular human beta(2)-adrenoceptor gene transfer and role of NFkappaB and CREB transcription factors. British journal of pharmacology *162*, 712-721.

Coller, B.S. (2005). Leukocytosis and ischemic vascular disease morbidity and mortality: is it time to intervene? Arteriosclerosis, thrombosis, and vascular biology *25*, 658-670.

Cronstein, B.N., Kimmel, S.C., Levin, R.I., Martiniuk, F., and Weissmann, G. (1992). A mechanism for the antiinflammatory effects of corticosteroids: the glucocorticoid receptor regulates leukocyte adhesion to endothelial cells and expression of endothelial-leukocyte adhesion molecule 1 and intercellular adhesion molecule 1. Proceedings of the National Academy of Sciences of the United States of America *89*, 9991-9995.

Cutolo, M. (2012). Chronobiology and the treatment of rheumatoid arthritis. Current opinion in rheumatology *24*, 312-318.

dela Paz, N.G., and D'Amore, P.A. (2009). Arterial versus venous endothelial cells. Cell and tissue research *335*, 5-16.

Dickmeis, T. (2009). Glucocorticoids and the circadian clock. The Journal of endocrinology *200*, 3-22.

Dimitrov, S., Benedict, C., Heutling, D., Westermann, J., Born, J., and Lange, T. (2009). Cortisol and epinephrine control opposing circadian rhythms in T cell subsets. Blood *113*, 5134-5143.

Druzd, D., de Juan, A., and Scheiermann, C. (2014). Circadian rhythms in leukocyte trafficking. Seminars in immunopathology *36*, 149-162.

Druzd, D., O. Matveeva, L. Ince, U. Harrison, W. He, C. Schmal, H. Herzel, A. H. Tsang, N. Kawakami, A. Leliavski, O. Uhl, L. Yao, L. E. Sander, C. S. Chen, K. Kraus, A. de Juan, S. M. Hergenhan, M. Ehlers, B. Koletzko, R. Haas, W. Solbach, H. Oster, and C. Scheiermann. 2017. 'Lymphocyte Circadian Clocks Control Lymph Node Trafficking and Adaptive Immune Responses', *Immunity*, 46: 120-32.

Dustin, M.L., Rothlein, R., Bhan, A.K., Dinarello, C.A., and Springer, T.A. (2011). Induction by IL 1 and interferon-gamma: tissue distribution, biochemistry, and function of a natural adherence molecule (ICAM-1). J. Immunol. 1986. 137: 245-254. Journal of immunology (Baltimore, Md : 1950) *186*, 5024-5033.

Dzhagalov, I., Giguere, V., and He, Y.W. (2004). Lymphocyte development and function in the absence of retinoic acid-related orphan receptor alpha. Journal of immunology (Baltimore, Md : 1950) *173*, 2952-2959.

Eichmann, A., and Brunet, I. (2014). Arterial innervation in development and disease. Science translational medicine *6*, 252ps259.

Elenkov, I.J., Wilder, R.L., Chrousos, G.P., and Vizi, E.S. (2000). The sympathetic nerve--an integrative interface between two supersystems: the brain and the immune system. Pharmacological reviews *52*, 595-638.

Elices, M.J., Osborn, L., Takada, Y., Crouse, C., Luhowskyj, S., Hemler, M.E., and Lobb, R.R. (1990). VCAM-1 on activated endothelium interacts with the leukocyte integrin VLA-4 at a site distinct from the VLA-4/fibronectin binding site. Cell *60*, 577-584.

Fawcett, B.a. (1994). Textbook of Histology.

Florey (1966). The endothelial cell. British medical journal *2*, 487-490.

Fortier, E.E., Rooney, J., Dardente, H., Hardy, M.P., Labrecque, N., and Cermakian, N. (2011). Circadian variation of the response of T cells to antigen. Journal of immunology (Baltimore, Md : 1950) *187*, 6291-6300.

Ghosh, S., May, M.J., and Kopp, E.B. (1998). NF-kappa B and Rel proteins: evolutionarily conserved mediators of immune responses. Annual review of immunology *16*, 225-260.

Gibbs, J.E., Blaikley, J., Beesley, S., Matthews, L., Simpson, K.D., Boyce, S.H., Farrow, S.N., Else, K.J., Singh, D., Ray, D.W.*, et al.* (2012). The nuclear receptor REV-ERBalpha mediates circadian regulation of innate immunity through selective regulation of inflammatory cytokines. Proceedings of the National Academy of Sciences of the United States of America *109*, 582-587.

Girard, J.P., Moussion, C., and Forster, R. (2012). HEVs, lymphatics and homeostatic immune cell trafficking in lymph nodes. Nature reviews Immunology *12*, 762-773.

Golombek, D.A., and Rosenstein, R.E. (2010). Physiology of circadian entrainment. Physiological reviews *90*, 1063-1102.

Hand, L. E., T. W. Hopwood, S. H. Dickson, A. L. Walker, A. S. Loudon, D. W. Ray, D. A. Bechtold, and J. E. Gibbs. 2016. 'The circadian clock regulates inflammatory arthritis', *Faseb j*, 30: 3759-70.

Hansen, J. (2001). Increased breast cancer risk among women who work predominantly at night. Epidemiology (Cambridge, Mass) *12*, 74-77.

Hashiramoto, A., Yamane, T., Tsumiyama, K., Yoshida, K., Komai, K., Yamada, H., Yamazaki, F., Doi, M., Okamura, H., and Shiozawa, S. (2010). Mammalian clock gene Cryptochrome regulates arthritis via proinflammatory cytokine TNF-alpha. Journal of immunology (Baltimore, Md : 1950) *184*, 1560-1565.

Haupt, C.M., Alte, D., Dorr, M., Robinson, D.M., Felix, S.B., John, U., and Volzke, H. (2008). The relation of exposure to shift work with atherosclerosis and myocardial infarction in a general population. Atherosclerosis *201*, 205-211.

Hidalgo, A., Chang, J., Jang, J.E., Peired, A.J., Chiang, E.Y., and Frenette, P.S. (2009). Heterotypic interactions enabled by polarized neutrophil microdomains mediate thromboinflammatory injury. Nature medicine *15*, 384-391.

Hidalgo, A., Peired, A.J., Wild, M., Vestweber, D., and Frenette, P.S. (2007). Complete identification of E-selectin ligands on neutrophils reveals distinct functions of PSGL-1, ESL-1, and CD44. Immunity *26*, 477-489.

Hogg, N., Henderson, R., Leitinger, B., McDowall, A., Porter, J., and Stanley, P. (2002). Mechanisms contributing to the activity of integrins on leukocytes. Immunological reviews *186*, 164-171.

Hoppensteadt, F.C., and Keller, J.B. (1976). Synchronization of periodical cicada emergences. Science (New York, NY) *194*, 335-337.

Howell, R. E., S. M. Albelda, M. L. Daise, and E. M. Levine. 1988. 'Characterization of beta-adrenergic receptors in cultured human and bovine endothelial cells', *J Appl Physiol (1985)*, 65: 1251-7.

Ignatowski, T.A., Gallant, S., and Spengler, R.N. (1996). Temporal regulation by adrenergic receptor stimulation of macrophage (M phi)-derived tumor necrosis factor (TNF) production post-LPS challenge. Journal of neuroimmunology *65*, 107-117.

Jung, U., and Ley, K. (1999). Mice lacking two or all three selectins demonstrate overlapping and distinct functions for each selectin. Journal of immunology (Baltimore, Md : 1950) *162*, 6755-6762.

Jung, U., Norman, K.E., Scharffetter-Kochanek, K., Beaudet, A.L., and Ley, K. (1998). Transit time of leukocytes rolling through venules controls cytokine-induced inflammatory cell recruitment in vivo. The Journal of clinical investigation *102*, 1526-1533.

Karatsoreos, I. N., and R. Silver. 2017. 'Chapter 27 - Body Clocks in Health and Disease A2 - Conn, P. Michael.' in, *Conn's Translational Neuroscience* (Academic Press: San Diego).

Krams, R.B., Magnus (2017). The ESC Textbook of Vascular Biology.

Kubo, T., Ozasa, K., Mikami, K., Wakai, K., Fujino, Y., Watanabe, Y., Miki, T., Nakao, M., Hayashi, K., Suzuki, K.*, et al.* (2006). Prospective cohort study of the risk of prostate cancer among rotating-shift workers: findings from the Japan collaborative cohort study. American journal of epidemiology *164*, 549-555.

Ley, K., Laudanna, C., Cybulsky, M.I., and Nourshargh, S. (2007). Getting to the site of inflammation: the leukocyte adhesion cascade updated. Nature reviews Immunology *7*, 678-689.

Lilly, L.S. (2010). Pathophysiology of Heart Disease: A Collaborative Project of Medical Students and Faculty.

Litinski, M., Scheer, F.A., and Shea, S.A. (2009). Influence of the Circadian System on Disease Severity. Sleep medicine clinics *4*, 143-163.

Liu, J., Malkani, G., Shi, X., Meyer, M., Cunningham-Runddles, S., Ma, X., and Sun, Z.S. (2006). The circadian clock Period 2 gene regulates gamma interferon production of NK cells in host response to lipopolysaccharide-induced endotoxic shock. Infection and immunity *74*, 4750-4756.

Logan, R.W., Wynne, O., Levitt, D., Price, D., and Sarkar, D.K. (2013). Altered circadian expression of cytokines and cytolytic factors in splenic natural killer cells of Per1(-/-) mutant mice. Journal of interferon & cytokine research : the official journal of the International Society for Interferon and Cytokine Research *33*, 108-114.

Looney, M.R., and Bhattacharya, J. (2014). Live imaging of the lung. Annual review of physiology *76*, 431-445.

Lopez, V. M., C. L. Decatur, W. D. Stamer, R. M. Lynch, and B. S. McKay. 2008. 'L-DOPA is an endogenous ligand for OA1', *PLoS Biol*, 6: e236.

Lu, H., Smith, C.W., Perrard, J., Bullard, D., Tang, L., Shappell, S.B., Entman, M.L., Beaudet, A.L., and Ballantyne, C.M. (1997). LFA-1 is sufficient in mediating neutrophil emigration in Mac-1-deficient mice. The Journal of clinical investigation *99*, 1340-1350.

Lucas, D., Battista, M., Shi, P.A., Isola, L., and Frenette, P.S. (2008). Mobilized hematopoietic stem cell yield depends on species-specific circadian timing. Cell stem cell *3*, 364-366.

Maestroni, G.J., Cosentino, M., Marino, F., Togni, M., Conti, A., Lecchini, S., and Frigo, G. (1998). Neural and endogenous catecholamines in the bone marrow. Circadian association of norepinephrine with hematopoiesis? Experimental hematology *26*, 1172-1177.

Majno, G., and Palade, G.E. (1961). Studies on inflammation. 1. The effect of histamine and serotonin on vascular permeability: an electron microscopic study. The Journal of biophysical and biochemical cytology *11*, 571-605.

Malpas, S.C. (2010). Sympathetic nervous system overactivity and its role in the development of cardiovascular disease. Physiological reviews *90*, 513-557.

Marshall, J.M. (1982). The influence of the sympathetic nervous system on individual vessels of the microcirculation of skeletal muscle of the rat. The Journal of physiology *332*, 169-186.

Mauvoisin, D., Dayon, L., Gachon, F., and Kussmann, M. (2015). Proteomics and circadian rhythms: it's all about signaling! Proteomics *15*, 310-317.

Mendez-Ferrer, S., Lucas, D., Battista, M., and Frenette, P.S. (2008). Haematopoietic stem cell release is regulated by circadian oscillations. Nature *452*, 442-447.

Miyamasu, M., Misaki, Y., Izumi, S., Takaishi, T., Morita, Y., Nakamura, H., Matsushima, K., Kasahara, T., and Hirai, K. (1998). Glucocorticoids inhibit chemokine generation by human eosinophils. The Journal of allergy and clinical immunology *101*, 75-83.

Motosugi, Y., H. Ando, K. Ushijima, T. Maekawa, E. Ishikawa, M. Kumazaki, and A. Fujimura. 2011. 'Tissue-dependent alterations of the clock gene expression rhythms in leptin-resistant Zucker diabetic fatty rats', *Chronobiol Int*, 28: 968-72.

Mormont, M.C., Waterhouse, J., Bleuzen, P., Giacchetti, S., Jami, A., Bogdan, A., Lellouch, J., Misset, J.L., Touitou, Y., and Levi, F. (2000). Marked 24-h rest/activity rhythms are associated with better quality of life, better response, and longer survival in patients with metastatic colorectal cancer and good performance status. Clinical cancer research : an official journal of the American Association for Cancer Research *6*, 3038-3045.

Mulcahy, D., Keegan, J., Cunningham, D., Quyyumi, A., Crean, P., Park, A., Wright, C., and Fox, K. (1988). Circadian variation of total ischaemic burden and its alteration with anti-anginal agents. Lancet (London, England) *2*, 755-759.

Muller, J.E., Stone, P.H., Turi, Z.G., Rutherford, J.D., Czeisler, C.A., Parker, C., Poole, W.K., Passamani, E., Roberts, R., Robertson, T.*, et al.* (1985).

Circadian variation in the frequency of onset of acute myocardial infarction. The New England journal of medicine *313*, 1315-1322.

Murfee, W. L., T. C. Skalak, and S. M. Peirce. 2005. 'Differential arterial/venous expression of NG2 proteoglycan in perivascular cells along microvessels: identifying a venule-specific phenotype', *Microcirculation*, 12: 151-60.

Nabah, Y.N., Mateo, T., Cerda-Nicolas, M., Alvarez, A., Martinez, M., Issekutz, A.C., and Sanz, M.J. (2005). L-NAME induces direct arteriolar leukocyte adhesion, which is mainly mediated by angiotensin-II. Microcirculation (New York, NY : 1994) *12*, 443-453.

Nance, D.M., and Sanders, V.M. (2007). Autonomic innervation and regulation of the immune system (1987-2007). Brain, behavior, and immunity *21*, 736-745.

Narasimamurthy, R., Hatori, M., Nayak, S.K., Liu, F., Panda, S., and Verma, I.M. (2012). Circadian clock protein cryptochrome regulates the expression of proinflammatory cytokines. Proceedings of the National Academy of Sciences of the United States of America *109*, 12662-12667.

Nguyen, K.D., Fentress, S.J., Qiu, Y., Yun, K., Cox, J.S., and Chawla, A. (2013). Circadian gene Bmal1 regulates diurnal oscillations of Ly6C(hi) inflammatory monocytes. Science (New York, NY) *341*, 1483-1488.

Nussbaum, J.C., Van Dyken, S.J., von Moltke, J., Cheng, L.E., Mohapatra, A., Molofsky, A.B., Thornton, E.E., Krummel, M.F., Chawla, A., Liang, H.E.*, et al.* (2013). Type 2 innate lymphoid cells control eosinophil homeostasis. Nature *502*, 245-248.

Papanicolaou, D.A., Tsigos, C., Oldfield, E.H., and Chrousos, G.P. (1996). Acute glucocorticoid deficiency is associated with plasma elevations of interleukin-6: does the latter participate in the symptomatology of the steroid withdrawal syndrome and adrenal insufficiency? The Journal of clinical endocrinology and metabolism *81*, 2303-2306.

Parker, J.D., Testa, M.A., Jimenez, A.H., Tofler, G.H., Muller, J.E., Parker, J.O., and Stone, P.H. (1994). Morning increase in ambulatory ischemia in

patients with stable coronary artery disease. Importance of physical activity and increased cardiac demand. Circulation *89*, 604-614.

Pearson Education, I. (2011). Cardiovascular System Blood.

Preitner, N., Damiola, F., Lopez-Molina, L., Zakany, J., Duboule, D., Albrecht, U., and Schibler, U. (2002). The orphan nuclear receptor REV-ERBalpha controls circadian transcription within the positive limb of the mammalian circadian oscillator. Cell *110*, 251-260.

Ralph, M.R., Foster, R.G., Davis, F.C., and Menaker, M. (1990). Transplanted suprachiasmatic nucleus determines circadian period. Science (New York, NY) *247*, 975-978.

Rogers, D.L., Sarah (2017). Overview of the vessels involved in bllod circulation.

Scharffetter-Kochanek, K., Lu, H., Norman, K., van Nood, N., Munoz, F., Grabbe, S., McArthur, M., Lorenzo, I., Kaplan, S., Ley, K.*, et al.* (1998). Spontaneous skin ulceration and defective T cell function in CD18 null mice. The Journal of experimental medicine *188*, 119-131.

Scheiermann, C., Kunisaki, Y., and Frenette, P.S. (2013). Circadian control of the immune system. Nature reviews Immunology *13*, 190-198.

Scheiermann, C., Kunisaki, Y., Lucas, D., Chow, A., Jang, J.E., Zhang, D., Hashimoto, D., Merad, M., and Frenette, P.S. (2012). Adrenergic nerves govern circadian leukocyte recruitment to tissues. Immunity *37*, 290-301.

Schernhammer, E.S., Kroenke, C.H., Laden, F., and Hankinson, S.E. (2006). Night work and risk of breast cancer. Epidemiology (Cambridge, Mass) *17*, 108-111.

Schernhammer, E.S., Laden, F., Speizer, F.E., Willett, W.C., Hunter, D.J., Kawachi, I., Fuchs, C.S., and Colditz, G.A. (2003). Night-shift work and risk of colorectal cancer in the nurses' health study. Journal of the National Cancer Institute *95*, 825-828.

Schloss, M.J., Hilby, M., Nitz, K., Guillamat Prats, R., Ferraro, B., Leoni, G., Soehnlein, O., Kessler, T., He, W., Luckow, B.*, et al.* (2017). Ly6C(high) Monocytes Oscillate in the Heart During Homeostasis and After Myocardial

Infarction-Brief Report. Arteriosclerosis, thrombosis, and vascular biology *37*, 1640-1645.

Segers, V. F., and R. T. Lee. 2008. 'Stem-cell therapy for cardiac disease', *Nature*, 451: 937-42.

Shearman, L.P., Sriram, S., Weaver, D.R., Maywood, E.S., Chaves, I., Zheng, B., Kume, K., Lee, C.C., van der Horst, G.T., Hastings, M.H.*, et al.* (2000). Interacting molecular loops in the mammalian circadian clock. Science (New York, NY) *288*, 1013-1019.

Shimba, A., G. Cui, S. Tani-Ichi, M. Ogawa, S. Abe, F. Okazaki, S. Kitano, H. Miyachi, H. Yamada, T. Hara, Y. Yoshikai, T. Nagasawa, G. Schutz, and K. Ikuta. 2018. 'Glucocorticoids Drive Diurnal Oscillations in T Cell Distribution and Responses by Inducing Interleukin-7 Receptor and CXCR4', *Immunity*, 48: 286-98.e6.

Silver, A.C., Arjona, A., Walker, W.E., and Fikrig, E. (2012). The circadian clock controls toll-like receptor 9-mediated innate and adaptive immunity. Immunity *36*, 251-261.

Silvestre, J.S. (2008). Vascular progenitor cells and diabetes: role in postischemic neovascularisation. Diabetes & metabolism *34 Suppl 1*, S33-36.

Spengler, M.L., Kuropatwinski, K.K., Comas, M., Gasparian, A.V., Fedtsova, N., Gleiberman, A.S., Gitlin, II, Artemicheva, N.M., Deluca, K.A., Gudkov, A.V.*, et al.* (2012). Core circadian protein CLOCK is a positive regulator of NF-kappaB-mediated transcription. Proceedings of the National Academy of Sciences of the United States of America *109*, E2457-2465.

Stein, C.M. (2012). Chapter 11 - β-Adrenergic Receptors A2 - Robertson, David. In Primer on the Autonomic Nervous System (Third Edition), I. Biaggioni, G. Burnstock, P.A. Low, and J.F.R. Paton, eds. (San Diego: Academic Press), pp. 59-61.

Sternberg, E.M. (2006). Neural regulation of innate immunity: a coordinated nonspecific host response to pathogens. Nature reviews Immunology *6*, 318-328.

Stouthard, J.M., Levi, M., Hack, C.E., Veenhof, C.H., Romijn, H.A., Sauerwein, H.P., and van der Poll, T. (1996). Interleukin-6 stimulates coagulation, not fibrinolysis, in humans. Thrombosis and haemostasis *76*, 738-742.

Straub, R.H., and Cutolo, M. (2007). Circadian rhythms in rheumatoid arthritis: implications for pathophysiology and therapeutic management. Arthritis and rheumatism *56*, 399-408.

Suarez-Barrientos, A., Lopez-Romero, P., Vivas, D., Castro-Ferreira, F., Nunez-Gil, I., Franco, E., Ruiz-Mateos, B., Garcia-Rubira, J.C., Fernandez-Ortiz, A., Macaya, C.*, et al.* (2011). Circadian variations of infarct size in acute myocardial infarction. Heart (British Cardiac Society) *97*, 970-976.

Sumagin, R., and Sarelius, I.H. (2006). TNF-alpha activation of arterioles and venules alters distribution and levels of ICAM-1 and affects leukocyte-endothelial cell interactions. American journal of physiology Heart and circulatory physiology *291*, H2116-2125.

Sumagin, R., and Sarelius, I.H. (2007). A role for ICAM-1 in maintenance of leukocyte-endothelial cell rolling interactions in inflamed arterioles. American journal of physiology Heart and circulatory physiology *293*, H2786-2798.

Sumagin, R., and Sarelius, I.H. (2013). Emerging understanding of roles for arterioles in inflammation. Microcirculation (New York, NY : 1994) *20*, 679-692.

Sun, Y., Yang, Z., Niu, Z., Peng, J., Li, Q., Xiong, W., Langnas, A.N., Ma, M.Y., and Zhao, Y. (2006). MOP3, a component of the molecular clock, regulates the development of B cells. Immunology *119*, 451-460.

Suzuki, S., Namiki, J., Shibata, S., Mastuzaki, Y., and Okano, H. (2010). The neural stem/progenitor cell marker nestin is expressed in proliferative endothelial cells, but not in mature vasculature. The journal of histochemistry and cytochemistry : official journal of the Histochemistry Society *58*, 721-730.

Tannenbaum, G.S., and Martin, J.B. (1976). Evidence for an endogenous ultradian rhythm governing growth hormone secretion in the rat. Endocrinology *98*, 562-570.

Tenkanen, L., Sjoblom, T., and Harma, M. (1998). Joint effect of shift work and adverse life-style factors on the risk of coronary heart disease. Scandinavian journal of work, environment & health *24*, 351-357.

Tofler, G.H., Gebara, O.C., Mittleman, M.A., Taylor, P., Siegel, W., Venditti, F.J., Jr., Rasmussen, C.A., and Muller, J.E. (1995). Morning peak in ventricular tachyarrhythmias detected by time of implantable cardioverter/defibrillator therapy. The CPI Investigators. Circulation *92*, 1203-1208.

Undar, L., Ertugrul, C., Altunbas, H., and Akca, S. (1999). Circadian variations in natural coagulation inhibitors protein C, protein S and antithrombin in healthy men: a possible association with interleukin-6. Thrombosis and haemostasis *81*, 571-575.

Westgate, E. J., Y. Cheng, D. F. Reilly, T. S. Price, J. A. Walisser, C. A. Bradfield, and G. A. FitzGerald. 2008. 'Genetic components of the circadian clock regulate thrombogenesis in vivo', *Circulation*, 117: 2087-95.

Westcott, E.B., and Segal, S.S. (2013). Perivascular innervation: a multiplicity of roles in vasomotor control and myoendothelial signaling. Microcirculation (New York, NY : 1994) *20*, 217-238.

Westfall, T.C. (2009). Sympathomimetic Drugs and Adrenergic Receptor Antagonists A2 - Squire, Larry R. In Encyclopedia of Neuroscience (Oxford: Academic Press), pp. 685-695.

Wilson, R.W., Ballantyne, C.M., Smith, C.W., Montgomery, C., Bradley, A., O'Brien, W.E., and Beaudet, A.L. (1993). Gene targeting yields a CD18-mutant mouse for study of inflammation. Journal of immunology (Baltimore, Md : 1950) *151*, 1571-1578.

Yang, Y.T., and McElligott, M.A. (1989). Multiple actions of beta-adrenergic agonists on skeletal muscle and adipose tissue. The Biochemical journal *261*, 1-10.

Young, M.R., Matthews, J.P., Kanabrocki, E.L., Sothern, R.B., Roitman-Johnson, B., and Scheving, L.E. (1995). Circadian rhythmometry of serum interleukin-2, interleukin-10, tumor necrosis factor-alpha, and granulocyte-macrophage colony-stimulating factor in men. Chronobiology international *12*, 19-27.

Yu, X., Rollins, D., Ruhn, K.A., Stubblefield, J.J., Green, C.B., Kashiwada, M., Rothman, P.B., Takahashi, J.S., and Hooper, L.V. (2013). TH17 cell differentiation is regulated by the circadian clock. Science (New York, NY) *342*, 727-730.

Zhang, D., G. Chen, D. Manwani, A. Mortha, C. Xu, J. J. Faith, R. D. Burk, Y. Kunisaki, J. E. Jang, C. Scheiermann, M. Merad, and P. S. Frenette. 2015. 'Neutrophil ageing is regulated by the microbiome', *Nature*, 525: 528-32.

6 Appendix

6. 1 Curriculum Vitae

Education

06/2013 – 07/2018	**PhD of Medical Research**, Graduate Program IRTG of the SFB914, Ludwig-Maximilians University Munich, Germany.
09/2007 – 09/2012	**Licenciatura en Biología** (Long cycle degree, 5 years) in Biology; Universidad Autónoma de Madrid (Madrid, Spain).
09/2011 – 06/2012	**Biology degree final project** Department of Epidemiology, Atherothrombosis and Imaging. National Center of Cardiovascular Research (CNIC), Madrid, Spain.

Research Experience

06/2013 -	**Ludwig-Maximilians-University, Munich, Germany** Walter Brendel Center of Experimental Medicine. PhD student.
05/2012 – 05/2013	**National Center of Cardiovascular Research (CNIC), Madrid, Spain.** Lab assistant.
09/2011 – 05/2012	**National Center of Cardiovascular Research (CNIC), Madrid, Spain** Pre-graduate student.

Grants

09/2010 – 09/2011	Erasmus Programme in Rome, Italy. Università degli Studi Roma Tre.
05/2015	Travel grant: ESCI. (Cluj-Napoca)

Publications

1.- de Juan A, Pick R, Chen CS, Ince L, Zhang D, Druzd D, Oster H, Zuchtriegel G, Reichel C, Söhnlein O, Frenette P, Scheiermann C. Sympathetic innervation of arteries drives rhythmic leukocyte adhesion to arteries and veins (***manuscript in preparation****).*

2.- He, W; Holtkamp, S; Hergenhan, S; Kraus, K; **de Juan, A**; Weber, J; Druzd, D; Ince, L; Chen, CS; Scheiermann, C. A circadian zip code of pro-migratory factors determines rhythmic trafficking of leukocyte subsets to organs (***manuscript submitted*** 2018*).*

3.- Druzd D, Matveeva O, Ince L, Harrison U, He W, Schmal C, Herzel H, Tsang AH, Kawakami N, Leliavski A, Uhl O, Yao L, Sander LE, Chen CS, Kraus K, **de Juan A**, Hergenhan SM, Ehlers M, Koletzko B, Haas R, Solbach W, Oster H, Scheiermann C. Lymphocyte Circadian Clocks Control Lymph Node Trafficking and Adaptive Immune Responses. **Immunity.** *2017 Jan* 17;46(1):120-132. doi: 10.1016/j.immuni.2016.12.011. Epub 2017 Jan 10.

4.- de Juan, A; Druzd, D.; Scheiermann, C. Recent Advances in Physiology: Role of the Circadian Clock in Health and Disease (Chapter 9: Regulation of Immunity by the Circadian Clock).

5.- Pineda-Torra, I; Gage, M; **de Juan,** A; Pello, OM. Isolation, Culture, and Polarization of Murine Bone Marrow-Derived and Peritoneal Macrophages. **Methods Mol Biol.** *2015*;1339:101-9. doi: 10.1007/978-1-4939-2929-0_6.

6.- Druzd, D; **de Juan, A**; Scheiermann, C. Circadian rhythms in leukocyte trafficking. **Semin Immunopathol.** 2014 Mar;36(2):149-62. doi: 10.1007/s00281-013-0414-4. Epub 2014 Jan 17. Review.

7.- Pello, OM; Chévre, R; Laoui, D; **de Juan, A**; Lolo, F; Andres-Manzano, M; Serrano, M; Vanginderachter, J; Andres, V. In vivo inhibition of c-Myc in myeloid cells impairs tumor-associated macrophage maturation and pro-tumoral activities. **PLoS One.** 2012;7(9):e45399. doi: 10.1371/journal.pone.0045399. Epub 2012 Sep 20.

Conferences

• 2nd International Conference on Leukocyte Trafficking (SFB 914). Munich, March 2018.

• XV European Biological Rhythms Society (EBRS) Congress. Amsterdam July-August 2017. Oral presentation.

• Experimental Biology. Chicago, April 2017. Oral presentation.

• Experimental Biology. San Diego, March 2016. Oral presentation.

• Kick-off SFB914. Villa Vigoni, Italy, October 2015. Poster presentation (Poster Prize).

• ESCI. Cluj-Napoca, May 2015. Oral presentation (Travel grant).

• Experimental Biology. Boston, March 2015. Oral and poster presentations.

• International Conference on Leukocyte Trafficking (SFB 914). Munich, March 2014.

• Madrid meeting on dendritic cells and macrophages. National Center of Biotechnology (CNB, CSIC) Madrid, May 2012.

6.2 Affidavit

I hereby declare, that the submitted thesis entitled

Sympathetic innervation of arteries drives rhythmic leukocyte adhesion to arteries and veins

is my own work. I have only used the sources indicated and have not made unauthorized use of services of a third party. Where the work of others has been quoted or reproduced, the source is always given.

I further declare that the submitted thesis or parts thereof have not been presented as part of an examination degree to any other university.

Munich, 23/07/2018 Alba de Juan

Place, date Signature doctoral candidate